

Copyright
by
Sergey Grebenshikov
2010

**The Thesis Committee for Sergey Grebenshikov
Certifies that this is the approved version of the following thesis:**

Impacts of Windmill Traffic on Pavement Structures

**APPROVED BY
SUPERVISING COMMITTEE:**

Supervisor:

Jorge A. Prozzi

Co-Supervisor:

Jolanda Prozzi

Randy B. Machemehl

Impacts of Windmill Traffic on Pavement Structures

by

Sergey Grebenshikov, B.S.E.

Thesis

Presented to the Faculty of the Graduate School of

The University of Texas at Austin

in Partial Fulfillment

of the Requirements

for the Degree of

Master of Science in Engineering

The University of Texas at Austin

August, 2010

Dedication

To broadening perspectives and advancing knowledge in all fields of human interest!

Acknowledgements

Many thanks to my advisors Jolanda and Jorge Prozzi, and to the University of Texas at Austin, for sponsoring my education. Many thanks to my family for supporting me throughout my life.

August, 2010

Abstract

Impacts of Windmill Traffic on Pavement Structures

Sergey Grebenshikov, M.S.E.

The University of Texas at Austin, 2010

Supervisor: Jorge A. Prozzi, Jolanda Prozzi

This report focuses on the impacts of traffic generated as a result of the windmill on pavement structures. The wind energy industry is a fast growing sector of the U.S. economy. Lately concerns have been raised over the transportation of heavy windmill components on the pavement infrastructure. This report analyzes the impacts of windmill traffic on two pavement structures in Texas: 1) rural interstate facility, and 2) rural collector roadway facility. Windmill traffic was disaggregated by windmill component and categorized into eight vehicle classes. Two traffic scenarios were developed and a damage ratio for pavement rutting was developed. Based on the rutting damage ratio, results showed that windmill traffic has a significant impact on rural collector facilities when compared against normal truck traffic activity. Meanwhile, impacts on rural interstate facilities were determined to be insignificant when compared to normal truck traffic activity.

TABLE OF CONTENTS

CHAPTER 1. INTRODUCTION AND METHODOLOGY	1
CHAPTER 2. THE WIND INDUSTRY IN THE U.S.	5
CHAPTER 3. TRENDS IN WIND TECHNOLOGY	10
3.1 <i>Growth in Wind Turbine Technology</i>	11
3.2 <i>Limiting Factors in Wind Technology</i>	12
CHAPTER 4. WINDMILL COMPONENTS	15
4.1 <i>Nacelle Unit</i>	15
4.2 <i>Rotor Hub and Blades</i>	17
4.3 <i>Windmill Towers</i>	20
CHAPTER 5. TRANSPORTATION OF WINDMILL COMPONENTS	22
CHAPTER 6. THE TRUCK TRANSPORT INDUSTRY	28
CHAPTER 7. THE WIND TRANSPORT VEHICLE FLEET	35
7.1 <i>Limitations of the Oversize/Overweight (OS/OW) Permit Dataset</i>	36
7.2 <i>Nacelle Transport Vehicle Fleet</i>	37
7.3 <i>Tower Transport Vehicle Fleet</i>	48
7.4 <i>Hub Transport Vehicle Fleet</i>	56
7.5 <i>Blade Transport Vehicle Fleet</i>	57
CHAPTER 8. ROADWAY NETWORK ANALYSIS	59
CHAPTER 9. PAVEMENT IMPACT ANALYSIS	61
9.1 <i>Pavement Selection</i>	63
9.1.1 <i>Interstate Highway 20</i>	65
9.1.2 <i>Farm-to-Market Road 1606</i>	67

9.2 <i>Traffic Characterization</i>	69
9.2.1 <i>Standard Traffic</i>	69
9.2.2 <i>Windmill Traffic</i>	74
9.3 <i>MEPDG Analysis</i>	79
9.4 <i>Analysis Results</i>	82
9.4.1 <i>IH-20 Impact Analysis Results</i>	83
9.4.2 <i>FM 1606 Impact Analysis Results</i>	89
CHAPTER 10. CONCLUSIONS OF STUDY	94
10.1 <i>Further Remarks</i>	95
Appendix A.....	98
References.....	100
VITA	104

LIST OF TABLES

Table 1: Length, Width, and Size Dimensions for Nacelle Units.....	17
Table 2: Size and Weight Dimensions for Blades and Rotor Hubs from Vestas and Aceonia.....	19
Table 3: Advantages and Disadvantages for each Transportation Mode Choice	22
Table 4: Maximum Permitted Legal Length, Width, Height, and Weight Limits for Trucks	26
Table 5: Max. Permitted Length, Width, Height, and Weight Limits for Cargo on Trains	26
Table 6: Types of Trailers Used for Hauling Windmill Components.....	29
Table 7: Field Entries in the Oversized/Overweight Database.....	35
Table 8: Number of Records found for each component in the OS/OW Dataset.....	36
Table 9: Trailer types used for hauling Nacelle Units.....	41
Table 10: Trailer types used for hauling Tower sections	49
Table 11: Distribution of Vehicle-Miles-Traveled over various facility types	60
Table 12: Structural Composition of IH-20.....	65
Table 13: Layer Gradation for IH-20	65
Table 14: Mixture Properties for HMA Layers	66
Table 15: Material Properties for Granular Layers and Subgrade	66
Table 16: Structural Composition of FM 1606.....	67
Table 17: Layer Gradation for Farm-to-Market 1606.....	68
Table 18: Mixture Properties for HMA Layer	68
Table 19: Material Properties for Granular Layers	68

Table 20: Standard Traffic Characteristics for Rural Interstates and Rural Collector Roads	70
Table 21: <i>Single</i> Axle Load Distribution for Class 5 and Class 9 Vehicles	73
Table 22: <i>Tandem</i> Axle Load Distribution for Class 9 Vehicles.....	73
Table 23: Percentage of Each Vehicle Class in the Windmill Fleet	75
Table 24: Single Axle Load Distribution Spectra for Windmill Traffic	76
Table 25: Tandem Axle Load Distribution Spectra for Windmill Traffic	77
Table 26: Tridem Axle Load Distribution Spectra for Windmill Traffic.....	78
Table 27: Quad Axle Load Distribution Spectra for Windmill Traffic.....	78
Table 28: Pavement Rutting During First 2 Years.....	86
Table 29: Pavement Rutting During Years 8-10.....	87
Table 30: Pavement Rutting During Years 18-20.....	87
Table 31: Damage Ratios for Windmill Traffic When Compared Against Standard Traffic	88
Table 32: Pavement Rutting During First 2 Years.....	90
Table 33: Pavement Rutting During Years 8-10.....	91
Table 34: Pavement Rutting During Years 18-20.....	92
Table 35: Damage Ratios for Windmill Traffic When Compared Against Standard Traffic	93

LIST OF FIGURES

Figure 1: Structure for Assessing the Impacts of Windmill Traffic on the Pavement Infrastructure.....	2
Figure 2: Methodology for Quantifying Impacts.....	3
Figure 3: Growth in the U.S. Wind Energy Sector	5
Figure 4: Wind Resources in the U.S. at 50 m above Ground Elevation	7
Figure 5: Rate of Investment Necessary to Meet the 20% Wind Scenario Goal.....	8
Figure 6: Required On-Shore and Off-Shore Power Capacity to Meet the 20% Wind Scenario Goal.....	8
Figure 7: GE 1.5 MW Windmill Compared Against the Statue of Liberty.....	10
Figure 8: Distribution of Wind Turbines Installed in the U.S.	11
Figure 9: The Development Path and Growth of Wind Turbines.....	12
Figure 10: Standard Windmill Nacelle Unit	16
Figure 11: Nacelle Weight vs. Power Output	16
Figure 12: Interior View of the Rotor Assembly	17
Figure 13: Rotor Assembly Weight vs. Power Output.....	18
Figure 14: Rotor Diameter vs. Power Output	19
Figure 15: Typical Windmill Tower	20
Figure 16: Weight of Windmill Towers based on Height	21
Figure 17: Wind Transload Centers on BNSF Railway Network.....	24
Figure 18: Wind Transload Centers on Union Pacific Network.....	25
Figure 19: Double-Drop (Lowboy) Trailer Compared with Standard Flatbed Trailer	30
Figure 20: Tandem Axle 30 Ton Blade Trailer by Peerless Limited	31

Figure 21: 13-Axle Trailer Assembly by International Specialized Trailer Mfg., LLC ..	32
Figure 22: Full Schnabel Trailer System.....	33
Figure 23: Half Schnabel Trailer System	33
Figure 24: GVW of Transport Vehicle Involved in Moving Nacelles.....	38
Figure 25: Vehicle Axle Spacing for Nacelle Transports.....	38
Figure 26: GVW for Standard and Non-Standard Vehicles	40
Figure 27: Number of Axles on Trailer for Standard and Non-Standard Tractors	41
Figure 28: Standard Tractor + 6-Axle Trailer.....	43
Figure 29: Standard Tractor + 7-Axle Trailer.....	44
Figure 30: Non-Standard Tractor + 7-Axle Trailer.....	45
Figure 31: Non-Standard Tractor + 9-Axle Trailer.....	46
Figure 32: Non-Standard Tractor + 15 Axle Trailer	47
Figure 33: GVW of the Tower Transport Fleet	48
Figure 34: Standard Tractor + Half Schnabel +3-Axle Dolly Trailer	51
Figure 35: Non-Standard Tractor + Half Schnabel + 4-Axle Dolly.....	52
Figure 36: Non-Standard Tractor + Half Schnabel + 5-Axle Dolly	53
Figure 37: Non-Standard Tractor + Half Schnabel + 5-Axle Dolly	54
Figure 38: Non-Standard Tractor + Jeep and Dolly Full Schnabel System	55
Figure 39: Standard Tractor + Extended Double Drop Trailer Combination.....	57
Figure 40: Standard Tractor + Specialized Blade Trailer.....	58
Figure 41: Pavement Cross-Sections of IH 20 and FM 1606.....	64
Figure 42: FHWA Vehicle Classification System	71

Figure 43: General <i>Tandem</i> Axle Load Spectra Across All Dates and Locations According to the California Study	72
Figure 44: Windmill Vehicle Fleet Used for Pavement Impact Analysis	75
Figure 45: Inner Workings of the MEPDG	79
Figure 46: Pavement Performance for IH-20.....	84
Figure 47: IH-20 Pavement Performance at Initial Stages of Design Life.....	85
Figure 48: IH-20 Pavement Performance for Years 8-10 of Design Life	86
Figure 49: IH-20 Pavement Performance During Years 18-20 of Design Life	87
Figure 50: Pavement Performance for FM 1606	89
Figure 51: FM 1606 Pavement Performance at Initial Stages of Design Life.....	90
Figure 52: FM 1606 Pavement Performance for Years 8-10 of Design Life	91
Figure 53: FM 1606 Pavement Performance During Years 18-20 of Design Life.....	92
Figure 54: Construction of Pad Site for Windmill Structure	96

LIST OF EQUATIONS

Equation 1: Permanent Deformation in the AC Layer	80
Equation 2: Permanent Deformation in Unbound Materials	81
Equation 3: Damage Ratio for Pavement Rutting.....	88

CHAPTER 1. INTRODUCTION AND METHODOLOGY

Over the last decade, wind energy has become a popular source of electricity generation throughout the world. The desire to produce clean, renewable and domestic energy has compelled many countries into developing their own wind resources. Today, the U.S. is one of the leaders in wind energy production, with over 35.6 GW of installed capacity (*AWEA, 2009*)¹. This rapid development of the wind industry in the U.S. has provided the country with a clean, renewable source of energy, and much needed job opportunities during the current economic downturn.

As the wind industry has grown, and seeing a wind blade whiz by on the freeway has gone from being a rare opportunity to a common-day sight, concerns have been raised over the impacts of hauling oversized and overweight windmill components on the pavement infrastructure. What are the impacts? After all, most rural pavement structures in Texas were designed decades ago for different traffic configurations.

Since the U.S. wind industry is a relatively new and growing part of the energy sector, very little research has been done that examines the transportation logistics of moving windmill components and their impacts on the pavement infrastructure. The main goal of this study is to do just that, to provide an in-depth look at the impacts of wind energy traffic on the pavement infrastructure. To get to this goal however, it is first important to provide a methodology and the steps to be taken to reach this ultimate objective. The methodology used for this study is illustrated in Figure 1 below.

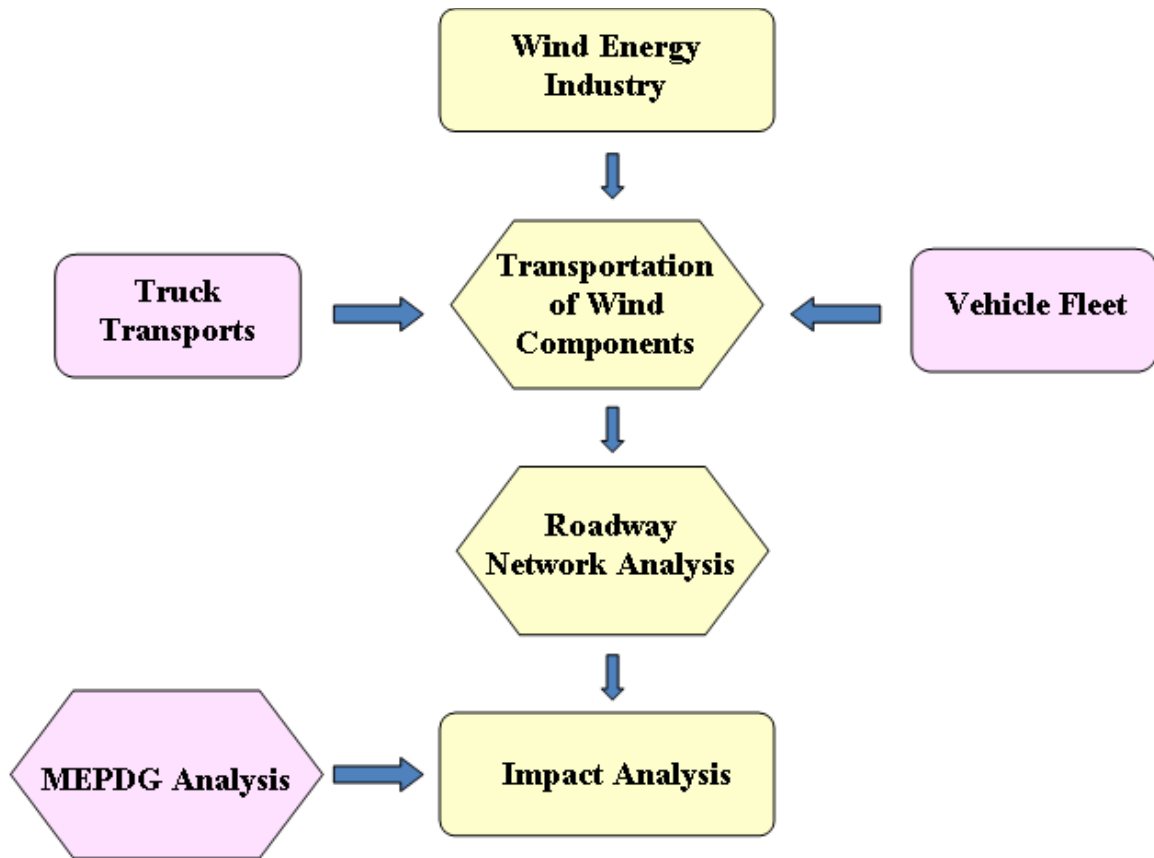


Figure 1: Structure for Assessing the Impacts of Windmill Traffic on the Pavement Infrastructure

From the figure, it can be seen that this study is structured into four main components; each component is addressed in a different section of this thesis. The first section provides information on the wind energy sector, and how it has grown and is expected to grow in the future. This section also provides insight into technological advances within the wind industry, as these will ultimately dictate the size and weight of windmill components being hauled across the country, and hence their impacts on the pavement infrastructure. The next two sections of this report focus in on the transportation sector. Transportation plays a significant role in the wind energy supply chain, therefore, understanding the transportation logistics of moving heavy windmill components, the vehicle fleet, and the types of roadway facilities that are impacted the most by these hauls

is imperative. Lastly, with the accumulated depth of knowledge gained, an impact analysis can be conducted.

To conduct an in-depth impact analysis to see how the transportation of heavy windmill components affects the pavement infrastructure, several steps need to be taken. Figure 2 illustrates a rational approach to this problem that was followed in this study.

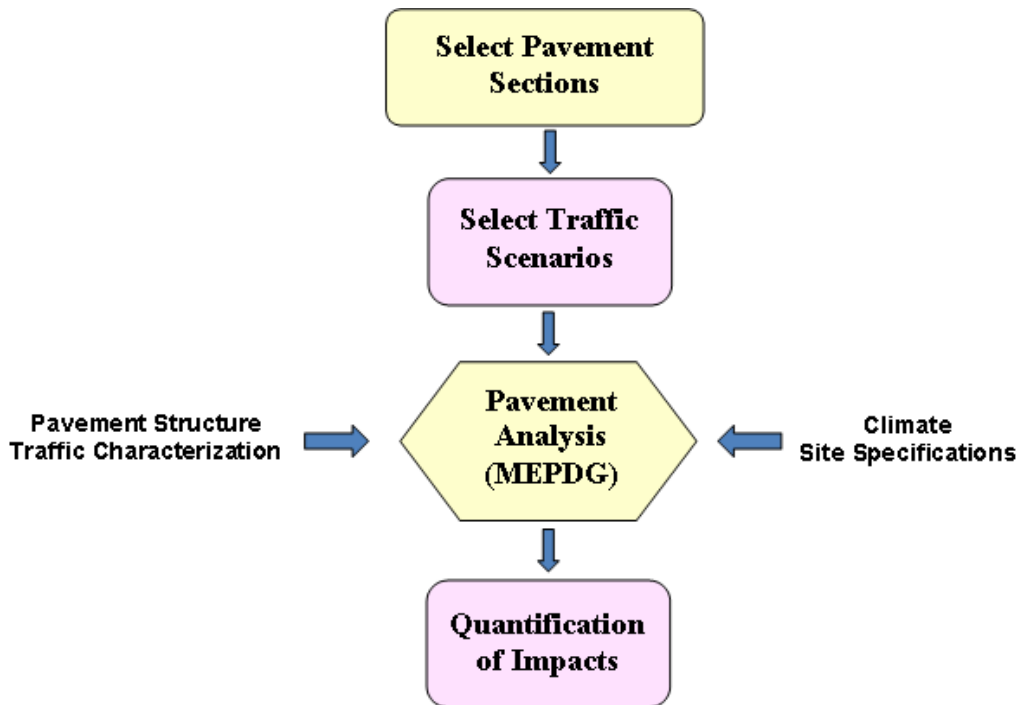


Figure 2: Methodology for Quantifying Impacts

From the figure, it can be seen that the approach calls for the selection of several pavement sections for the analysis. Two pavement sections were selected for the analysis in this study. These sections were selected to be representative of the following:

- Rural Interstate Pavement Section
- Rural Collector Road Pavement Section

Thereafter, the approach calls for the selection of several traffic scenarios. Since the ultimate goal of this study is to quantify the impacts of windmill traffic on two pavement

sections, it becomes necessary to evaluate these impacts against some base-case traffic scenario. Without this comparison, the analysis holds no frame of reference and is incomplete. Therefore two traffic scenarios were chosen for evaluation. These scenarios are as follows:

- Standard traffic given by the normal AADTT expected on the two roadway facilities.
- Windmill traffic, or the ADTT associated with moving 2, 5, 10, or 20 windmills per day on the two roadway facilities.

The next step in the methodology calls for the analysis of these two pavement and traffic scenarios. To carry out this task, the Mechanistic-Empirical Pavement Design Guide version 1.1 (or MEPDG) was used (*TRB, ND*)². The MEPDG is a pavement analysis tool that is accompanied with a computer software which allows the user to model the structure of a pavement and then to subject it to an array of traffic and climate scenarios. Under these scenarios, the analysis produces estimates of pavement performance in terms of rutting, cracking and roughness. The MEPDG is considered the most comprehensive pavement design and analysis software tool to date and its inner workings shall be further discussed in the subsequent chapters of this thesis (*AASHTO, 2008*)³.

The last step in the methodology calls for a quantification of pavement impacts. Impacts are typically quantified by evaluating various physical distresses such as pavement roughness, rutting, and fatigue cracking as they evolve during the service life of a pavement (*AASHTO, 1993*)⁴. For this study, pavement impacts will be evaluated by observing only one type of distress- permanent deformation or pavement rutting. Rutting within the pavement layers can pose a serious safety concern as it may lead to vehicle hydroplaning during a heavy storm (*AASHTO, 1993*)⁴. After the impacts have been quantified, a discussion of the results will ensue, followed by the conclusions derived from this study.

CHAPTER 2. THE WIND INDUSTRY IN THE U.S.

The wind energy industry is a growing part of the U.S. energy sector. Over the last decade, it has grown at an exponential rate. At the end of year 2000, there were 2,566 MW of wind power installed nationwide. By the end of year 2009, this number had increased to 35,603 MW (AWEA, 2009)¹. This accounted for approximately 2% of the U.S. electric energy demand. Figure 3 illustrates how the industry has grown over the past decade.

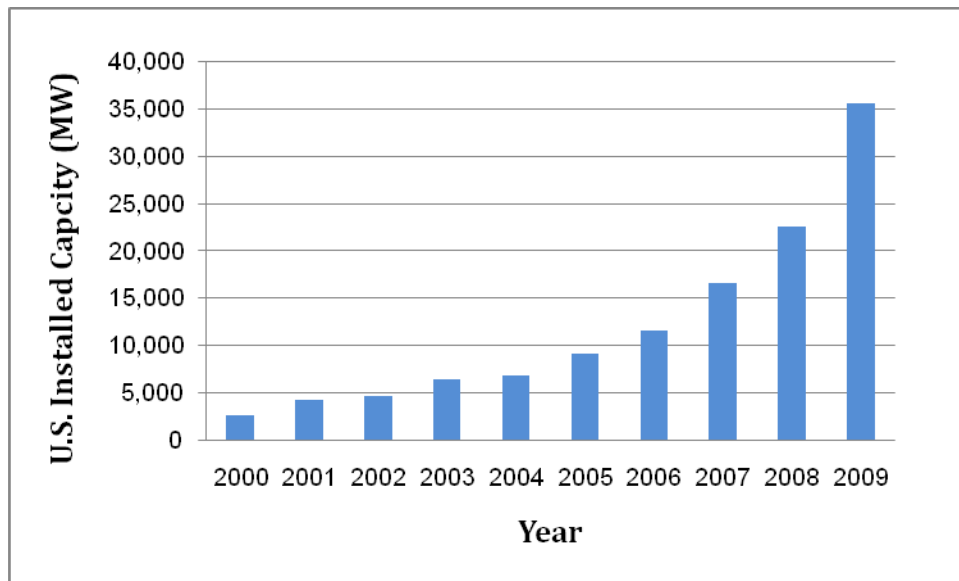


Figure 3: Growth in the U.S. Wind Energy Sector

The growth in the wind energy sector has been fueled by a volatile global energy market, and a need for the United States to become more energy independent by generating cost effective, clean, and renewable energy. This need for a clean, domestic energy source had led the U.S. Department of Energy into investigating a scenario where 20% of the nation's electricity demand would be generated from wind. In their report *20% Wind Energy by 2030*, the Department of Energy concluded that the U.S. has sufficient wind resources to meet the nation's energy demands several times over. They

had also outlined a plan for a national effort and the level of economic investment that would be necessary to attain a 20% wind energy goal by year 2030 (*U.S. DOE, 2008*)⁵.

To promote clean, renewable energy and to meet the national goal of 20% wind power by 2030, the U.S. government has provided the wind industry with a series of incentives over the past two decades. Some of the more prevailing incentives include a production tax credit (PTC) of 2.1 cents/kilowatt-hour for commercial wind farm developers, which was created under the Energy Policy Act in 1992 and extended through the end of year 2012 by the American Recovery and Reinvestment Act of 2009 (*AWEA, ND*)⁶. As part of that act, the U.S. government has allowed wind farm developers to substitute the PTC with a 30% investment tax credit which qualifies to be converted into a grant from the U.S. Treasury. As part of this provision, the Treasury Department provided \$1.5 billion in grants to the wind industry in 2009, which helped provide power to approximately 800,000 homes nationwide.

These incentives, amongst others, have acted as an impetus for the development of wind energy resources throughout the country. Most of the development has occurred in the wind belt areas of the Great Plains and along the nation's coast lines where the wind blows the hardest. Figure 4 highlights these areas, showing the highest level of potential along the Atlantic and Pacific coastlines, the Gulf of Mexico, and the Great Lakes.

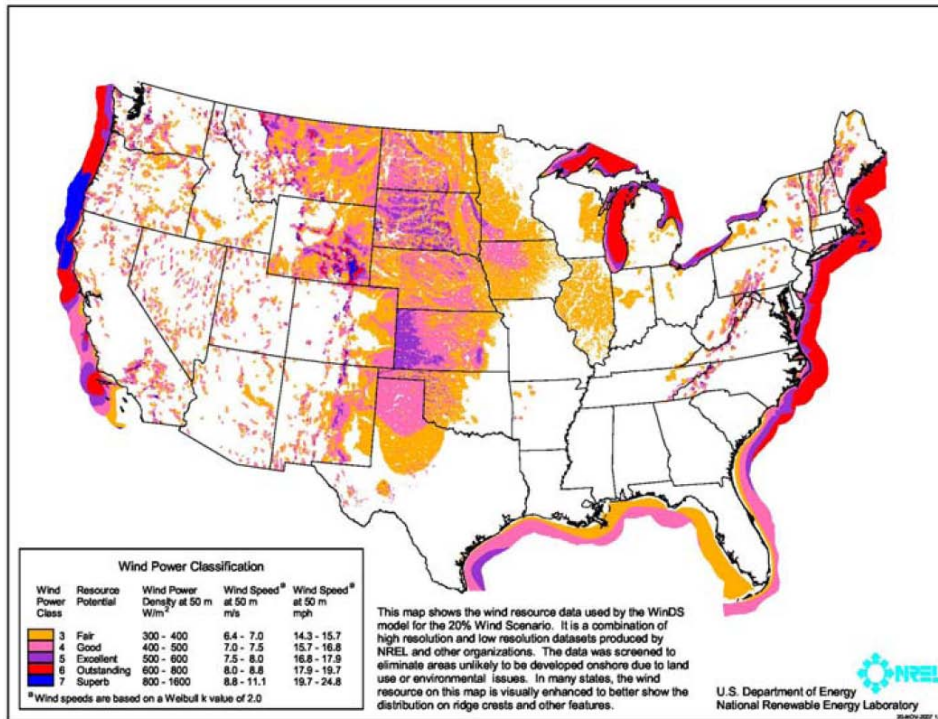


Figure 4: Wind Resources in the U.S. at 50 m above Ground Elevation
(Source: U.S. DOE, 2008)⁵

Although the current 35.6 GWs of wind energy capacity installed in the U.S. accounts for about 20% of wind capacity installed worldwide, it is quite far from meeting the 20% energy demand of this nation. According to the report published by U.S. DOE, a net capacity of about 300 GW (or 300,000 MW) will be necessary to meet 20% of the nation's electricity demand by year 2030 (U.S. DOE, 2008)⁵. This scenario, outlined in Figure 5 below, would require increasing the level of investment to approximately 16,000 MW of annual installed capacity by year 2018, and a continued level of investment at about the same rate through year 2030.

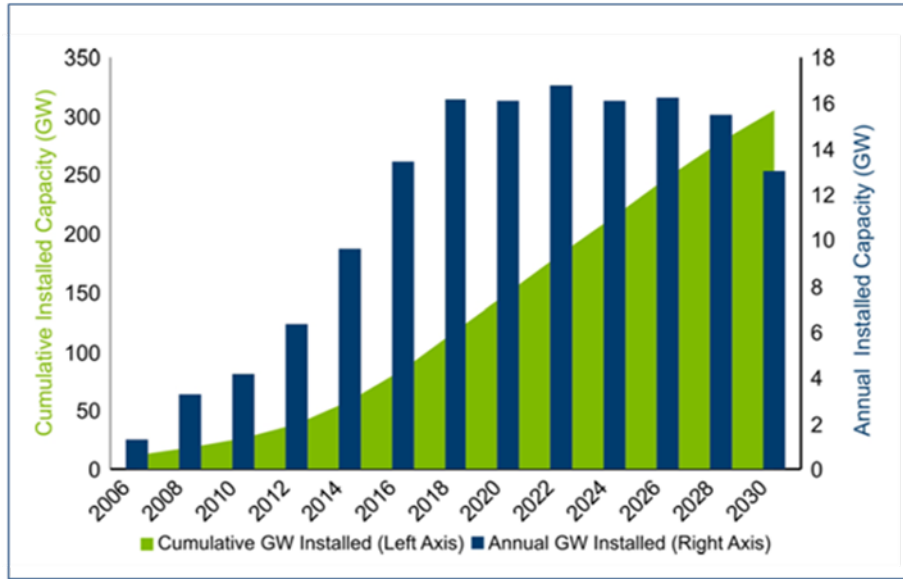


Figure 5: Rate of Investment Necessary to Meet the 20% Wind Scenario Goal
(Source: U.S. DOE, 2008)⁵

Out of the 300 GW capacity, the scenario estimates that approximately 50 GW (or 16.7%) can be developed offshore along the U.S. coastline. The distribution of off-shore to onshore wind capacity development, based on the *20% Wind Energy by 2030* scenario is presented in Figure 6.

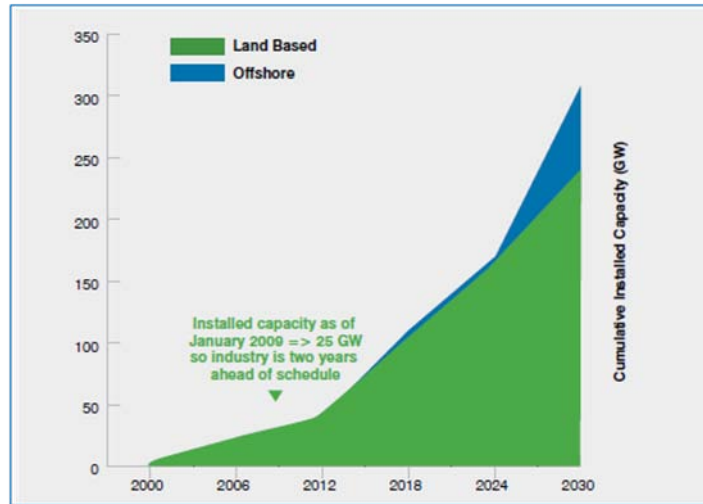


Figure 6: Required On-Shore and Off-Shore Power Capacity to Meet the 20% Wind Scenario Goal
(Source: AWEA, 2010)⁷

From the figures and the information presented in this chapter, it can be seen that the U.S. Wind Energy industry is quite a few leaps away from meeting its national goal. However, manufacturing and installation of wind turbines has steadily continued throughout the first decade of the 21st century. The manufacturing sector has grown by 12 times since 2004, with over 50% of new wind turbine components being manufactured in domestic facilities (*AWEA, 2010*)⁷. Also, at the end of 2009, as noted in Figure 6, the U.S. Wind Energy industry was about two years ahead of schedule proposed by the *20% Wind Energy* scenario.

Although the wind industry is taking quick and steady steps to meet the nation's demand for clean renewable energy, the future of the industry faces two main obstacles:

- 1) A long-term binding commitment from the U.S. government in wind energy.
- 2) Adequate transmission capacity to deliver electricity from points of production to major centers of consumption.

Currently, the U.S. government has made no binding long-term commitment to the installation of renewable energy. Unlike China and Europe, that have guaranteed wind developers long-term incentives, the U.S. market is driven mainly by short-term tax credits that have to be re-negotiated every several years. As a result, wind farm developers are apprehensive about large capital investment in full-scale manufacturing an installation of wind turbines to meet the *20% Wind Energy* goal. One legislature, the National Renewable Electricity Standard (RES), pushes for a national standard which would ensure that 25% of the U.S. electricity demand would be met by renewable sources by year 2025 (*AWEA, ND*)⁶. A strong national investment in renewable energy would allow for a steady growth in the wind energy market, and it would encourage the development of adequate transmission lines.

CHAPTER 3. TRENDS IN WIND TECHNOLOGY

To better follow this study, it is first important to understand the trends in current and future wind technology and to understand some terms in the wind energy industry, specifically the difference between a windmill and a wind turbine, as defined by this report. A turbine is a mechanical system that uses torque to produce electricity. A wind turbine consists of a set of blades, fixed upon a rotor hub that are used to capture the force of wind, and a generator system to convert the mechanical energy from the rotor into an electrical current. Hence, a commercial windmill is a wind turbine placed on a support tower that can generate enough electricity for commercial production.

A commercial windmill is a massive structure. When fully erected, it can rise as high as 400 feet in the air and have a blade-span that rivals that of a Boeing 747 (Tombari, 2007)⁸. To demonstrate the sheer size and magnitude of a commercial windmill, Figure 7 illustrates a typical 1.5 MW windmill constructed by GE Energy when compared against the Statue of Liberty.

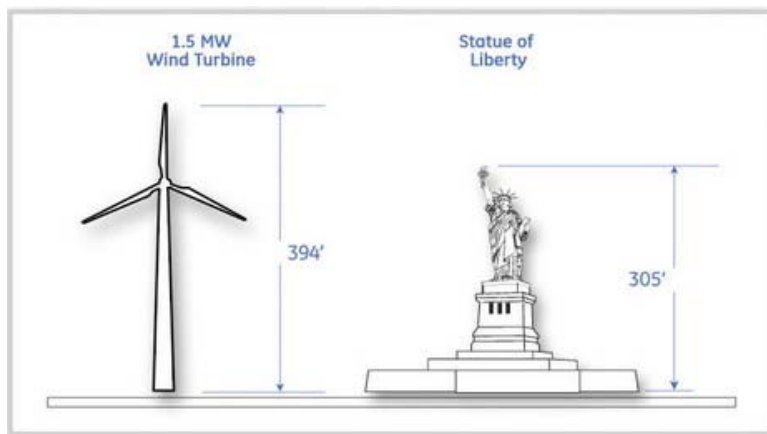


Figure 7: GE 1.5 MW Windmill Compared Against the Statue of Liberty
(Source: GE Energy)⁹

Today, the 1.5 MW windmill is the most common windmill on the U.S. market. In 2008, it accounted for over 50% of all windmills installed throughout the nation. This

is illustrated by Figure 8. By far, the largest provider of wind turbines in the U.S. was GE Energy, accounting for 47% of all wind turbines installed in 2008 (AWEA, 2009)¹.

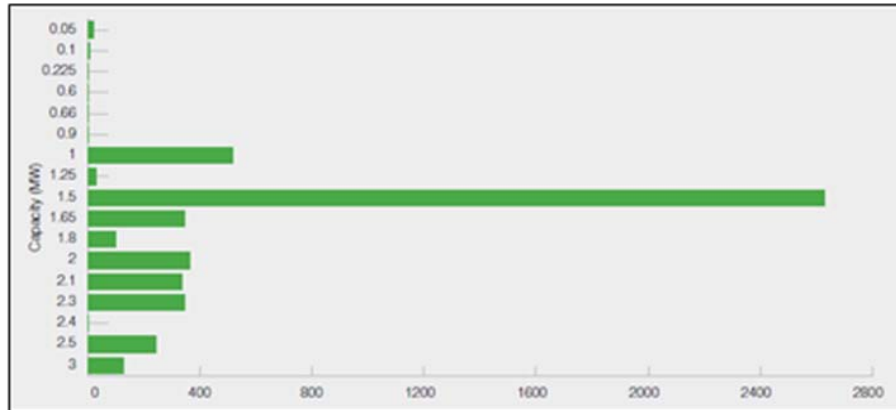


Figure 8: Distribution of Wind Turbines Installed in the U.S.
(Source: AWEA, 2009)¹

3.1 Growth in Wind Turbine Technology

The size of windmills has grown almost linearly for the last three decades. As more investment is made into research and development, every generation of windmills grows bigger, with larger rotors and a higher power capacity. Figure 9 illustrates how growth in the power capacity and rotor size of wind turbines has changed worldwide in the past 30 years and how it is predicted to change in the future.

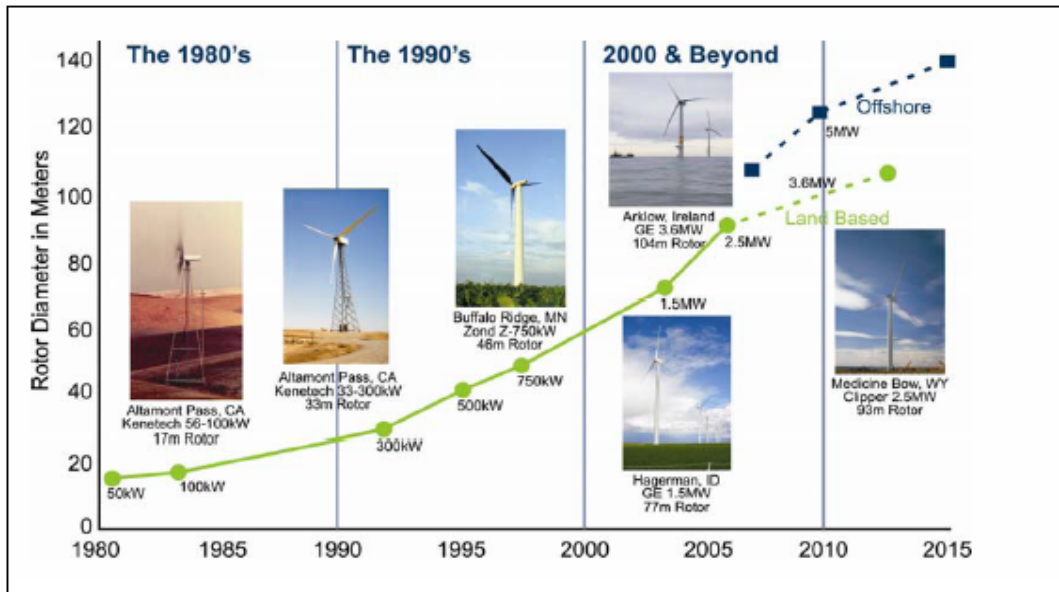


Figure 9: The Development Path and Growth of Wind Turbines
 (Source: U.S. DOE, 2008)⁴

From the figure, it can be seen that in 2004, the 1.5 MW windmill was on the cutting edge of technological development. Today, manufacturers such as Siemens and Vestas are working on developing wind turbines that are as large as 4.5-5.0 MW in size. There are several reasons for developing larger wind turbines. Larger turbines have the ability to capture more energy by accessing stronger winds at higher altitudes. The power availability found in wind is proportional to the cube of its speed. Therefore, having a wind turbine nestled on top of a taller tower will allow the windmill to generate more power. The size of the rotor blades also plays an important role. Larger rotor blades have a bigger sweep area and generate more lift from the passing wind, resulting in more energy captured by the wind turbine (US DOE, 2008)⁵. In summary, turbines placed at higher altitudes with larger swept areas produce more electricity at lower costs.

3.2 Limiting Factors in Wind Technology

The desire to improve energy capture makes it economically favorable to develop larger commercial windmills. Typically, the annual energy production from a wind turbine is

never as much as its name plate capacity rating. Wind does not always blow at the same rate, and therefore the productivity of turbines, at most wind sites is between 20-40% percent of its capacity rating. This is called a turbine's capacity factor. According to the U.S. Energy Information Administration, in 2008 an average home in the U.S. consumed about 30.6 kWh per day (*U.S. EIA, ND*)¹⁰. Therefore, a 1.0 MW windmill located at a site with a power capacity factor of 40 percent, could power approximately 313 homes, annually. A 2.0 MW windmill at the same site, could power twice as many homes while generating twice as much revenue for the developer, and only requiring a marginal portion of additional capital costs.

Some economists however, have argued that according to the square-cube law, the mass and cost associated with constructing larger wind turbines can eventually outgrow the energy output revenue, making super-large windmills economically unfavorable to develop (*US DOE, 2008*)⁵. The principle of the square-cub law states that:

“When an object undergoes a proportional increase in size, its new volume is proportional to the cube of the multiplier and its new surface area is proportional to the square of the multiplier.”-Wikipedia¹¹

Applying this principle to wind energy economics, it can be said that as the rotor of a wind turbine increases in size, the energy output will increase with the rotor's diameter by a square-factor, while the volume of material needed, and therefore the turbine's mass and cost, will increase with the rotor's diameter by a cube-factor (*US DOE, 2008*)⁵. Hence at one point, the cost of the turbine will outgrow its power revenue.

Although this is a possibility, wind engineers have been able to skirt the square-cube law by continuous innovation in design. By placing wind turbines at higher altitudes, engineers have been able to increase the capacity factors and improve the reliability of their units. Innovation in generator design has also reduced the size, weight and maintenance demands of wind turbines. For example, such recent models as the Siemens SWT-3.0 MW turbine and the Clipper 2.5 MW Liberty turbine have eliminated

the need for a gearbox by using rare-earth permanent magnets in their generators. This innovation significantly reduces the weight and size of the turbine, and according to Siemens, “eliminates the most complex part of the design” (*Siemens, 2010*)¹².

Rising costs in raw materials such as steel has also inspired research in stronger and lighter materials such as carbon fiber. For example, it was found that windmill blades made from carbon fiber can reduce the load carrying requirements for the entire structure, allowing other components such as the windmill tower to be designed using less steel, and hence allowing for overall savings in the design (*US DOE, 2008*)⁵.

CHAPTER 4. WINDMILL COMPONENTS

In the development of wind farms, transportation of windmill components from the manufacturing plant to the construction site is a critical step in the process. Without the right components, the wind farm cannot be built. Overall, a commercial windmill is constructed from four main components that have to be transported to the site:

- Nacelle Unit
- Rotor Hub
- Blades (3 per windmill)
- Tower (typically delivered in 2-5 pieces)

4.1 Nacelle Unit

The nacelle unit is the main part of the wind turbine. It encases the gearbox, the generator, the main control system, the yaw system and the main shaft. Within the nacelle unit, the rotor connects to the main shaft which spins a generator. The generator converts the mechanical energy from the rotor to a voltage which then drives an electrical current. Often times the nacelle unit also houses a gearbox which helps increase the speed of the shaft between the rotor hub and the generator, allowing for higher conversion rates. The yaw system is used to move the rotor system in alignment with the wind for optimum energy capture and the brakes are used to stop the rotation of the shaft in case of a power overload (*U.S.DOE, 2008*)⁵. Figure 10 presents a typical commercial windmill nacelle unit in operation today.

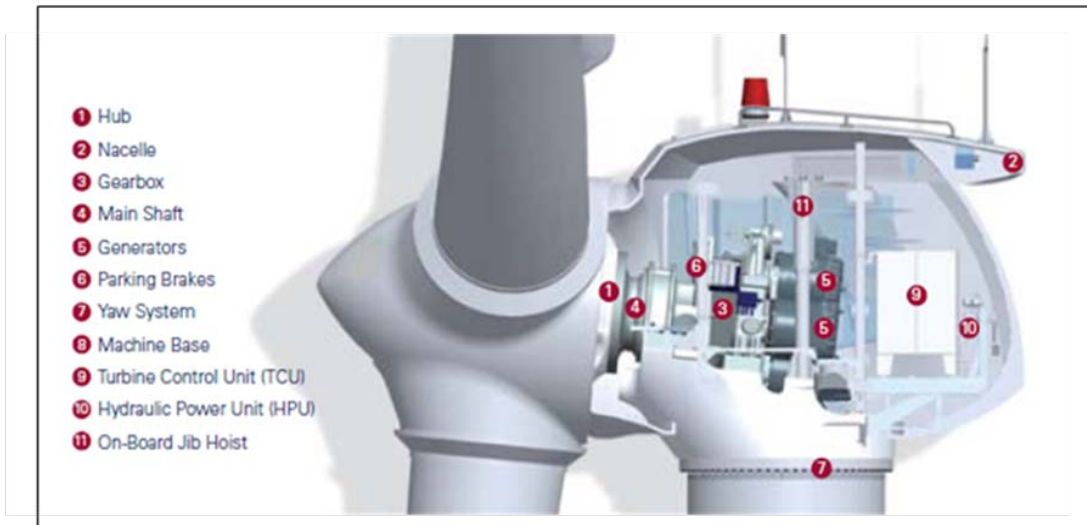


Figure 10: Standard Windmill Nacelle Unit
 (Source: *Clipper Liberty 2.5 MW Wind Turbine*)¹³

As the power capacity of windmills has increased, the size and weight of windmill components has also increased correspondingly. The weight of the nacelle unit, for instance, has increased in a linear fashion with respect to the windmill's power output. Figure 11 presents typical weights of nacelle units from five of the industry's leaders in wind turbine manufacturing.

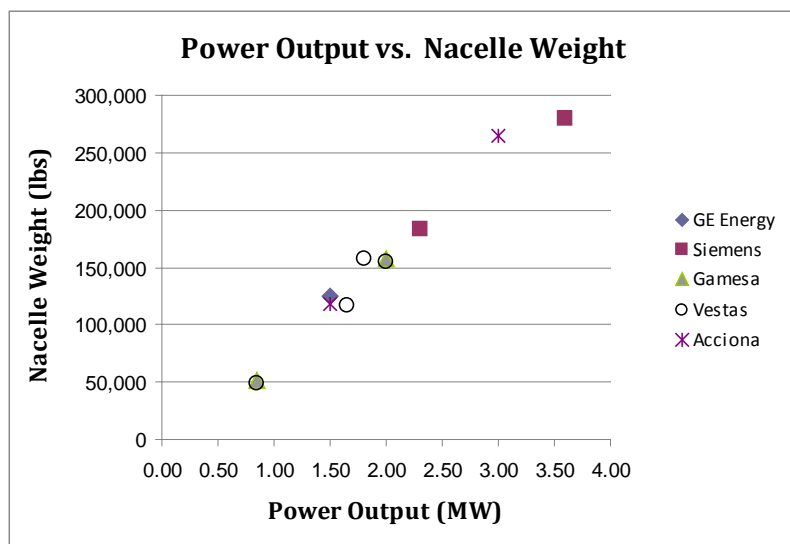


Figure 11: Nacelle Weight vs. Power Output
 (Source: *Acciona*¹⁶, *GE Energy*¹⁴, *Siemens*¹², *Gamesa*¹⁵, *Vestas*¹⁷ Product Brochures)

Using linear regression and fitting a line to the data, it can be shown that the weight of the nacelle increases by about 87,400 lbs for every 1.0 MW of power output in a linear fashion ($\beta_0 = -16662.98$, $\beta_1 = 87400.13$, $W_{nacelle} = -16,662.98 + 87,400.13 * P_{output}$).

The size dimensions of nacelle units can also be evaluated by evaluating various models on the market today. Although this information is less readily available, dimensions for 5 models made by three manufacturers are presented in Table 1 below.

Table 1: Length, Width, and Size Dimensions for Nacelle Units

Manufacturer	Vestas		Siemens	Acciona	
	1.8 MW	3.0 MW	3.0 MW	1.5 MW	3.0 MW
Length (ft)	34.12	45.93	22.31	41.01	57.41
Width (ft)	11.15	12.80	13.78	13.78	14.76
Height (ft)	13.12	12.80	13.78	13.12	13.12

4.2 Rotor Hub and Blades

The rotor system is the part of the assembly that captures the passing wind. It is composed of a rotor hub and a set of 3 blades. The blades are fit inside the hub which attaches to the main shaft, and a cover is placed over the entire assembly. Figure 12 illustrates an interior view of the rotor assembly with the hub in the center, and the three blades spanning out equidistantly from the sides.



Figure 12: Interior View of the Rotor Assembly

(Source: www.mywindpowersystem.com)

Similarly to the nacelle unit, the weight of the rotor assembly has also grown in proportion to the power capacity of the windmill. Figure 13 illustrates data on how the weight of rotors has grown from four of the industry's leading manufacturers.

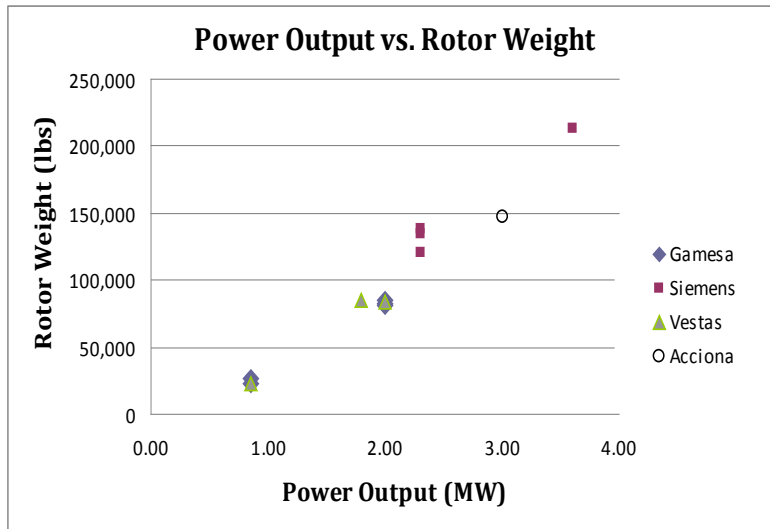


Figure 13: Rotor Assembly Weight vs. Power Output
 (Source: Gamesa¹⁵, Siemens¹², Vestas¹⁷, and Acciona¹⁶ Product Brochures)

The weight of the rotor and the windmill's power capacity are both related to the diameter of the rotor by the square-cube law, and hence cannot be expected to grow in a linear fashion. Figure 14 illustrates how the weight is influenced by the diameter of the rotor.

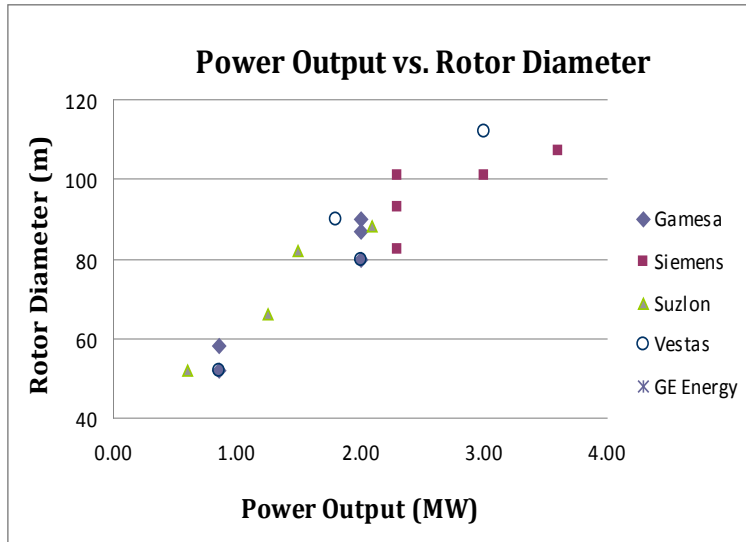


Figure 14: Rotor Diameter vs. Power Output

(Source: Gamesa¹⁵, Siemens¹², Suzlon¹⁹, Vestas¹⁸, and GE Energy¹⁴ Product Brochures)

The size dimensions for blades and rotor hubs can also be evaluated by comparing various models on the market today. Tables 2 presents data on the weight and size dimensions of blades and rotor hubs from Vestas and Acciona, two of the leaders in wind technology.

Table 2: Size and Weight Dimensions for Blades and Rotor Hubs from Vestas and Acciona

Component	Manufacturer	Vestas		Acciona
		1.8 MW	2.0 MW	3.0 MW
Hub	Height (ft)	13.78	13.78	14.76
	Diameter (ft)	10.83	10.83	13.12
	Weight (lbs)	40,320	40,320	80,640
Blade	Length (ft)	127.95	144.36	159.78
	Chord (ft)	11.48	11.48	-
	Weight (lbs)	14,560	15,008	23,296

As it can be seen from the table, the length of rotor blades can span up to 160 ft for a 3.0 MW windmill, however, data from the American Wind Energy Association specified that future 5.0 MW offshore wind turbines may have blades up to 200 ft in length (AWEA, 2010)⁷. Meanwhile rotor hubs weigh between 40,000-80,000 lbs.

4.3 Windmill Towers

The windmill tower is the last piece of the assembly. It provides support to the rotor and the nacelle, and lifts the assembly to higher elevation where the blades can safely clear the ground. Modern commercial windmills are typically tapered tubular steel towers that range anywhere from 44 to 100 meters (144-328 ft) in height and have diameters which range from 4.5 to 5.4 meters (14.76-17.72 ft) at the base. The diameter of the tower is an important parameter as it spreads the load of the nacelle and the rotor over a larger surface area, requiring less material for construction. However, towers with diameters greater than 14 ft may require special transportation needs as will be discussed in the next chapter (U.S. DOE, 2008)⁵.

Modern day commercial windmill towers are hollow on the inside and may provide enough space for a service lift, a power cabin, and a lighting and ventilation system for maintenance activities. They are typically delivered on site in 2 to 5 sections depending on the tower's dimensions and weight. Figure 15 illustrates an example of a tower's internal configuration.



Figure 15: Typical Windmill Tower
(Source: Vestas V821-65 1.65 MW Product Brochure)¹⁸

Just as with the other windmill components, towers have grown in weight and size over the past decade. The desire for higher energy output at more consistent rates has driven engineers to place turbines at higher elevations, requiring significantly higher and heavier tower sections to support the structural load. Figure 16 illustrates industry data on how the weight of the windmill tower has increased consistently with its height.

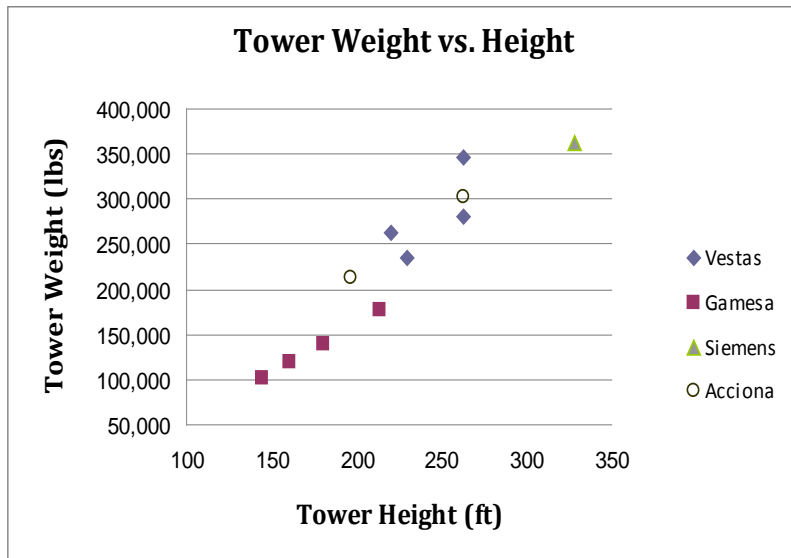


Figure 16: Weight of Windmill Towers based on Height
(Source: Vestas¹⁷, Gamesa¹⁵, Siemens¹², and Acciona¹⁶ Product Brochures)

From the figure it can be seen that, in general, the weight of the windmill tower grows linearly with tower height. However, the innovation in windmill technology that was discussed in the previous chapter is also evident from this figure. Vestas Inc. for example, were able to cut the weight of their 80 m (262 ft) tower by nearly 67,000 lbs through innovation and technology. As the wind industry grows around the world, such innovations will be more common place as engineers attempt to reduce costs by cutting the amount of materials necessary for construction.

CHAPTER 5. TRANSPORTATION OF WINDMILL COMPONENTS

As it was shown in the previous chapter, windmill components are large and massive pieces of equipment and, therefore, require special transportation accommodations. Windmill components are transported by three modes: truck, rail, and barge. Out of these three, truck transportation is currently the most pragmatic mode of choice, however all three modes have their own advantages and disadvantages (AWEA, ND)²⁰. These are presented in Table 3 below.

Table 3: Advantages and Disadvantages for each Transportation Mode Choice

Mode of Transportation	Advantages	Disadvantages
Truck	<ul style="list-style-type: none"> ● Short and long-range transport ● Flexibility of schedule ● Direct Access to Construction Site ● Shipment of Individual Parts 	<ul style="list-style-type: none"> ● Oversized/overweight routing regulations ● Increased transportation costs
Rail	<ul style="list-style-type: none"> ● Economical for long-range transport ● Economical for transport in bulk quantities 	<ul style="list-style-type: none"> ● Oversized/overweight routing regulations ● Retrofitting of rail carts ● Limited access to final site
Barge	<ul style="list-style-type: none"> ● Economical for long-range transport ● Economical for transport in bulk quantities ● No oversized/overweight routing regulations 	<ul style="list-style-type: none"> ● Limited to <i>no</i> site access to final destination

From the table it can be seen that both truck transport and rail can provide reliable ground services to the wind industry. One advantage of rail transport is its ability to move components in mass quantity. A case study conducted by BNSF railway has shown that 6 rotor hubs or 2 nacelle units can be transported on one railroad cart without any specific modifications. Meanwhile, BNSF railway has also demonstrated its ability to transport 60 wind blades on one of its mile long unit trains after retrofitting the carts to hold the components (BNSF, 2010)²¹.

In retrospect, truck transportation requires a tractor-trailer combination for the movement of each individual windmill component along with two extra escort vehicles to accompany the oversized/overweight vehicle on its route. To move a single windmill would require 7-10 oversized/overweight vehicles along with 14-20 escort vehicles. Moving windmill components by truck can sometimes raise the costs of the turbine by 15-25% (*AWEA, ND*)²⁰. In a case study conducted by BNSF, it was shown that the manufacturer saved as much as \$1 million in transportation costs by moving windmill components for 30 new windmills by rail from Corpus Christi, TX to Glenrock, WY (*BNSF, 2010*)²¹. Hence, having the ability to move large pieces of equipment in bulk can drastically reduce transportation costs.

One advantage that truck transport holds over rail is its direct access to the final wind farm site. Since most wind development projects are located in remote rural locations, often times they are only accessible by roads. Therefore, even if the components were to be shipped using rail or barge, a leg of the journey would still have to be made by truck. Point-to-point delivery is one of the main reasons why truck transport, although it may cost more for bulk deliveries, is still the more pragmatic mode of choice.

Recent trends in the railroad industry however, have shown that rail transport is starting to play a larger role in the transportation logistics of windmill components. BNSF railway, for example has invested in a number of wind transload sites throughout its railway network, which allows them to ship and unload components 150-200 miles away from most wind development locations in the country. A map of these transload centers is illustrated in Figure 17 below.

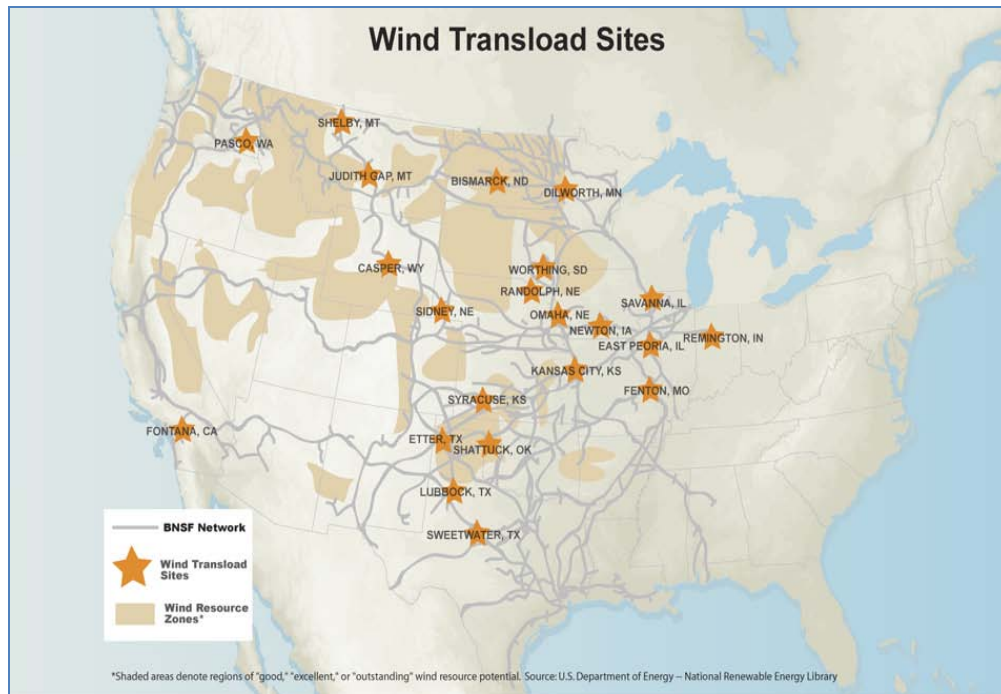


Figure 17: Wind Transload Centers on BNSF Railway Network
*(Source: BNSF Railway, 2010)*²²

Meanwhile, Union Pacific is in the process of making similar investments in the wind industry. Figure 18 illustrates the location of UP’s wind transload centers, marking current sites with blue stars and future pre-qualified distribution centers with yellow stars.

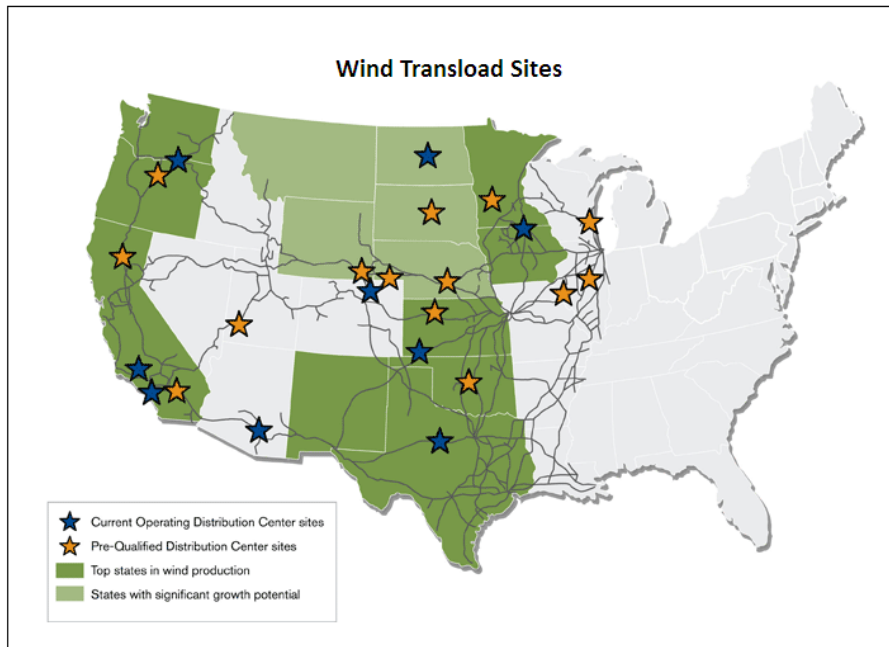


Figure 18: Wind Transload Centers on Union Pacific Network
 (Source: Union Pacific Railway, ND)²³

Transportation of windmill components, both by rail and truck requires special routing for several reasons. Often times the right-of-way for both modes is limited and, therefore, it is important that vertical clearances at bridge underpasses and horizontal clearances on sharp turns are not violated. Also, weight tolerances on certain bridges cannot be exceeded due to the danger of structural collapse (*TxDOT, ND*)²⁴. Since many windmill components are oversized and overweight, special care must be paid to the way they are routed along the rail and roadway network.

To ensure that certain dimensional limits and weight tolerances are not exceeded, state transportation agencies and railroad companies have created practical legal limits for their transportation networks. These limits ensure that all cargo meets a certain length, width, height, and weight requirement. Otherwise, the carrier is forced to apply for a special routing permit which limits them to stay on only those routes that can sustain the oversize and overweight load. Table 4 illustrates legal limits placed on trucks from

two state transportation agencies and, likewise, Table 5 illustrates legal limits placed on cargo traveling on the BNSF, Union Pacific, and the CSX railway lines.

Table 4: Maximum Permitted Legal Length, Width, Height, and Weight Limits for Trucks

Maximum Permitted Limits	Texas	California
Length (Truck + Trailer Combination)	65'	65'
Width	102" (8' 6")	102" (8' 6")
Height	14'	14'
Weight (lbs)	80,000	80,000

(Source: TxDOT²⁴, CalTrans²⁵)

Table 5: Max. Permitted Length, Width, Height, and Weight Limits for Cargo on Trains

Maximum Permitted Limits	CSX	Union Pacific	BNSF
Length (Cargo)	60'	No Overhang	89'
Width (Cargo)	11'	11'	11'
Height*	11' (Cargo)	17' above top of rail	17' above top of rail
Weight (Cargo)	150,000 lbs	220,000 lbs	Varies based on location

(Source: CSX²⁷, BNSF²², Union Pacific²⁶ Railroads)

From the two tables, it can be seen that the dimensional limits for rail transports are less restrictive than those for trucks. This may be due to the reason that rail corridors were mainly designed for the movement of cargo and, therefore, design specifications for weight tolerances on bridges, along with vertical and horizontal clearance distances at geometrically confining areas are not as constraining as they are on the roadway network. Also, since rail traffic travels on designated guide-ways, there is a lower probability that the train will interact with other vehicles such as passenger cars and, therefore, safety is less of a concern.

From the previous chapter it was seen that windmill components are often times oversized and overweight. The base section of a tower for example, can have a diameter of 5.4 meters (17.7 ft) and weigh up to 150,000 lbs. Meanwhile, nacelle units can range from 50,000 to 280,000 lbs in weight and have heights and widths of up to 14 ft. Windmill blades typically span over 100 ft in length. Therefore, most windmill

components would not meet the legal load dimensions and would require special route permitting from both transportation agencies and railway companies.

The primary advantage that truck transportation holds over rail is the vastness of the U.S. roadway network. During the case study conducted by BNSF, it was evident that the U.S. railroad network is not nearly as extensive as the roadway network. For example, in the transportation of windmill components from Corpus Christi, TX, to Glenrock, WY, BNSF could not move all of the components on its network alone, and had to rely on the CSX network to reroute some of their trains. Development of wind farms is a time sensitive issue, and project costs due to transportation delays can offset the benefits of the project. Although truck transportation may cost more in the long run, the reliability of timely delivery still makes it the preferred mode of choice.

The last mode of choice that was presented in Table 3 was transportation via river barge. This mode of transportation would be the ideal because barge transports have the ability to transport components in large quantities without imposing any dimensional limits on the cargo. However, barge transport relies on waterways which typically have *no* or *very limited* access to the final project site. Finally, storage space at ports and crane capacity to load and unload the cargo is seen as a major constraint (AWEA, ND)²⁰.

CHAPTER 6. THE TRUCK TRANSPORT INDUSTRY

The growth in the U.S. wind industry has provided the trucking industry with challenges and opportunities to capitalize on the current market. As windmill components have grown in weight and size to reflect the desire for higher powered turbines, trucking companies have come up with various solutions to transport these components. Currently the trucking industry is dominated by two types of tractors and four types of trailers that are used routinely for moving windmill components. The tractor vehicles can be split into two classes:

- Standard tractor vehicle (single steering axle and one tandem back axle).
- Non-standard tractor vehicle (single steering axle and a non-tandem combination back axle).

Trailers can be divided into four main categories:

- Extended Lowboy (Double-Drop Deck) Trailer
- Dolly + Deck + Jeep Trailer System
- Dolly+ Schnabel-neck Trailer System
- Specialized Long Stretch Trailer

Since each windmill component serves a specific function and has specific dimensions, a variety of trailers are used for the haul. For example, windmill blades are too long to fit on a regular flatbed trailer, hence, they require a specialized long stretch trailer for the haul. Meanwhile, the weight of the nacelle unit requires a specialized Jeep + Dolly combination trailer to properly distribute the load over the entire axle spectra. Table 6 presents common practices in the trucking industry for matching specific windmill components with various types of trailers used for the haul.

Table 6: Types of Trailers Used for Hauling Windmill Components

Rotor Hub	<ul style="list-style-type: none"> ▪ Lowboy Trailer
Rotor Blade	<ul style="list-style-type: none"> ▪ Long Stretch Trailer
Nacelle Unit	<ul style="list-style-type: none"> ▪ Lowboy Trailer ▪ Dolly/Deck/Jeep Trailer
Tower Sections	<ul style="list-style-type: none"> ▪ Lowboy Trailer ▪ Dolly Trailer ▪ Schnabel/Dolly Trailer ▪ Double (Full) Schnabel Trailer

From Table 6, it can be seen that the lowboy (double-drop) trailer can be used for hauling rotor hubs, nacelle units, and some tower sections. A lowboy trailer is a simple standard flatbed trailer that is double dropped from its original height of 60” to a height of 24” above the ground. This 36” drop allows the trailer to carry many components which would not otherwise pass legal dimensional limits imposed by the federal and state transportation agencies. The average load carrying capacity of a lowboy can range from 25-42 metric tons (56,000-95,000 lbs) so it is limited to carrying smaller sized nacelle units and only some tower sections. The lowboy trailer is mostly employed for hauling rotor hubs, since most hubs in the industry weigh around 40,000 lbs and are small enough to fit on the deck of the trailer. Figure 19 presents the dimensions for a typical drop-down trailer when compared to a standard flatbed used in the industry today.

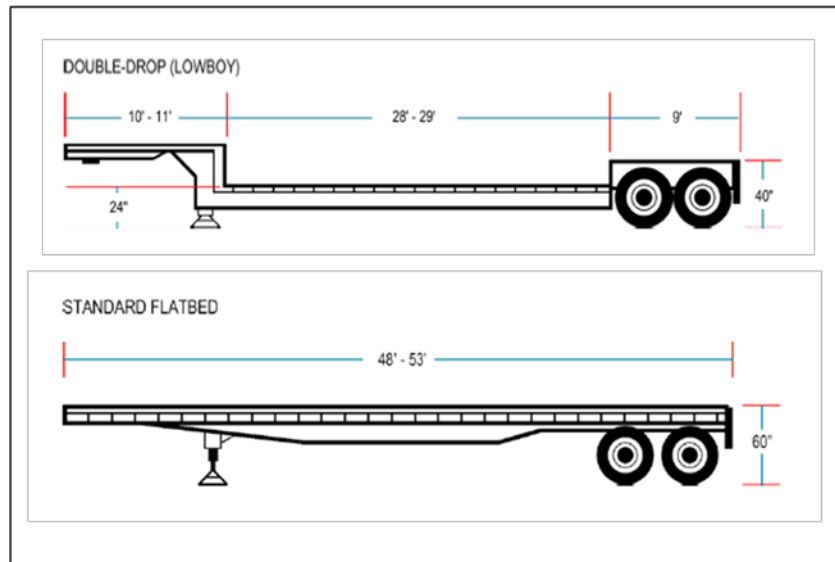


Figure 19: Double-Drop (Lowboy) Trailer Compared with Standard Flatbed Trailer

(Source: *BLM Deck Division, Inc*)²⁸

Rotor blades are typically transported using a specialized long stretch trailer. These types of trailers are typically 53 ft in length and can be extended up to 150 ft in length to accommodate the length of the blade. Often times they are equipped with a steerable back axle for easier navigation of turns. The back axle typically consists of a tandem, tridem, or quad combination axle group (*IST Trailers, ND*)³⁰. Figure 20 illustrates a specialized stretch trailer manufactured by Peerless Limited for the movement of windmill blades.

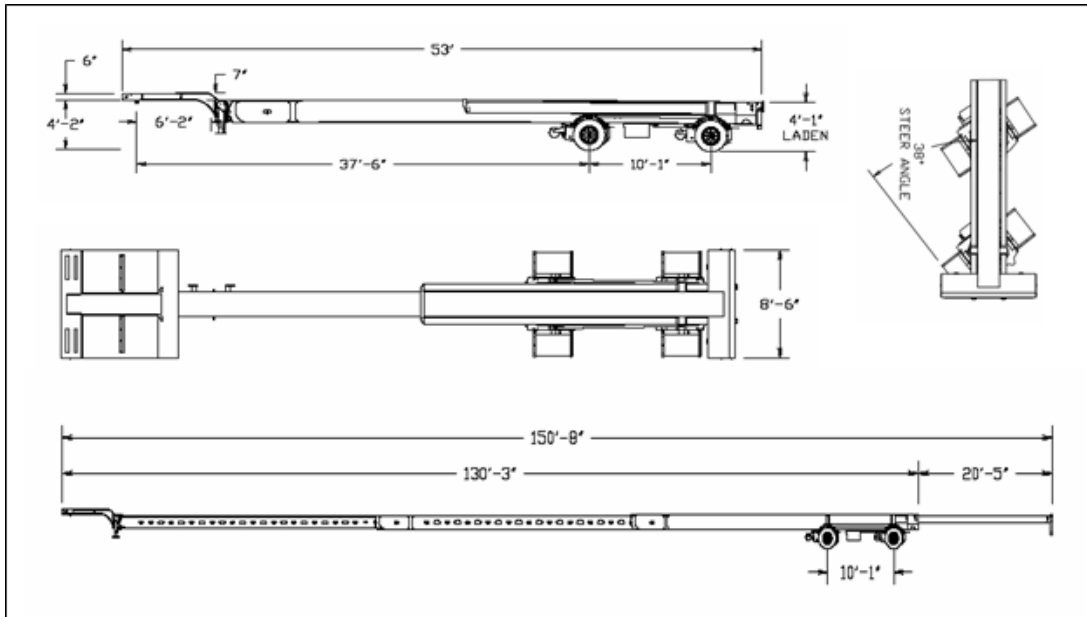


Figure 20: Tandem Axle 30 Ton Blade Trailer by Peerless Limited
 (Source: Peerless Limited)²⁹

The nacelle unit is typically transported using a jeep and dolly combination trailer. The jeep section is often times a tridem-axle suspension system that weighs from 10,000-12,000 lbs and attaches directly to the tractor. The dolly system complements the back of the trailer and can have various types of suspensions. The most common dolly system employs either a tridem-axle suspension or a dual tridem-axle suspension and can weigh from 9,000-25,000 lbs (*IST Trailers, ND*)³⁰. Figure 21 illustrates an example of a 13-axle tractor-trailer combination vehicle with a jeep and dolly system that is most commonly used for moving nacelle units today. This particular type of trailer is capable of carrying a load of 85 tons (or 190,400 lbs).

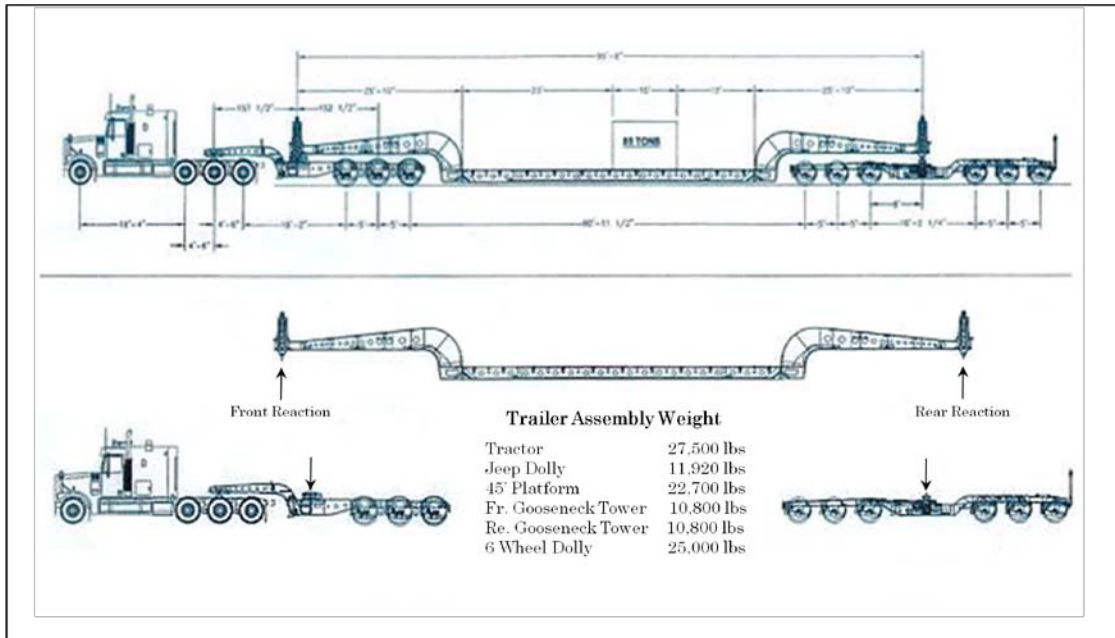


Figure 21: 13-Axle Trailer Assembly by International Specialized Trailer Mfg., LLC
*(Source: IST Trailers)*³⁰

Schnabel-neck systems are most commonly used for carrying tower sections. A Schnabel-neck is a C-shaped steel structure that attaches to a Jeep dolly or a tractor vehicle and is equipped with a hook-in system to connect to the loaded tower. A Schnabel neck is typically accompanied by a dolly system at the rear of the trailer on which the back end of the tower section rides. There are mainly two types of Schnabel trailers employed by the wind industry:

- Double (Full) Schnabel Trailer
- Half Schnabel Trailer

The differences between the two configurations are illustrated in Figures 22 and 23.

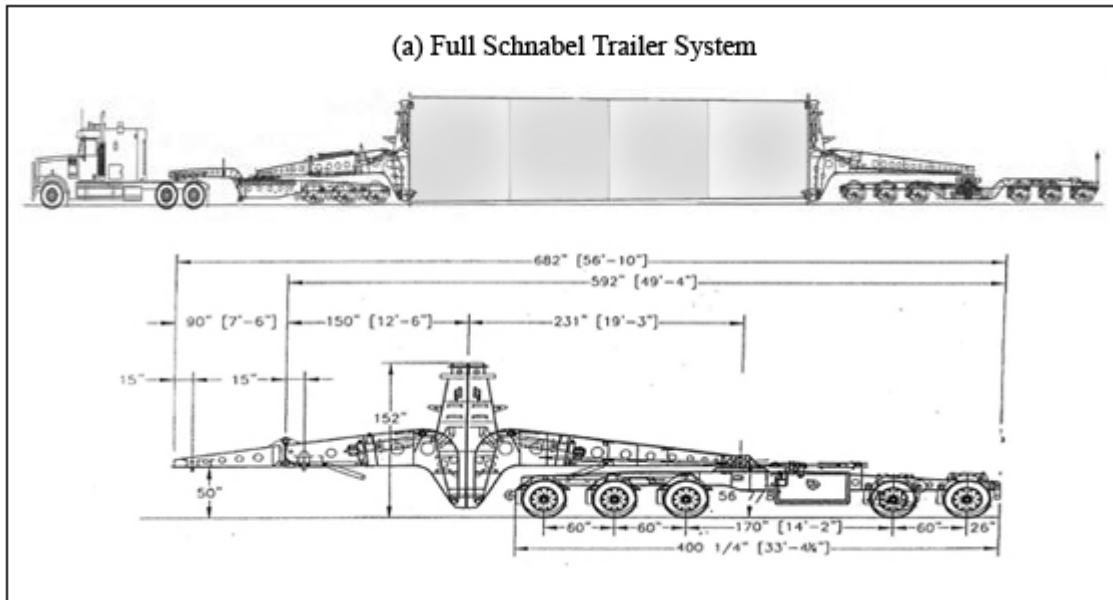


Figure 22: Full Schnabel Trailer System
(Source: IST Trailers)³⁰

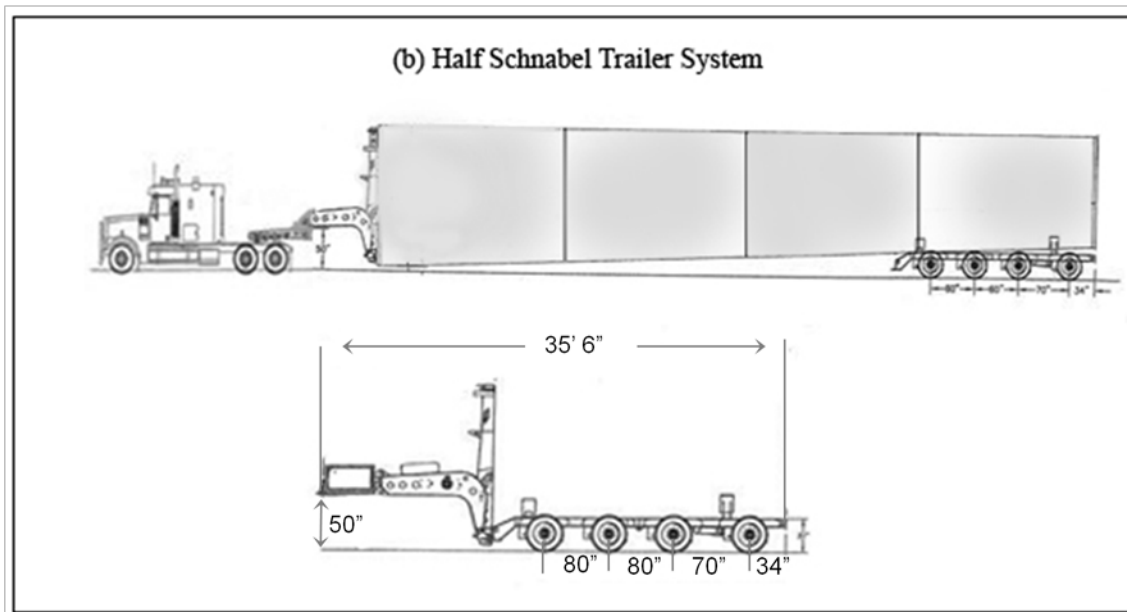


Figure 23: Half Schnabel Trailer System
(Source: IST Trailers)³⁰

Full Schnabel trailers are typically employed for moving base and mid tower section of the windmill assembly, as these sections are bigger and require grips on both

sides of the tower. Meanwhile half-Schnabel trailers are employed for moving lighter mid-tower sections and top tower sections of the windmill assembly.

CHAPTER 7. THE WIND TRANSPORT VEHICLE FLEET

To understand the impacts of hauling oversized and overweight windmill components on the pavement infrastructure, it is first important to disaggregate the transport vehicle fleet and identify certain characteristics specific to each vehicle class. From the previous chapter it was seen that generally there were two types of tractors and four types of trailers employed for moving windmill components. However, each type of tractor-trailer combination will have its variability in size, weight, number of axles, axle load spectra, and axle spacing dimensions to accommodate the component being transported. While the previous chapter presented generalities on the transport vehicle fleet, this chapter aims at further disaggregating the fleet by examining real data.

The data used for the task were obtained from oversize/overweight permits data collected by the Texas Department of Transportation (TxDOT) for the years of 2007-2009. That dataset was queried for permit records associated with the wind industry, and overall, it was found that there were 47,490 permits issued to the wind industry in the last three years. Each record in the dataset contains 103 fields of information about the vehicle, route, and cargo being transported. Some of this information is presented in Table 7 below.

Table 7: Field Entries in the Oversized/Overweight Database

Field No.	Field Description	Field No.	Field Description
1	Permit Number	21	Gross Vehicle Weight
2	Load Description	25-29	Route Information
6-7	Width	30-53	Axle Spacing
9-10	Height	54-78	Reported Weight On Axle
12-13	Length	79-103	Number of Tires per Axle

The data from Table 7 were used to conduct an analysis to determine the impacts of heavy windmill traffic on the pavement infrastructure. Field 2, which provided information on the load description, was used to classify the vehicle fleet by windmill component. Fields that provided information on the width, height, and length of the vehicle were used to develop dimensions specific to each class within the vehicle fleet.

Route information was used to determine which facilities were impacted the most by the movement of windmill components. And finally, gross vehicle weight (GVW) data along with reported weight on axles and the number of tires per axle were used to create an axle load spectra for each vehicle class. This information was then input into the Mechanistic-Empirical Pavement Design Guide (MEPDG) to calculate pavement rutting. Chapter 1 discussed the steps and methodology used for estimating pavement impacts. The objective of this chapter is to disaggregate the vehicle fleet by windmill component and to discuss the dimensions of each vehicle class along with their respective axle loading spectra.

7.1 Limitations of the Oversize/Overweight (OS/OW) Permit Dataset

Overall, there were 47,490 wind related route entries in the oversize/overweight permit dataset obtained from TxDOT. The route entries were first grouped by the components being hauled. Table 8 presents information on the number of records found for each component. It should be noted that about 6.5 percent of records in the dataset included permits for other windmill components such as casting molds, tower flanges, crane equipment, service lift systems, and other maintenance components. For the most part, however, components for the construction of the windmill itself were hauled.

Table 8: Number of Records found for each component in the OS/OW Dataset

Windmill Component	No. Records	Percentage
Rotor Hubs	4,066	8.56%
Windmill Blades	15,854	33.38%
Nacelle Units	3,629	7.64%
Tower Sections	20,835	43.87%
Other	3,106	6.54%

In the OS/OW dataset, not all entries had the full information necessary to carry out the analysis for grouping and classifying the vehicle fleet. For example, if the vehicle was under the maximum legal load limit, then information on the vehicle's axle spacing and the reported weight on each axle was not available. This posed a concern for

disaggregating the vehicle fleet employed in carrying windmill blades and rotor hubs. As most blades and rotor hubs are light enough to meet the maximum legal load limit, information on the vehicle fleet's axle spacing and load spectra was limited. Therefore, with the information gathered for this report, three assumptions were made and maintained throughout the analysis process: 1) extended lowboy trailers were used for moving rotor hubs, 2) specialized long stretch trailers were used for moving windmill blades, and 3) the maximum gross vehicle weight for both tractor-trailer combinations was 80,000 pounds.

It is also worth mentioning that the dataset collects information on the *reported* axle load spectra and *not* on the actual axle load spectra itself. The reported axle load spectra is the information that the transportation company provides to the state transportation agency in the permitting process and, to some degree, it may not be completely representative of the actual data. Information on the actual load spectra would have to be obtained from WIM stations. However, since this information was unavailable at the time of writing this thesis, the reported axle load spectra was used to carry out the impact analysis. Based on the information available in the OS/OW dataset, the following sections outline the characteristics of each vehicle fleet.

7.2 Nacelle Transport Vehicle Fleet

Information on the nacelle transport vehicle fleet was gathered from 3,629 records found in the OS/OW dataset obtained from TxDOT. Out of these, there were 261 incomplete records, which left 3,368 records with information on the vehicles' axle spacing and their reported axle load spectra. Information on the GVW of the fleet was first analyzed.

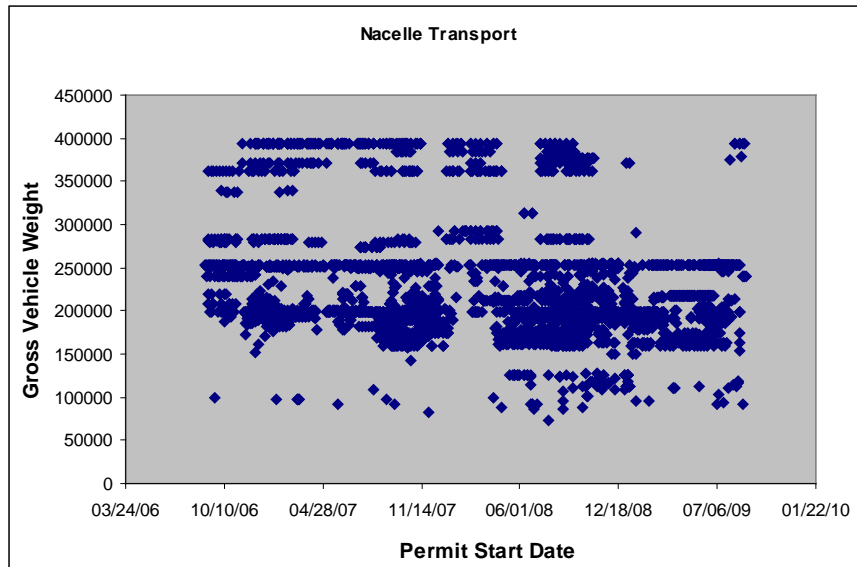


Figure 24: GVW of Transport Vehicle Involved in Moving Nacelles

From the data in Figure 24, it was seen that the GVW of nacelle transports ranged from 80,000- 400,000 lbs. over the 3-year observation period. This implies that the range of nacelles being installed in Texas also varied quite significantly. The vehicle fleet was further analyzed by the distribution of the first four axle spacings for the tractor-trailer vehicle combinations.

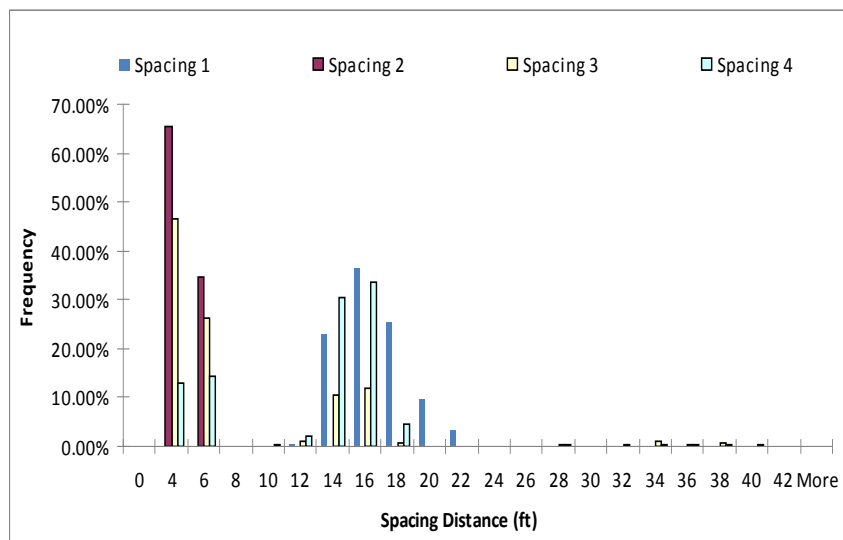


Figure 25: Vehicle Axle Spacing for Nacelle Transports

In general, axles can be split into two categories (Prozzi and Hong, 2006)³¹:

- Single axles: axles spaced more than 96 inches (8 ft.) apart (includes all steering axles).
- Combination axles: axles spaced between 40-96 inches (3.33-8 ft) apart (includes tandem, tridem, quad, and higher level combination axles).

From the peaks in Figure 25, it can be seen that all tractor vehicles had one steering axle and at least one tandem rear axle. From the first two peaks of *Spacing 3*, it can be seen that a significant portion of tractor vehicles had a tridem rear axle. In general, the vehicle fleet employed two types of tractor vehicles:

- Standard tractor (single steering axle and a tandem rear axle)
- Non-standard tractor (single steering axle and a tridem rear axle)

Out of these, the non-standard tractor vehicle was used for 72.6% of the hauls. Applying the Wilcoxon rank-sum test, which compares the means of two independent continuous populations to determine if both populations belong to the same distribution (Montgomery & Runger, 2007)³¹, it was determined that the standard and non-standard tractors came from two different populations of fleets and, therefore, were not used for moving the same types of load. ***Standard tractor vehicles were used for moving nacelles that were significantly lighter with a smaller maximum power output***, while non-standard tractors were reserved for larger, heavier nacelles with higher power output. The application and results of the Wilcoxon rank-sum test can be found in Appendix A. Figure 26 shows how the distribution of gross vehicle weights differed for the two tractor fleets.

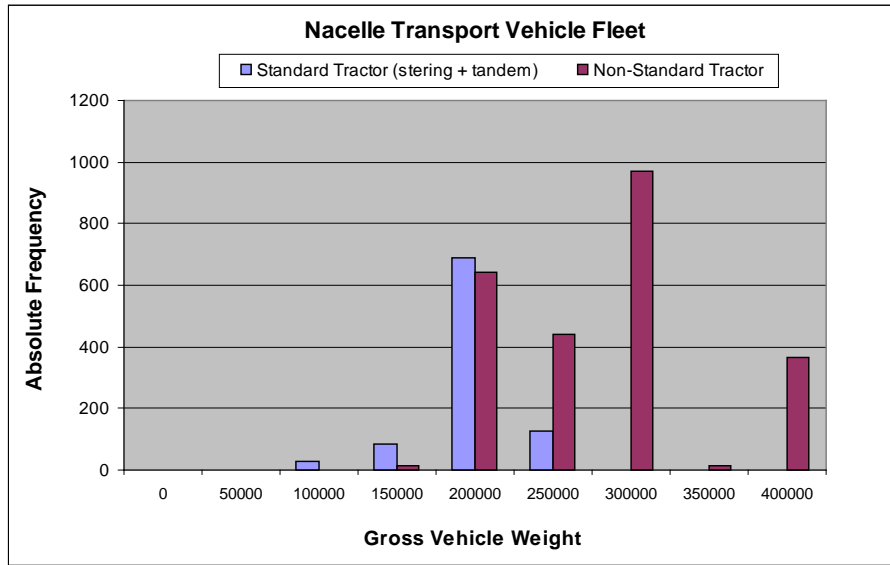


Figure 26: GVW for Standard and Non-Standard Vehicles

From the figure, it can be seen that there is a significant amount of overlap between the two types of tractors. Standard tractors, however, tend to have a much more limited range of GVWs and hence the cargo that they carry. Using the two distributions, a proportion statistic was determined for hauling weights over 250,000 lbs., as it signifies a shift from overweight vehicles to super-heavy vehicles. In accordance with TxDOT’s Permitting Division, a vehicle is considered to be super-heavy when it:

“...exceeds 254,300 pounds (total gross weight), or exceeds the maximum permissible weight on any axle or axle group, or exceeds 200,000 pounds with less than 95 feet of axle spacing-” TxDOT²³

From the sample size attained for this study, it was seen that **93.41% of all super-heavy vehicles relied on non-standard tractors** for hauling nacelle units.

The trailer fleet was analyzed by studying axle-spacing histogram data. In general, it was found that standard tractor vehicles most commonly employed 6-axle and 7-axle trailers for moving nacelle units. Meanwhile, non-standard tractor vehicles most commonly employ 7-axle, 9-axle, and 15-axle trailers. Figure 27 presents the distribution

for the number of trailer-axles for standard and non-standard tractor vehicles. Similarly, the breakdown of total and relative percentages is also illustrated in Table 9.

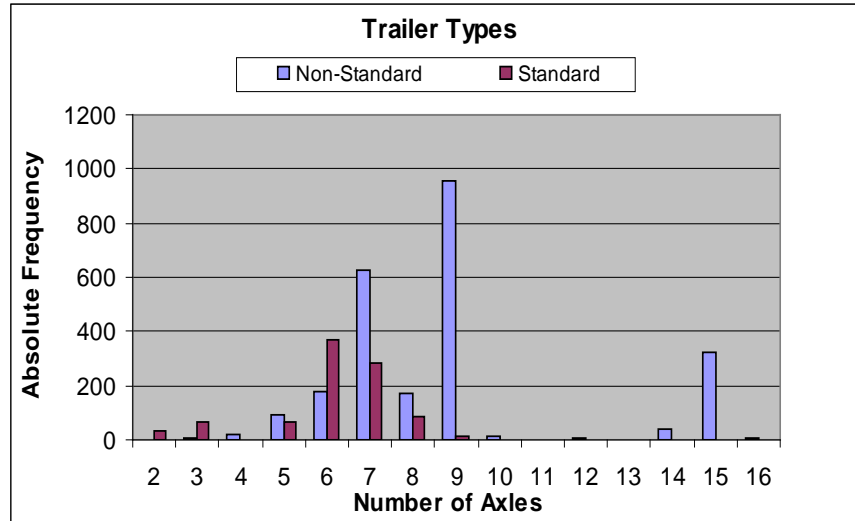


Figure 27: Number of Axles on Trailer for Standard and Non-Standard Tractors

Table 9: Trailer types used for hauling Nacelle Units

Trailer Axles	Standard (tractor)		Non-Standard (tractor)		Total	
	Count	Percentage	Count	Percentages	Count	Percentage
2	36	1.1%	2	0.1%	38	1.1%
3	66	2.0%	8	0.2%	74	2.2%
4	1	0.0%	21	0.6%	22	0.7%
5	65	1.9%	91	2.7%	156	4.6%
6	372	11.0%	179	5.3%	551	16.4%
7	281	8.3%	625	18.6%	906	26.9%
8	89	2.6%	171	5.1%	260	7.7%
9	14	0.4%	957	28.4%	971	28.8%
10	0	0.0%	13	0.4%	13	0.4%
11	0	0.0%	0	0.0%	0	0.0%
12	0	0.0%	4	0.1%	4	0.1%
13	0	0.0%	0	0.0%	0	0.0%
14	0	0.0%	39	1.2%	39	1.2%
15	0	0.0%	326	9.7%	326	9.7%
16	0	0.0%	8	0.2%	8	0.2%
Σ	924		2444		3368	

Based on the information gathered from this section, Figures 25, 26, 27, 28, and 29 present the length, width, and height dimensions for the five most common combination-vehicles listed above. Likewise, the reported axle load spectra, along with axle spacing, and the number of tires per each axle are also presented in these figures. Some summary statistics for the entire nacelle carrying vehicle fleet are presented below:

- Transport vehicle widths with cargo vary from 8 ft. 10 in. to 18 ft. 11 in.
- The majority of vehicles (90.7%) do not meet the TxDOT legal height limit of 14 ft.
- A high proportion of transport vehicles (35.0%) do not meet the TxDOT legal permitted length limit of 125 ft.
- A significant proportion of transport vehicles (9.7%) do not meet the TxDOT legal overall length limit of 180 ft.

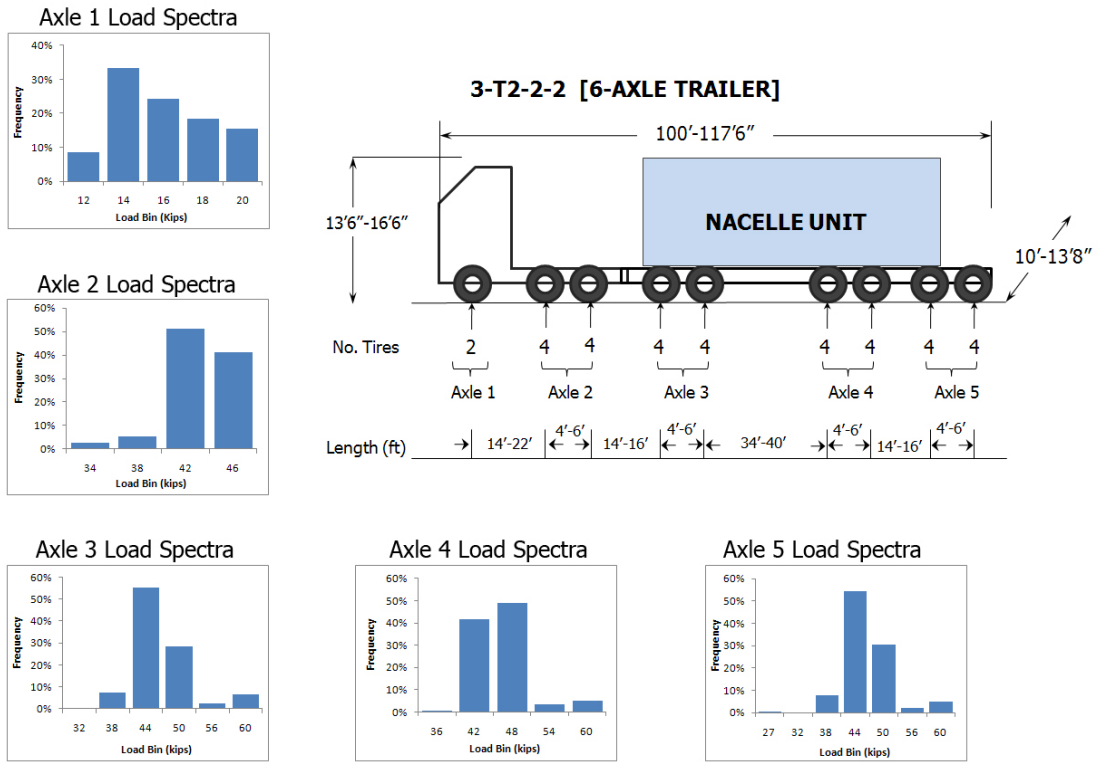


Figure 28: Standard Tractor + 6-Axle Trailer

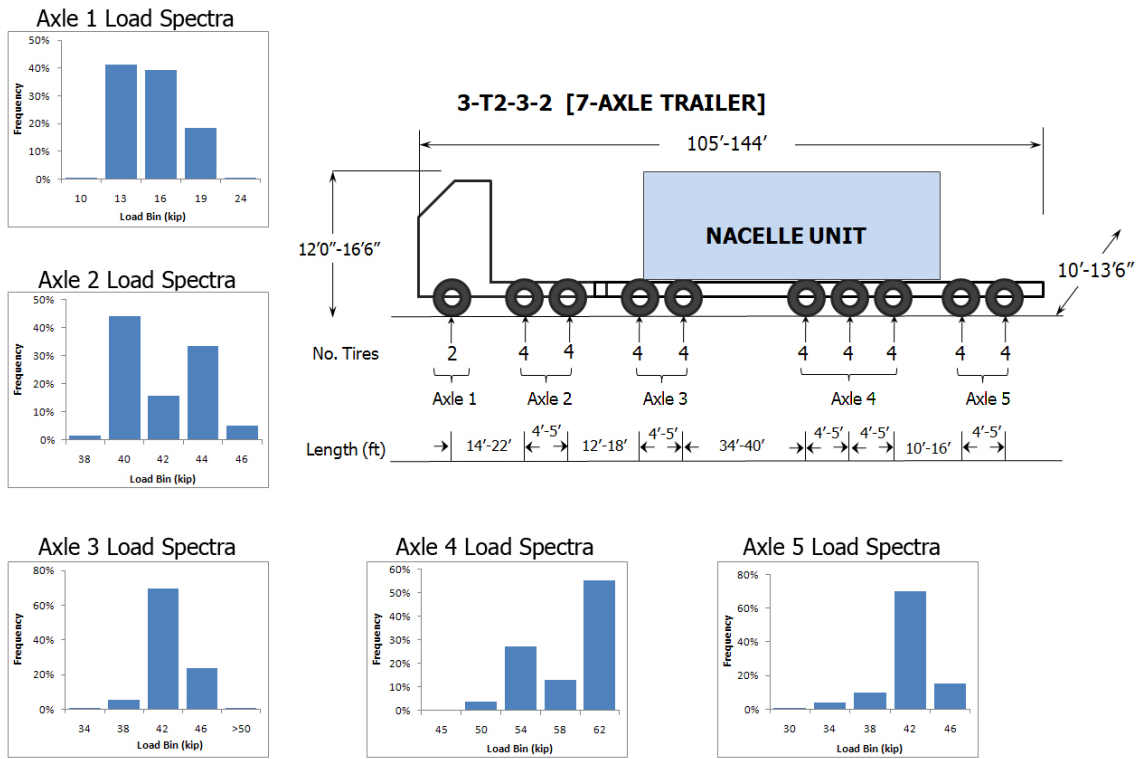


Figure 29: Standard Tractor + 7-Axle Trailer

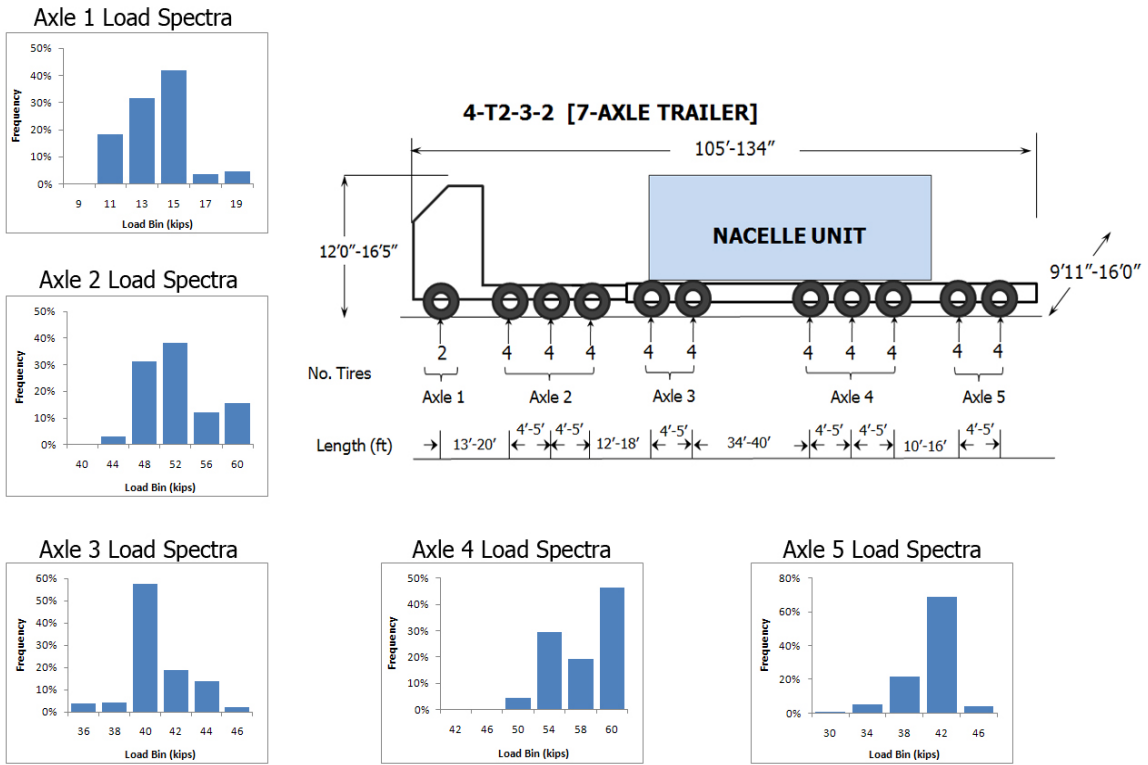


Figure 30: Non-Standard Tractor + 7-Axle Trailer

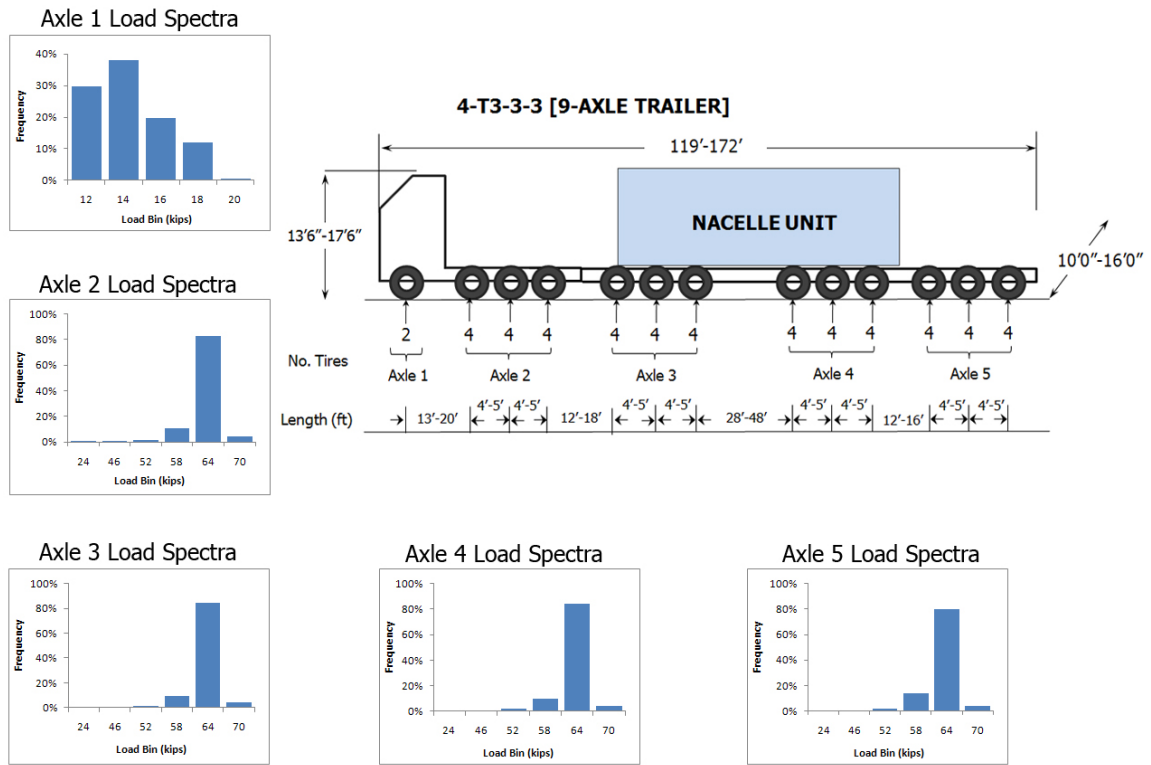


Figure 31: Non-Standard Tractor + 9-Axle Trailer

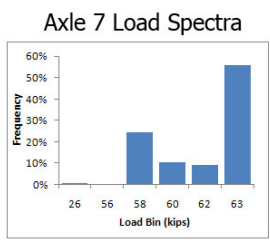
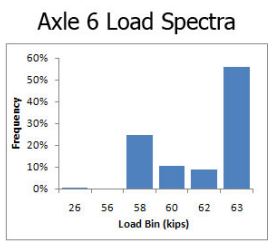
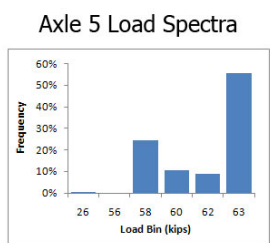
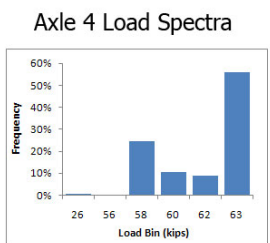
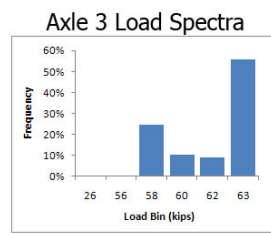
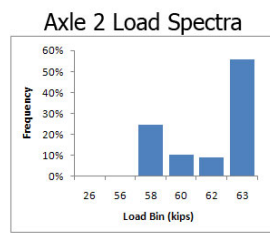
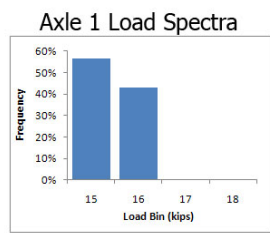
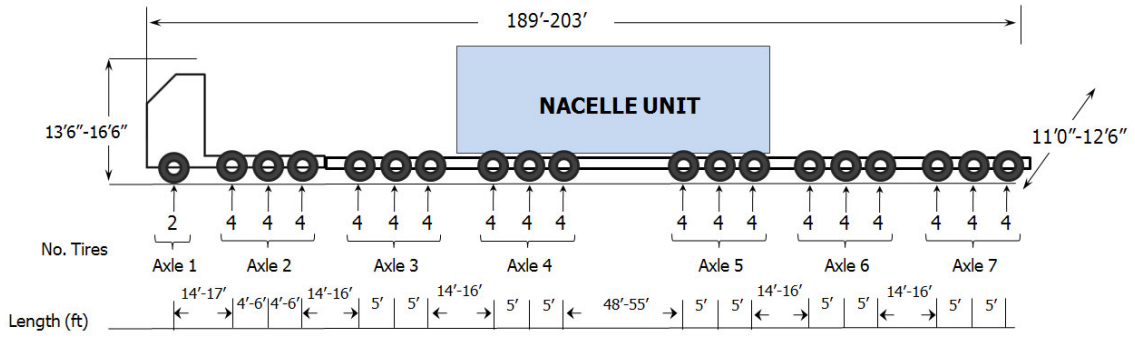


Figure 32: Non-Standard Tractor + 15 Axle Trailer

7.3 Tower Transport Vehicle Fleet

Tower sections are the second heaviest components that have to be hauled. As described earlier, the tower is typically moved in 2 to 5 sections and several types of vehicles are employed in the haul, the most common being the Schnabel-trailer combination vehicle. Overall, the OS/OW dataset contained 20,835 records for tower sections, out of which 20,433 had complete information on the vehicles' GVW and the axle load spectra. As with the nacelle transport fleet, the GVWs of the tower transport fleet was first analyzed.

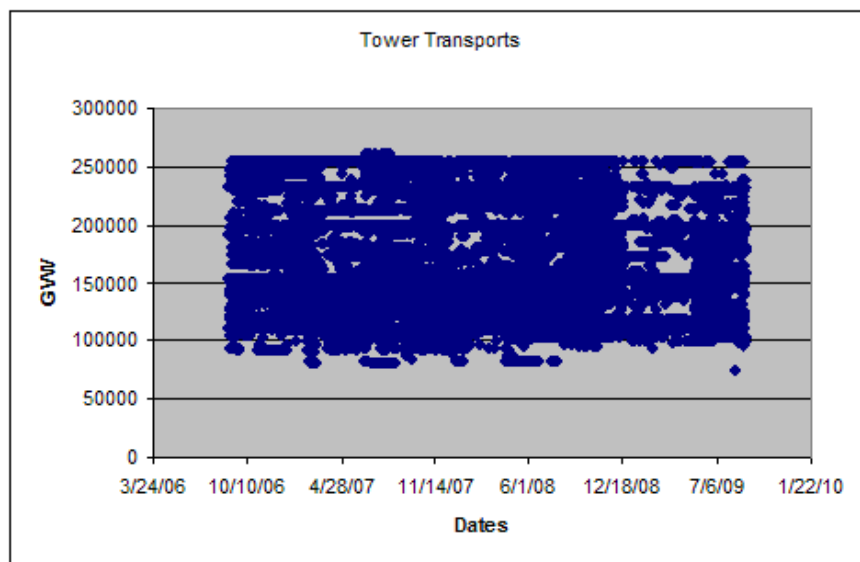


Figure 33: GVW of the Tower Transport Fleet

From Figure 33, it can be seen that the gross vehicle weights of tower transports ranged from 80,000-250,000 lbs., and only a small percentage of vehicles (8.7%) exceeded the super-heavy load limit of 250,000 lbs. For the three years of observation no significant trends could be established from the data.

The tractors can be divided into three types of vehicles:

- Standard Tractor (Steering axle + Tandem back axle)
- Non-standard Tractor (Steering axle + Tridem back axle)
- Non-standard Tractor (Steering axle + Quad back axle)

Out of these, the standard 3-axle tractor was used for 37.5% of the hauls, while the non-standard 4-axle tractor was used for 62.3% of the hauls. The 5-axle tractor was employed in 0.2% of the hauls. The trailer fleet was also analyzed by once again studying axle-spacing histogram data. From Table 10, it can be seen that the 3, 4, 5, and 9-axle trailers were the most common trailers used in hauling tower sections.

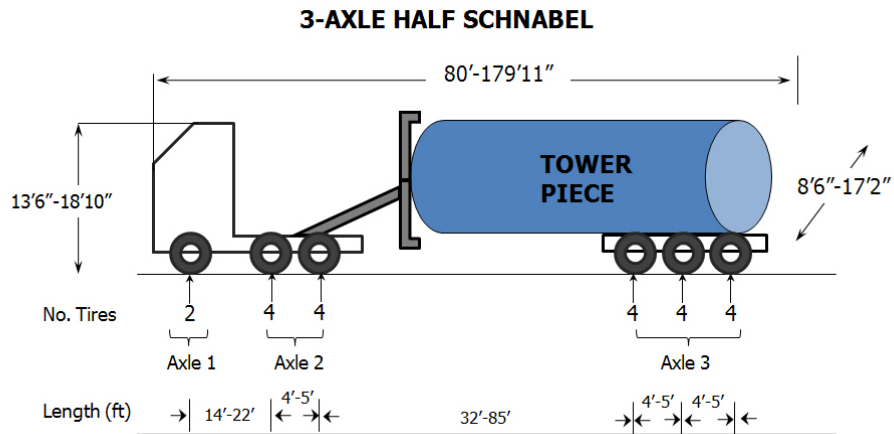
Table 10: Trailer types used for hauling Tower sections

Trailer Axles	Standard Tractor		4-Axle Tractor		5-Axle Tractor		Total	
	Count	Percentage	Count	Percentage	Count	Percentage	Count	Percentage
2	488	2.4%	25	0.1%	0	0.0%	513	2.5%
3	3652	17.9%	1002	4.9%	9	0.0%	4663	22.8%
4	772	3.8%	2807	13.7%	4	0.0%	3583	17.5%
5	775	3.8%	3242	15.9%	36	0.2%	4053	19.8%
6	779	3.8%	1059	5.2%	0	0.0%	1838	9.0%
7	254	1.2%	589	2.9%	0	0.0%	843	4.1%
8	562	2.8%	400	2.0%	0	0.0%	962	4.7%
9	370	1.8%	3588	17.6%	0	0.0%	3958	19.4%
10	5	0.0%	11	0.1%	0	0.0%	16	0.1%
Σ	7,657		12,723		49		20,429	

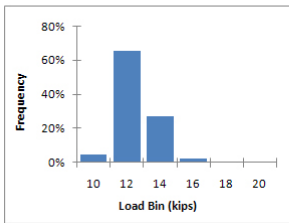
Figures 34 to 37 present the length, width, and height dimensions for the four most common combination-vehicles listed above. Likewise, the reported axle load spectra, along with axle spacing, and the number of tires per each axle are also presented in these figures. Some summary statistics for the entire tower transport vehicle fleet are presented below:

- Transport vehicle widths with tower vary from 8 ft. 6 in. to 17 ft. 7 in.
- The majority of vehicles (95.6%) do not meet the TxDOT legal height limit of 14 ft.
- A high proportion of transport vehicles (31.5%) do not meet the TxDOT legal permitted length limit of 125 ft.

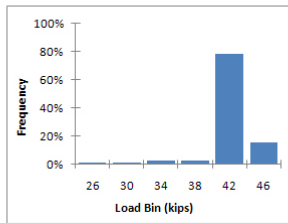
- A significant proportion of transport vehicles (7.1%) do not meet the TxDOT legal overall length limit of 180 ft.



Axle 1 Load Spectra



Axle 2 Load Spectra



Axle 3 Load Spectra

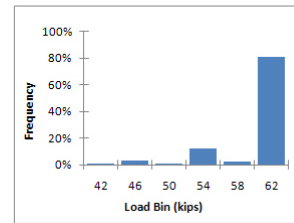
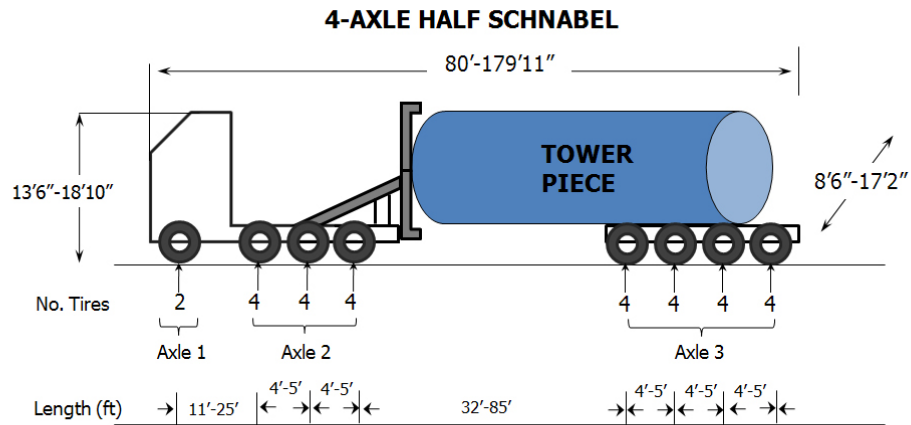
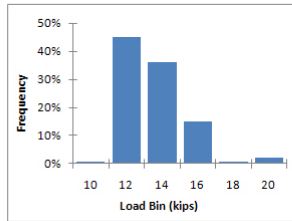


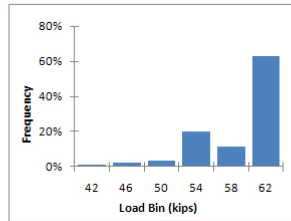
Figure 34: Standard Tractor + Half Schnabel +3-Axle Dolly Trailer



Axle 1 Load Spectra



Axle 2 Load Spectra



Axle 3 Load Spectra

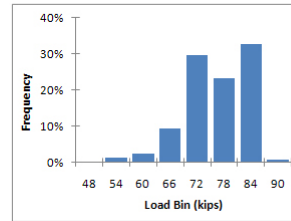
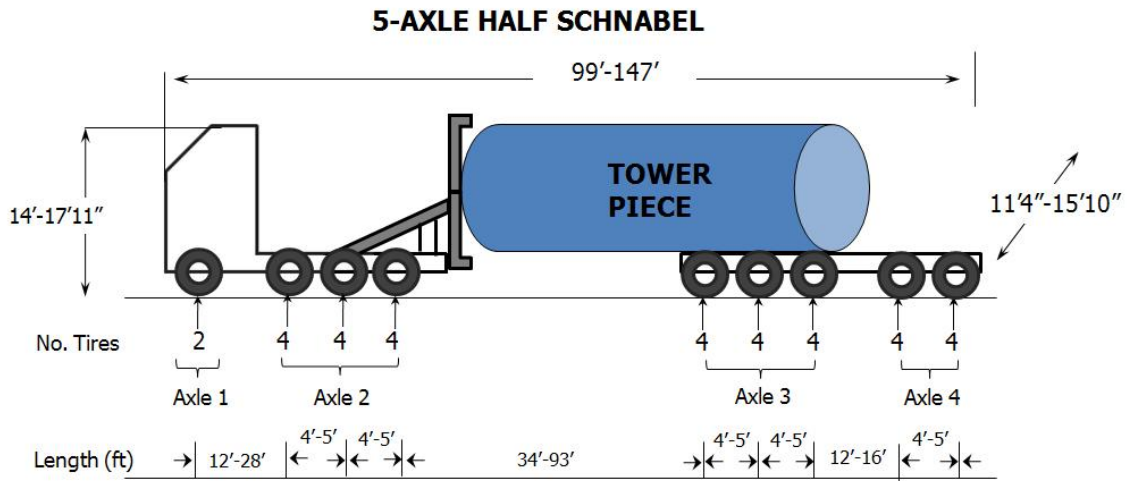
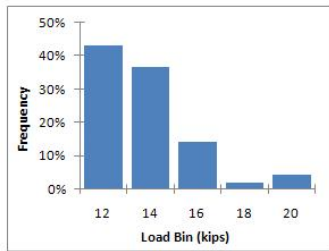


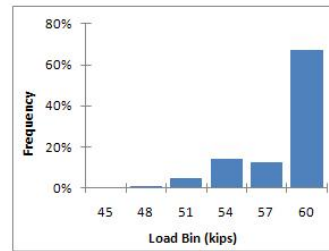
Figure 35: Non-Standard Tractor + Half Schnabel + 4-Axle Dolly



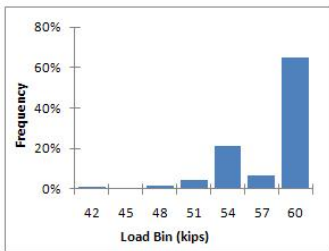
Axle 1 Load Spectra



Axle 2 Load Spectra



Axle 3 Load Spectra



Axle 4 Load Spectra

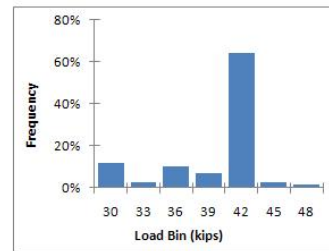
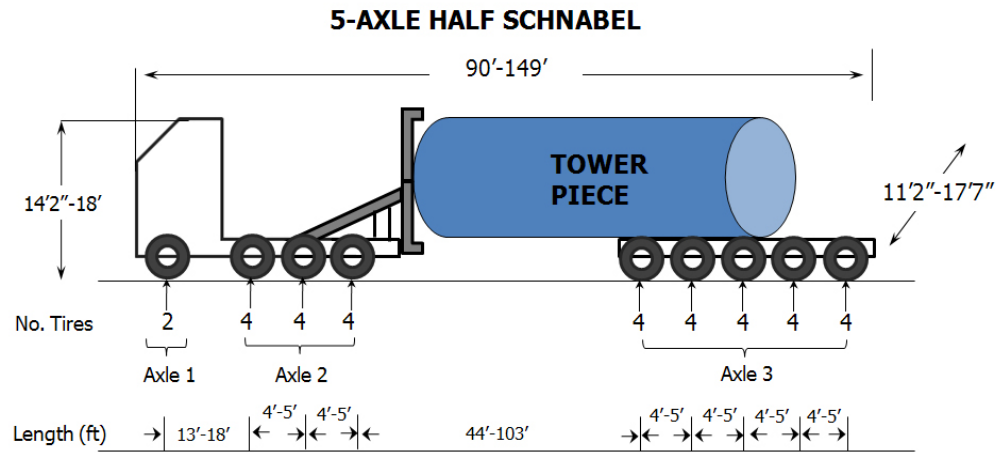
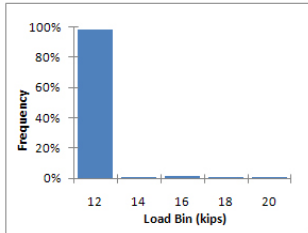


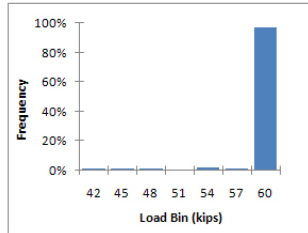
Figure 36: Non-Standard Tractor + Half Schnabel + 5-Axle Dolly



Axle 1 Load Spectra



Axle 2 Load Spectra



Axle 3 Load Spectra

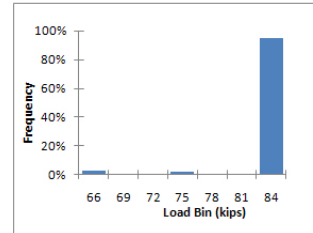


Figure 37: Non-Standard Tractor + Half Schnabel + 5-Axle Dolly

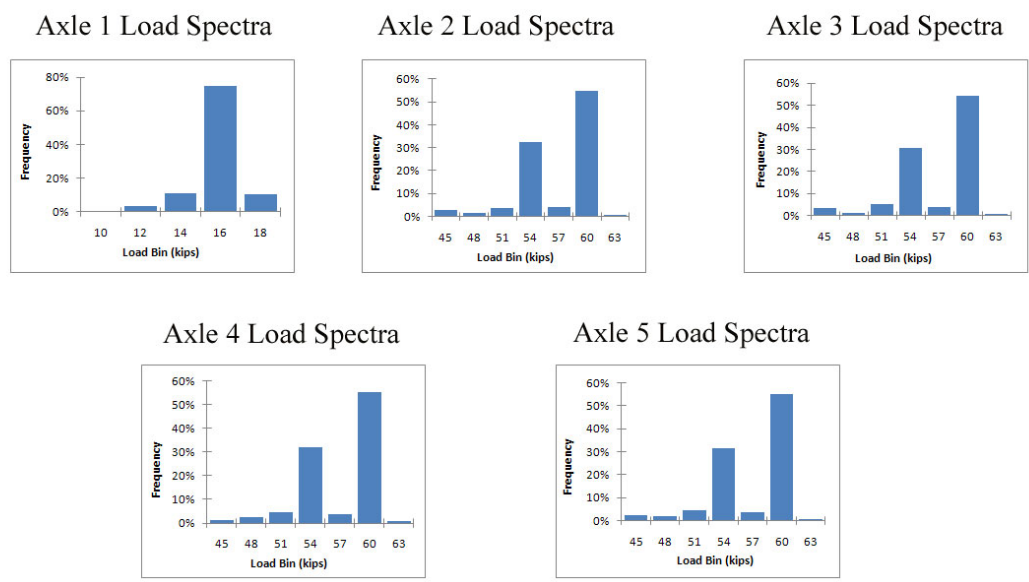
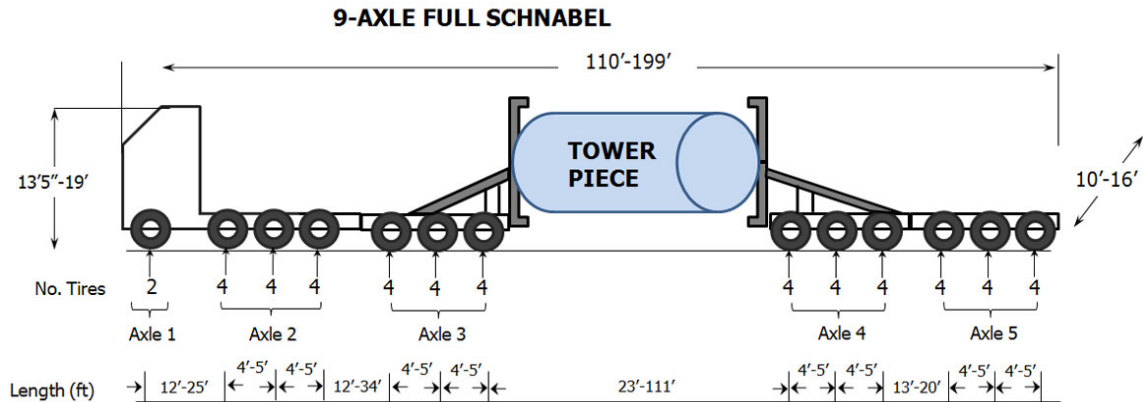


Figure 38: Non-Standard Tractor + Jeep and Dolly Full Schnabel System

7.4 Hub Transport Vehicle Fleet

As it was described in the previous chapters, rotor hubs are lighter components and are most commonly transported by the double drop trailer-tractor combination vehicle. Examining the OS/OW dataset obtained from TxDOT, it was seen that 74.7% of permits designated for the transport of hubs, were issued to vehicles that met the legal weight limit of 80,000 lbs. The other 25.3% of permits were issued to vehicles that exceeded the legal weight limit. These vehicles typically employed a standard tractor and a 2-axle or 3-axle combination trailer for transporting the hub. Based on these data, several generalizations were made about a typical hub transport vehicle:

- Standard tractor vehicle (steering axle + tandem back axle)
- Tandem rear axle double drop trailer
- Maximum gross vehicle weight of 80,000 lbs (12,000 lbs max. on steering axle, and 34,000 lbs max. on the two tandem axle combinations)

Based on these assumptions, and the length, height, and width dimensions obtained from the OS/OW dataset, a typical hub transport vehicle is presented in Figure 39 below.

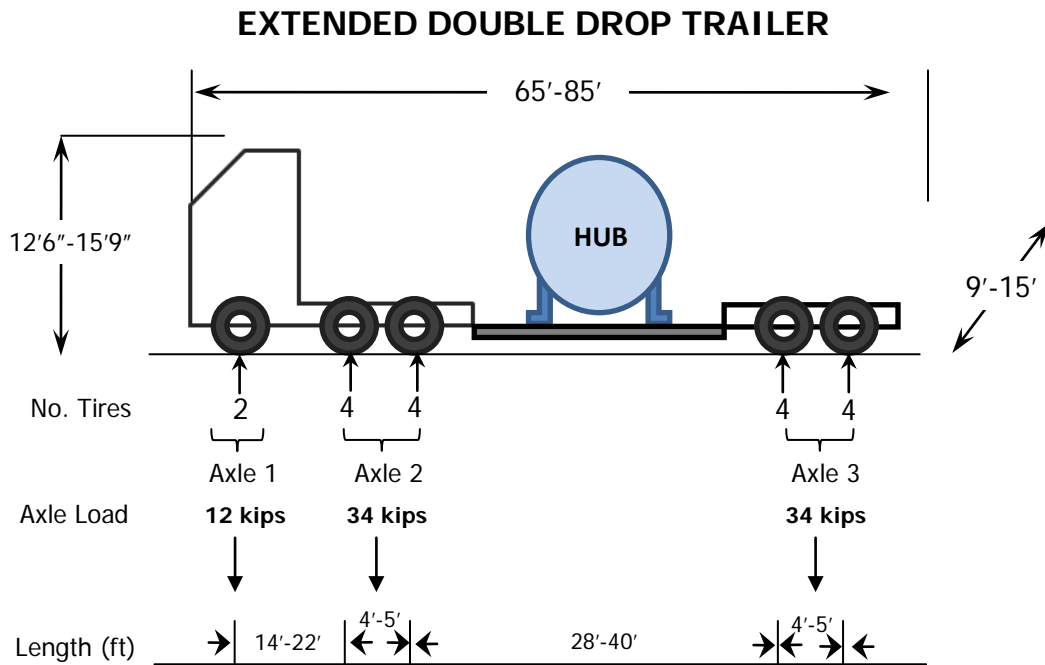


Figure 39: Standard Tractor + Extended Double Drop Trailer Combination

7.5 Blade Transport Vehicle Fleet

Information on the blade transport vehicle fleet was gathered from 15,854 permit records. As with the rotor hubs, it was seen that 94.1% of all permits were issued to vehicles that met the legal load limit of 80,000 lbs. Out of the vehicles that did not meet the legal load limit, the majority employed a long stretch blade trailer described in Chapter 6. Based on this information, once again several generalizations were made about a typical blade transport vehicle:

- Standard tractor vehicle (steering axle + tandem rear axle)
- Specialized long stretch blade trailer (tandem rear axle)
- Maximum gross vehicle weight of 80,000 lbs (12,000 lbs max. on steering axle, and 34,000 lbs max. on the two tandem axle combinations)

Based on these assumptions, and the length, height, and width dimensions obtained from the OS/OW dataset, a typical blade transport vehicle is presented in Figure 40 below.

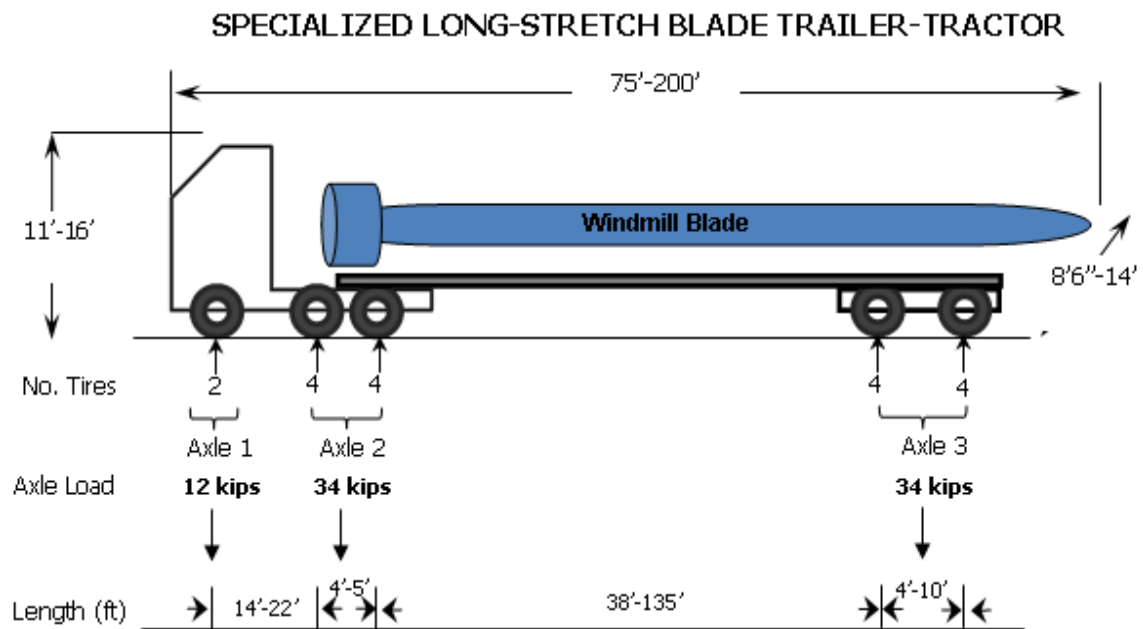


Figure 40: Standard Tractor + Specialized Blade Trailer

CHAPTER 8. ROADWAY NETWORK ANALYSIS

Windmill components are transported over a network of roadway facilities before they reach their final destination. For example, for longer hauls, it can be expected that windmill components will be transported over the interstate system, as it is the fastest and most efficient network of roads. It can also be expected that rural collector facilities such as farm-to-market, ranch-to-market and county roads will be utilized because most wind farms are located in rural areas that are only accessible by these types of roads. The structural design of these two types of facilities will significantly differ from one another. Interstate systems are designed to carry higher traffic volumes, while rural collector systems may be designed to carry several hundred vehicles per day. Therefore, the pavement impacts from transporting windmill components can be expected to differ significantly from one facility to the other.

To understand which roadway facilities are most commonly used in the transportation of windmill components, route information data from the OS/OW dataset were analyzed. Route information data provided the permit's starting and ending location, along with the description of the route. Drawing a random sample of permits from the OS/OW dataset, and plotting each permit's route in Google Maps, provided a representative distribution of facilities used in the transportation of windmill components, along with the average length of haul. Table 11 provides the results from the route analysis.

Table 11: Distribution of Vehicle-Miles-Traveled over various facility types

Sample Size (n)=97		
Functional Class	Miles (VMT)	Percentage
Interstate	19,297.80	49.24%
US Highway	10,757.70	27.45%
State Freeway	6,678.10	17.04%
Farm Roads	1,391.10	3.55%
Lps/Bltwys/Bus	1,054.80	2.69%
Unaccounted	14.35	0.04%
Total VMT	39,193.85	100.00%

From the table it can be seen that a sample of 97 records was taken from the dataset. The total vehicle-miles traveled for the sample was calculated to be 39,193 miles. The average distance per haul was 416 miles. Almost 50 percent of all vehicle-miles-traveled occurred on the interstate system, while only 3.6% of vehicle-miles-traveled occurred on rural collector facilities such as farm-to-market roads. This can be expected since farm-to-market roads typically serve as the final destination access points on the distribution network. They are, however, a critical part of the distribution network and travel on these facilities may be short, but frequent.

CHAPTER 9. PAVEMENT IMPACT ANALYSIS

The distribution of vehicle-miles traveled provides a good understanding of which facilities are impacted the most in the transportation of windmill components and, hence, which facilities should be targeted for further pavement impact analysis. For meeting the objectives of this study, two facilities were chosen for analyzing the impacts of hauling windmill components. These facilities were as follows:

- Rural interstate highway facility
- Rural collector roadway facility (or farm-to-market road)

These two facilities are critical links in the distribution network of windmill components. From the previous chapter, it was seen that wind truck traffic mainly travels on the interstate system over long distances. Much of that haul is over long stretches of rural road. Therefore, understanding the damage caused to a typical rural interstate facility becomes important for the analysis. At the same time, understanding the impacts of wind truck traffic on sparser traveled rural collector roads is also important. They serve as the final link in the distribution network of windmill components and are traveled frequently over short distances during the construction process of the wind farm site.

To further analyze the impacts of windmill traffic on these two facilities, it is first important to understand their structural composition. The structural make-up of a pavement will depend on several design variables such as performance period, amount of traffic during that period, and environmental conditions to which the facility is exposed (*AASHTO, 1993*)⁴. Also the strength and type of materials used for construction will have a significant impact on the structural integrity and thickness of the pavement structure.

In general there are two types of pavement structures: flexible pavements and rigid pavements. Flexible pavements are pavements constructed from bituminous and granular material, or asphalt concrete. Rigid pavements on the other hand, are constructed with Portland cement concrete. The United States has about 2.5 million

miles of paved roads, out of which 94 percent are flexible pavements. Rigid pavements constitute about 6 percent of all paved surfaces and are typically confined to the urban roadway network (*Huang, 2004*)³³.

Based on these observations, the two facilities analyzed for this report were chosen to have a *flexible pavement* design. In general, flexible pavements are layered systems, each layer constructed from a different material. Stronger materials with a higher stiffness, such as asphalt concrete are placed at the top of the layered system and are used for the riding surface of the road, while weaker granular materials with a lower stiffness are placed at the bottom of the layered system, near the roadbed soil. A typical flexible pavement section may be constructed anywhere from 3 to 6 layers. Typically one or two hot-mix-asphalt (HMA) layers are employed for the construction of the riding surface, followed by two stabilizing granular layers called the base and the subbase. This is followed by a weaker material subgrade layer which rests on top of the compacted roadbed soil (*Huang, 2004*)³³.

The purpose of the layered system is to optimize material usage and to minimize two types of pavement distresses: 1) rutting which can be described as permanent deformation of the asphalt concrete within the path of the wheel and 2) fatigue cracking which are structural cracks within the pavement, mainly caused by excessive traffic over extended periods of time. Minimizing these two types of distresses is critical for maintaining an efficient roadway infrastructure. Both distresses reduce the serviceability life of a pavement, leading to reductions in ride quality of the roadway surface, increased vehicle operating costs, and safety concerns for drivers. For example, bottom-up fatigue cracks formed within the asphalt concrete, can open up pathways for water to infiltrate into the underlying layers of the structure, causing strength reductions of the base and the subgrade layers which can ultimately lead to accelerated pavement deterioration. Rutting, or permanent deformation in the wheel path of the surface layers can reduce the pavement's drainage capabilities and lead to water accumulation during a heavy storm which may cause vehicle hydroplaning, and possibly other safety concerns (*AASHTO, 1993*)⁴.

Rutting and fatigue cracking can be minimized by limiting the level of stresses and strains within the flexible pavement structure. For example, permanent deformation is thought to be controlled by the amount of vertical compressive strain at the bottom of the subgrade layer. Thus, by constructing a thicker pavement structure, or one with stronger materials, the compressive strain at the bottom of the subgrade can be controlled and the magnitude of permanent deformation on the surface layer can be minimized. Meanwhile bottom-up fatigue cracking is thought to be caused by excessive horizontal tensile strains at the bottom of the HMA layer. By manipulating the thickness of the HMA layer, the amount of tensile strain at the bottom of the layer can also be controlled, which would lead to reductions in overall crack propagation (*Huang, 2004*)³³.

9.1 Pavement Selection

In selecting two pavement sections for the impact analysis, many aspects of the design have to be considered. Pavement selection should be done carefully, with mindfulness for each layer's material properties. For example, for hot-mix asphalt layers, aggregate gradation, asphalt binder grade, percentage of asphalt and percentage of air voids in the mixture are important variables for characterizing asphalt layer properties. It is known that an excessive amount of air voids within the asphalt mixture can lead to premature rutting, while an excessive amount of binder can lead to asphalt bleeding. For granular layers such as the base and subbase, aggregate gradation and the material's Atterberg limits play an important role in understanding material behavior. Clayey materials, for instance, tend to have expansive properties and should be avoided in construction of the base and subbase layers, as volumetric changes in these layers will cause unexpected variations in the roughness of the surface course.

In selecting the actual pavement sections, the *Texas Flexible Pavements Database*³⁴ was referenced. The Texas Flexible Pavement Database was developed under TxDOT Research Project 0-5513. It serves as a data pool for providing information on material properties, pavement structural characteristics, highway traffic

information, environmental conditions, and performance data for numerous pavement sections across the state of Texas. The database was used to query for two pavement sections, one rural interstate and one farm-to-market road that were found to be used by the wind industry during the route study. These sections were as follows:

- IH-20 near Colorado City in Mitchell County, TX (Section ID: TXLT08002)
- FM 1606 near San Antonio in Bexar County, TX (Section ID: TXLT15010)

The structure of these pavement sections is illustrated below in Figure 41.

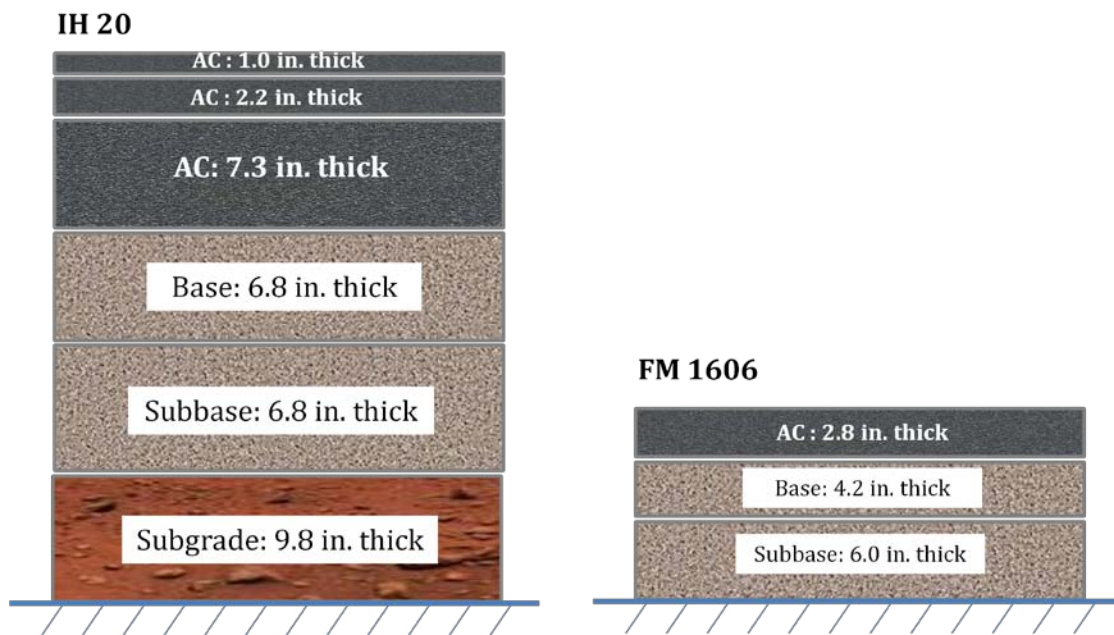


Figure 41: Pavement Cross-Sections of IH 20 and FM 1606

From the figure, it can be seen that the rural interstate section has a significantly thicker structure than the farm-to-market road. In total, the IH-20 section has 10.5 inches of asphalt concrete and 13.6 inches of granular material. Comparatively, the FM 1606 pavement section is composed of 2.8 inches of asphalt concrete and 10.2 inches of granular material. The disparity in structural design is greatly dependent on the

functional hierarchy of the road, and the level of traffic it is designed to handle over a 20-year period. Clearly, an interstate highway is a higher priority facility that is designed to carry significantly greater volumes of traffic than the farm-to-market road, hence, the pavement structure is significantly stronger. To further understand the material properties of each pavement structure, the following two sub-sections break down each pavement by their layer properties.

9.1.1 INTERSTATE HIGHWAY 20

Interstate Highway 20, located near Colorado City in Mitchell County, Texas is comprised of six structural layers. These layers and their details are presented in Table 12.

Table 12: Structural Composition of IH-20

IH 20	Layer	Details	Thickness
Layer 1	HMA	AC-10	1
Layer 2	HMA	AC-10	2.2
Layer 3	HMA	AC-10	7.3
Layer 4	Base	A-2-6	6.8
Layer 5	Subbase	A-2-4	8.8
Layer 6	Subgrade	A-6	118 (semi-inf.)

From the table it can be seen that there are three hot-mix asphalt concrete layers, followed by two granular layers and a semi-infinite subgrade layer. The aggregate gradation for each one of the layers is presented below in Table 13.

Table 13: Layer Gradation for IH-20

Layer Gradation	Percent Passing (%)					
Sieve Size	Layer 1	Layer 2	Layer 3	Layer 4	Layer 5	Layer 6
3 in				100	100	100
2 in				100	100	100
1 1/2 in	100	100	100	100	100	100
1 in	100	100	94	97	97	99.5

3/4 in	100	100	87.5	93.5	93.5	99.5
1/2 in	100	100	79	88	88	98.5
3/8 in	98.5	98.5	71.5	85	85	97.5
No. 4	63.5	63.5	53.5	77	77	94
No. 10	42	42	33.5	64	64	86.5
No. 40	27	27	21.5	48.5	48.5	82
No. 80	16	16	16.5	38.5	38.5	73.5
No. 200	9.45	9.45	13.75	30	30	48.45

Furthermore, the mixture properties for the three HMA layers are presented in Table 14, while the material properties for the two granular layers and the subgrade are presented in Table 15.

Table 14: Mixture Properties for HMA Layers

HMA Mix Properties	Layer 1	Layer 2	Layer 3
Binder Viscosity Grading	AC-10	AC-10	AC-10
AC _{WEIGHT} (%)	5.3%	5.8%	5.5%
G _{mm}	2.443	2.409	2.427
G _{mb}	2.377	2.378	2.281
VMA (%)	11.98%	11.45%	15.60%
V _{air voids} (%)	2.7%	1.30%	5.98%
VFA	77.5%	88.6%	61.7%
V _{eff-binder} (%)	9.3%	10.1%	9.6%
Unit Weight (lbs/ft ³)	148.3	148.4	142.4

Table 15: Material Properties for Granular Layers and Subgrade

Layer Material Properties	Layer 4	Layer 5	Layer 6
Liquid Limit	37	24	24
Plastic Limit	20	20	14
Plasticity Index	17	4	10
Maximum Dry Density	-	122	-
Optimum Moisture	-	11	-
Material Type	Granular	Granular	Clayey
AASHTO Classification	A-2-6	A-2-4	A-6
Modulus (psi)	20,500	21,500	14,500

From Table 14, it can be seen that the HMA layers were constructed with a binder viscosity grading of AC-10. The viscosity grading of asphalt relates to the binder’s “hardness” or “softness.” A low viscosity grading implies that the asphalt is “soft” or has reduced resistance to flow, while a high viscosity grading implies that the binder is “hard” or has a greater resistance to flow. Before the introduction of Superpave in the 1990’s, the most common asphalt binder used in the U.S. for paving was the AC-20 grade binder (*Roberts, 1996*)³⁵. However, it can be seen that for this particular pavement section an AC-10 viscosity grade binder was used.

From Table 15, it can be seen that according to the AASHTO Soil Classification System, the base and subbase layers are classified as A-2-6 and A-2-4 which can be categorized as granular materials with silty or clayey gravel and sand. The subgrade layer is classified as an A-6 in accordance with the AASHTO Soil Classification System which describes it as a clayey soil (*Das, 2001*)³⁶.

9.1.2 FARM-TO-MARKET ROAD 1606

Farm-to-market road 1606 near San Antonio, TX, is comprised of four structural layers. These layers along with their details are presented in Table 16.

Table 16: Structural Composition of FM 1606

FM 1606	Layer	Details	Thickness
Layer 1	HMA	AC-20	2.8
Layer 2	Base	A-2-6	4.2
Layer 3	Subbase	A-2-6	6
Layer 4	Subgrade	A-6	semi-infinite

From the table it can be seen that the pavement structure is composed of a single HMA layer and two granular layers which are classified as A-2-6 by the AASHTO Classification System. To further characterize each layer, Table 17 presents the aggregate gradation for the first three layers.

Table 17: Layer Gradation for Farm-to-Market 1606

Layer Gradation	Percent Passing (%)		
	Layer 1	Layer 2	Layer 3
3 in	100	100	100
2 in	100	100	100
1 1/2 in	100	100	100
1 1/4 in	100	100	100
1 in	100	76	76
7/8 in	100		
3/4 in	100	59	59
1/2 in	91	45	45
3/8 in	77	40	40
No. 4	52	32	32
No. 10	28	27	27
No. 40	12	22	22
No. 80	8	18	18
No. 200	5.5	16	16

Furthermore, Table 18 presents the mixture properties for the HMA layer and Table 19 presents the material properties for the base, subbase, and subgrade layers.

Table 18: Mixture Properties for HMA Layer

HMA Mix Properties	Layer 1
Binder Viscosity Grading	AC-20
AC _{WEIGHT} (%)	5.7%
Gmm	2.421
Gmb	2.324
VMA (%)	14.4
V _{air voids} (%)	4.0
VFA	72.2%
V _{eff-binder}	10.4
Unit Weight (lbs/ft ³)	145.0

Table 19: Material Properties for Granular Layers

Layer Material Properties	Layer 2	Layer 3	Layer 4
Liquid Limit	26	26	33
Plastic Limit	15	15	19

Plasticity Index	11	11	14
Material Type	Granular	Granular	Clayey
AASHTO Classification	A-2-6	A-2-6	A-6
Modulus (psi)	20,500	20,500	14,500

9.2 Traffic Characterization

The second step in the impact analysis is to characterize the traffic conditions under which the pavement sections are to be tested. In pavement performance evaluation, only truck traffic is considered for the analysis, as passenger vehicles and pick-up trucks were found to cause an insignificant amount of damage to the pavement structure (*Huang, 2004*)³³. Therefore traffic conditions can be thought of as “truck traffic” conditions, and they can be characterized into two main groups: 1) Standard traffic, and 2) windmill traffic.

Standard traffic can be characterized as the usual amount of truck traffic activity expected to be endured by the facility on a daily basis. Windmill traffic can be characterized as the truck traffic associated with moving a certain number of windmill components on the facility on a daily basis. The following two sub-sections will describe the specifics behind each type of traffic scenario.

9.2.1 STANDARD TRAFFIC

Interstate highway facilities and farm-to-market roads receive significantly different volumes of traffic. A farm-to-market road may experience several hundred trucks per day, while an interstate facility may experience traffic in the order of several thousand trucks per day. Therefore, the standard traffic scenario for the two facilities will be quite different from one another.

To understand the traffic scenario which would be considered normal or “standard” for the two facility types, data from the 2007 Highway Performance Management System (HPMS) database was used. The HPMS database is an ongoing effort sponsored by the federal government that collects data pertaining to highway

performance (Prozzi, 2009)³⁷. In Texas, data are collected for several thousand roadway sections spread over the entire state transportation network. Ninety eight fields are collected for each roadway section in the HPMS database. These fields classify each section by its functional class and include data on the average annual daily traffic (AADT), along with the annual percentages of single-unit and combination-unit trucks on that particular section. Therefore, the HPMS dataset was determined to be a reliable source for estimating standard or “normal” traffic conditions.

Overall, there were 71 rural interstate sections and 281 rural collector road sections identified in the 2007 Texas HPMS dataset. AADTT ranged from 1,897 to 19,742 trucks per day on rural interstate sections, and 7 to 4,060 trucks per day on rural collector roadway facilities. Averages were used to characterize the standard traffic conditions for the two facilities. These are presented in Table 20 below.

Table 20: Standard Traffic Characteristics for Rural Interstates and Rural Collector Roads

Traffic Characteristics	IH-20	FM 1606
ADTT	9,026	425
% SU	13.4%	42.9%
% CU	86.6%	57.1%

From the table it can be seen that on average, rural interstates experienced a significantly higher proportion of combination unit trucks than single unit trucks. The split between the two truck categories was almost even for rural collector facilities.

To simplify the standard traffic scenario, it was assumed that all single unit trucks were of a Class 5 category according to the FHWA Vehicle Classification System, while all combination-unit trucks were of a Class 9 category according to the FHWA Vehicle Classification System. The FHWA Vehicle Classification System is illustrated in Figure 42 below (Prozzi and Hong, 2006)³¹.

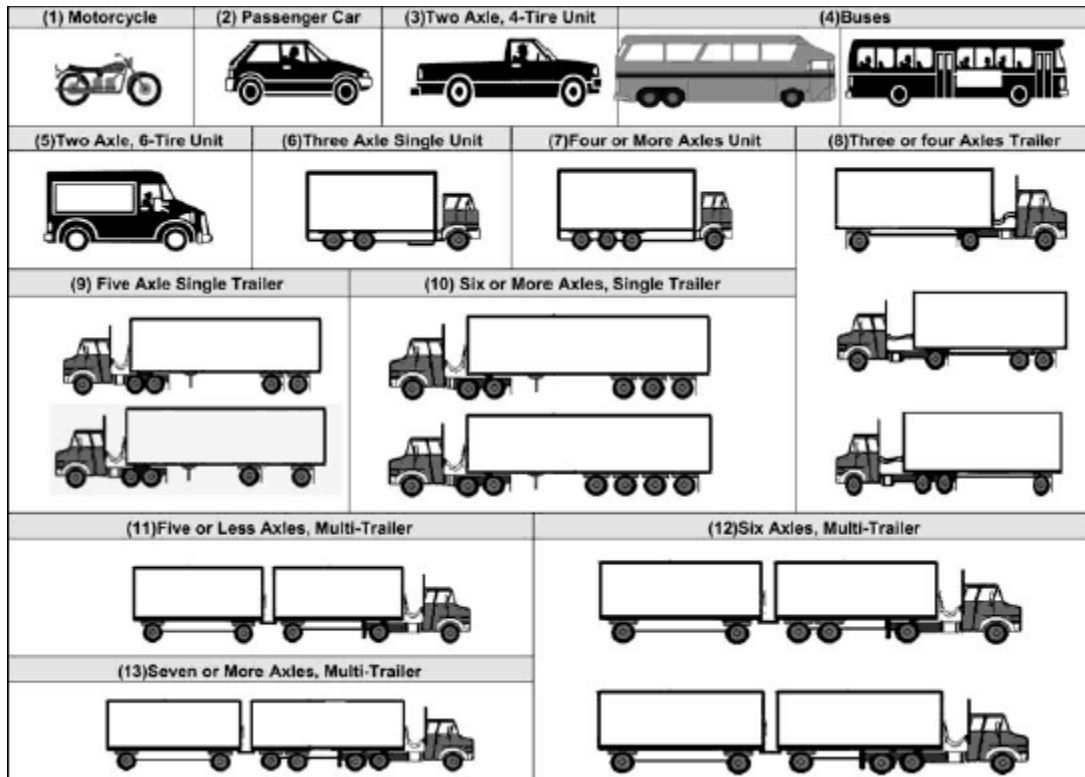


Figure 42: FHWA Vehicle Classification System

(Source: Prozzi and Hong, 2006)

Although in actuality the vehicle fleet is more diverse than just these two class categories, these assumptions are not too far-fetched from the real world scenario. Two research studies have been conducted in the past twenty years that support these assumptions. A study on the characteristics of axle load spectra conducted by Lu and Harvey at the University of California, Berkeley collected traffic data on the California State Highway network from years 1991-2001. This study showed that an overbearing amount of vehicles on California roads were of a Class 9 category (Prozzi and Hong, 2006)³¹. It also showed that vehicle classes 9, 5, 11, and 8 accounted for 90 percent of all truck traffic. These results are illustrated in Figure 43.

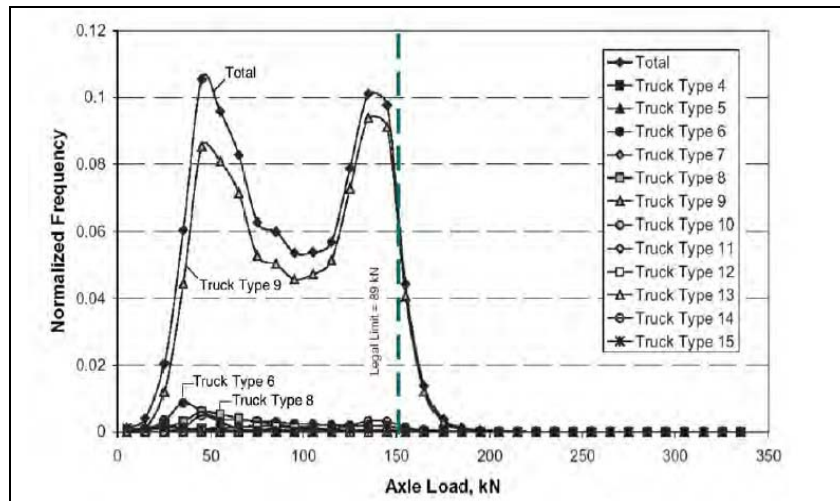


Figure 43: General Tandem Axle Load Spectra Across All Dates and Locations According to the California Study
(Source: Prozzi and Hong³⁰, 2006)

The other study on traffic classification was conducted by Lee and Nabil at the Center for Transportation Research at the University of Texas. Research conducted by Lee and Nabil showed that out of all trucks, the dominant class was the 3S2 5-axle truck (Class 9) accounting for 63% of all truck traffic in Texas. Meanwhile, the two axle single-unit truck (Class 5) accounted for 25% of all truck traffic (Prozzi and Hong, 2006)³¹. Therefore the decision to simplify the standard traffic scenario into just two vehicle classes (Class 9 for combination trucks and Class 5 for single unit trucks) is based off previous supporting research.

The last step in traffic characterization is to define the *axle load spectra* for each vehicle class in the standard traffic scenario. Since it was decided that there were only two vehicle classes, axle load spectra was defined for only the Class 5 and Class 9 vehicles. To define the axle load spectra, state default values for steering axle, single axle, and tandem axle, developed for the *Texas Flexible Pavements Database* were used. Based on these values, the single and tandem axle load spectra are presented for Class 5 and Class 9 vehicles in Table 21 and Table 22 below.

Table 21: *Single* Axle Load Distribution for Class 5 and Class 9 Vehicles

Weight	Class 5	Class 9	Weight	Class 5	Class 9
3,000	4.97	0.98	23,000	0.2	0
4,000	11.4	10.06	24,000	0.13	0
5,000	9.11	7.74	25,000	0.09	0
6,000	4.82	2.32	26,000	0.06	0
7,000	4.41	2.94	27,000	0.04	0
8,000	5.66	5.72	28,000	0.03	0
9,000	7.66	9.77	29,000	0.02	0
10,000	11.71	18.05	30,000	0.02	0
11,000	13.21	21.42	31,000	0.01	0
12,000	9.06	13.51	32,000	0.01	0
13,000	4.77	5.18	33,000	0.01	0
14,000	2.89	1.55	34,000	0	0
15,000	2.29	0.48	35,000	0	0
16,000	1.98	0.17	36,000	0	0
17,000	1.67	0.07	37,000	0	0
18,000	1.32	0.03	38,000	0	0
19,000	0.98	0.01	39,000	0	0
20,000	0.69	0	40,000	0	0
21,000	0.47	0	41,000	0	0
22,000	0.31	0	Total (%)	100	100

Table 22: *Tandem* Axle Load Distribution for Class 9 Vehicles

Weight	Class 9	Weight	Class 9	Weight	Class 9
6,000	1	32,000	9.03	58,000	0.02
8,000	3.83	34,000	8.97	60,000	0.01
10,000	6.98	36,000	5.75	62,000	0.01
12,000	8.43	38,000	2.77	64,000	0.01
14,000	8.05	40,000	1.33	66,000	0
16,000	6.78	42,000	0.76	68,000	0
18,000	5.55	44,000	0.49	70,000	0
20,000	4.82	46,000	0.32	72,000	0
22,000	4.57	48,000	0.21	74,000	0
24,000	4.54	50,000	0.14	76,000	0
26,000	4.5	52,000	0.09	78,000	0
28,000	4.66	54,000	0.06	80,000	0
30,000	6.29	56,000	0.03	82,000	0

9.2.2 WINDMILL TRAFFIC

Windmill traffic can be characterized as the truck traffic associated with moving a certain amount of windmill components on a roadway facility. For this study several windmill traffic scenarios were considered in the impact analysis:

- 2 windmill per day moved on facility
- 5 windmills per day moved on facility
- 10 windmills per day moved on facility
- 20 windmills per day moved on facility

From the previous chapters, it was seen that moving a single windmill requires anywhere from 7 to 10 oversized and overweight trucks. For this analysis it was assumed that *nine oversized/overweight trucks* shall be required to move the entire windmill to the construction site:

- 1 vehicle for moving the nacelle
- 4 vehicles for moving the tower (1 for base, 2 for mid-section, and 1 for top section)
- 1 vehicle for moving the rotor hub
- 3 vehicles for moving the blades

Therefore, the “2 windmills per day” scenario can be thought of as *18 wind trucks per day*, and the “5 windmills per day” scenario can be thought of as *45 wind trucks per day*.

As was shown in previous chapters, moving windmill components requires the utilization of a specialized vehicle fleet. Therefore, windmill traffic can be categorized by a select number of vehicle classes. To simplify the windmill vehicle fleet which was discussed in Chapters 6 and 7, only 8 vehicles were chosen to represent the entire fleet for the analysis. Two vehicles were chosen to represent the nacelle transport fleet, four vehicles were chosen to represent the tower transport fleet, and one vehicle was chosen to

represent each the hub and blades transport fleets. The vehicle fleet used for the analysis is presented in Figure 44 below.

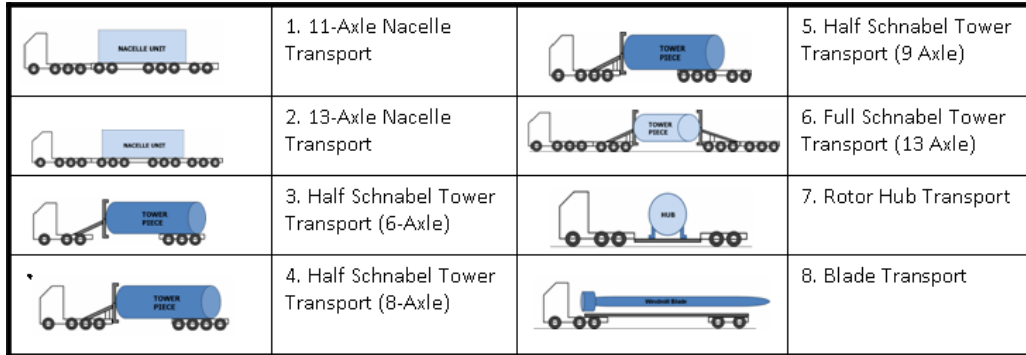


Figure 44: Windmill Vehicle Fleet Used for Pavement Impact Analysis

The break down by percentages of each vehicle class (as defined by Figure 44) within the windmill vehicle fleet is presented in Table 23.

Table 23: Percentage of Each Vehicle Class in the Windmill Fleet

Classification	Description	Percentage
Class 1	11-Axle Nacelle Transport	5.6
Class 2	13-Axle Nacelle Transport	5.6
Class 3	6-Axle Half Schnabel Tower Transport	11.1
Class 4	8-Axle Half Schnabel Tower Transport	11.1
Class 5	9-Axle Half Schnabel Tower Transport	11.1
Class 6	13-Axle Full Schnabel Tower Transport	11.1
Class 7	Rotor Hub Transport	11.1
Class 8	Windmill Blade Transport	33.3
	Total	100

Several important details should be considered when referring to Table 23. Since there are two vehicle classes present to represent the nacelle transport fleet, and only one nacelle unit is required per windmill, the percentages on the two vehicle classes are split so that half of the nacelle units are transported by the 11-Axle Nacelle Transport and the

other half are transported by the 13-Axle Nacelle Transport. It should also be noted that since each windmill requires three blades, 33.3 percent of all windmill traffic is generated by Blade Transport vehicles.

The last step in traffic characterization is to define the *axle load spectra* for each vehicle class. Tables 24 to 27 present the single, tandem, tridem, and quad axle load spectra for the vehicle classes in the windmill vehicle fleet, as defined by this report. This information was obtained from the reported axle load spectra found in the OS/OW database for years 2007-2009.

Table 24: Single Axle Load Distribution Spectra for Windmill Traffic

Weight	Class 1	Class 2	Class 3	Class 4	Class 5	Class 6	Class 7	Class 8
3,000	0	0	0	0.04	0	0	0.98	0.98
4,000	0	0	0	0	0	0	10.06	10.06
5,000	0	0	0	0	0	0	7.74	7.74
6,000	0	0	0	0	0	0	2.32	2.32
7,000	0	0	0	0	0	0	2.94	2.94
8,000	0	0	0	0	0	0	5.72	5.72
9,000	0.2	0	0	0	0	0	9.77	9.77
10,000	5.85	0	4.88	0.85	0	0.02	18.05	18.05
11,000	12.32	0	0	0	0	0	21.42	21.42
12,000	21.29	29.64	65.31	44.9	42.99	3.55	13.51	13.51
13,000	10.23	15.19	0	0	0	0	5.18	5.18
14,000	33.4	22.89	26.89	36.19	36.41	11.26	1.55	1.55
15,000	8.56	8.54	0	0	0	0	0.48	0.48
16,000	3.13	11.18	2.57	14.95	14.21	74.97	0.17	0.17
17,000	0.42	1.37	0	0	0	0	0.07	0.07
18,000	3.97	10.55	0.27	0.79	1.95	10.2	0.03	0.03
19,000	0.63	0.32	0	0	0	0	0.01	0.01
20,000	0	0.32	0.08	2.28	4.44	0	0	0
Total	<i>100%</i>							

** As defined in this report*

Table 25: Tandem Axle Load Distribution Spectra for Windmill Traffic

Weight	Class 1	Class 3	Class 5	Class 7	Class 8
6,000	0	0	0	1.01	1.01
8,000	0	0	0	3.83	3.83
10,000	0	0	0	6.98	6.98
12,000	0	0	0	8.43	8.43
14,000	0	0	0	8.05	8.05
16,000	0	0	0	6.78	6.78
18,000	0	0	1.07	5.55	5.55
20,000	0	0	0	4.82	4.82
22,000	0	0	0.53	4.57	4.57
24,000	0	0	0	4.54	4.54
26,000	0	0.54	0.51	4.49	4.49
28,000	0	0	0.89	4.66	4.66
30,000	0.1	0.08	8.88	6.29	6.29
32,000	0	0	1.78	9.03	9.03
34,000	2.61	2.55	5.33	8.97	8.97
36,000	1.88	0	5.33	5.75	5.75
38,000	12.94	2.55	2.84	2.77	2.77
40,000	28.71	0	65.72	1.33	1.33
42,000	43.74	78.7	2.49	0.76	0.76
44,000	6.78	0	0.36	0.49	0.49
46,000	3.24	15.58	4.09	0.32	0.32
48,000	0	0	0	0.21	0.21
50,000	0	0	0	0.14	0.14
52,000	0	0	0	0.09	0.09
54,000	0	0	0	0.06	0.06
56,000	0	0	0	0.03	0.03
58,000	0	0	0	0.02	0.02
60,000	0	0	0.18	0.01	0.01
62,000	0	0	0	0.01	0.01
64,000	0	0	0	0.01	0.01
Total	<i>100%</i>	<i>100%</i>	<i>100%</i>	<i>100%</i>	<i>100%</i>

** As defined in this report*

Table 26: Tridem Axle Load Distribution Spectra for Windmill Traffic

Weight	Class 1	Class 2	Class 3	Class 4	Class 5	Class 6
12,000	0	0	0	0	0	0
15,000	0	0	0	0	0	0.03
18,000	0	0	0	0	0	0.01
21,000	0	0	0	0	0	0.03
24,000	0	0.11	0	0	0	0.02
27,000	0	0	0	0	0	0.03
30,000	0	0	0	0	0	0.03
33,000	0	0	0	0	0	0.02
36,000	0	0	0	0.04	0	0.02
39,000	0	0	0.05	0.04	0	0.03
42,000	0.73	0	0.52	0.89	0.44	0.22
45,000	4.8	0.19	2.75	1.74	0.19	2.1
48,000	12.53	0.29	1.07	1.75	1.33	1.72
51,000	26.62	0.42	3.09	2.57	4.53	4.51
54,000	14.09	4.11	9.17	19.2	17.85	31.65
57,000	8.87	6.8	1.67	8.67	9.59	3.92
60,000	32.36	83.94	81.54	64.24	66.07	54.88
63,000	0	0	0.14	0.86	0	0.78
66,000	0	1.61	0	0	0	0
69,000	0	0	0	0	0	0
72,000	0	2.53	0	0	0	0
Total	<i>100%</i>	<i>100%</i>	<i>100%</i>	<i>100%</i>	<i>100%</i>	<i>100%</i>

** As defined in this report*

Table 27: Quad Axle Load Distribution Spectra for Windmill Traffic

Weight	Class 4	Weight	Class 4	Weight	Class 4
24,000	0	51,000	0.36	78,000	16.6
27,000	0	54,000	0.9	81,000	28.84
30,000	0	57,000	0.79	84,000	3.78
33,000	0	60,000	1.75	87,000	0.39
36,000	0	63,000	4.39	90,000	0.43
39,000	0	66,000	4.89	93,000	0.71
42,000	0	69,000	5.75	96,000	0
45,000	0.04	72,000	23.77	99,000	0
48,000	0.04	75,000	6.53	102,000	0.04
Total	<i>100%</i>				

** As defined in this report*

9.3 MEPDG Analysis

The final step of the analysis corresponds to the estimation of pavement impacts under the traffic scenarios described in the previous section. To estimate pavement impacts, a tool is required that can model pavement response and performance when subjected to traffic and environmental effects. The Mechanistic-Empirical Pavement Design Guide version 1.10 was the software tool used for this analysis.

The MEPDG was created under a joint effort by the AASHTO Joint Task Force on Pavements (JTFP), National Cooperative Highway Research Program (NCHRP) and the Federal Highway Administration (FHWA) to bring researchers and pavement engineers a state-of-the-art tool for designing pavement structures and analyzing pavement performance (AASHTO, 2008)³. As the name implies, the MEPDG combines both mechanistic principles and empirical models to predict pavement performance. Figure 45 illustrates the inner workings of the design guide.

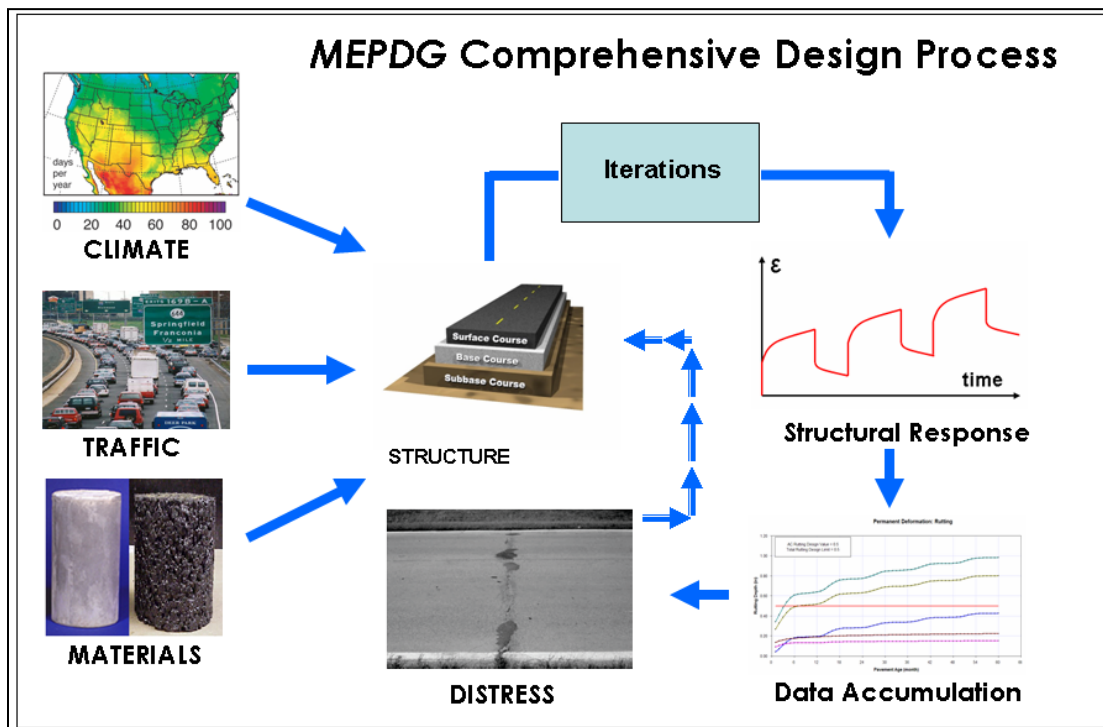


Figure 45: Inner Workings of the MEPDG

From the figure, it can be seen that the design guide takes into consideration the effects of traffic and the environment on the pavement structure. It then uses structural response models to estimate critical responses such as stresses, strains, and displacements within the pavement structure. For flexible pavements, the mechanical responses are estimated by a multi-layer linear elastic software program embedded within the design guide (AASHTO, 2008)². These responses are then utilized in a damage model to accumulate pavement damage (month by month) over the design period. The accumulated damage is then related to a specific distress such as pavement rutting or bottom-up cracking, by the application of distress prediction equations, or transfer functions (Prozzi and Hong, 2006)³⁰.

In general, transfer functions are derived from material performance under laboratory tests. For rutting in the asphalt layer for example, the rate of accumulation of plastic deformation is measured in the laboratory using a repeated load permanent deformation tri-axial test. This test applies pulse loads on a specimen to develop a relationship between the plastic strain in the specimen and its permanent deformation. The relationship between deformation and number of load cycles is then used to develop the transfer function.

For pavement rutting, there are two main transfer functions used by the design guide. The first equation calculates rutting in the asphalt concrete (AC) layers, while the second equation calculates rutting in unbound material layers. The total rut depth is the summation of the estimated rutting in the asphalt layers and the unbound layers of the pavement structure (NCHRP, 2004)³⁷. The two equations for rutting are presented below.

Equation 1: Permanent Deformation in the AC Layer

$$\Delta_{p(HMA)} = \varepsilon_{p(HMA)} h_{HMA} = \beta_{1r} \kappa_z \varepsilon_{r(HMA)} 10^{k_{1r}} N^{k_{2r} \beta_{2r}} T^{k_{3r} \beta_{3r}}$$

where:

- $\Delta_{p(HMA)}$ = Accumulated permanent vertical deformation in the HMA layer (in.),
 $\epsilon_{p(HMA)}$ = Accumulated permanent axial strain in the HMA layer (in./in.),
 $\epsilon_{r(HMA)}$ = Elastic strain calculated by the structural response model at mid-depth
of each HMA layer (in.),
 h_{HMA} = Thickness of the HMA layer/sublayer (in.),
 N = Number of axle load repetitions
 T = Mix or pavement temperature (°F),
 κ_z = Depth confinement factor
 $k_{1r,2r,3r}$ = Global field calibration factors
 $\beta_{1r,2r,3r}$ = Local or mixture field calibration factors

$$\kappa_z = (C_1 + C_2 * depth) * 0.328196^{depth}$$

$$C_1 = -0.1039 * H_{ac}^2 + 2.4868 * H_{ac} - 17.342$$

$$C_2 = 0.0172 * H_{ac}^2 - 1.7331 * H_{ac} + 27.428$$

where:

D = Depth below the surface (in.),

H_{ac} = Total HMA thickness (in.)

From the equation, it can be observed that the MEPDG predicts AC rutting based on a relationship between elastic strains and plastic strains in the asphalt pavement layers. The deformation predicted by the transfer function is then accumulated over the design life of the pavement to predict overall rutting in the AC layers. From the right side of the equation it can also be seen that model can be calibrated to better represent local conditions.

Equation 2: Permanent Deformation in Unbound Materials

$$\delta_a(N) = \beta_{s_1} k_1 \epsilon_v h \left(\frac{\epsilon_0}{\epsilon_r} \right) \left| e^{-\left(\frac{p}{N}\right)^\beta} \right|$$

where:

δ_a	=	permanent deformation for the unbound layer
N	=	Number of repetitions
ϵ_v	=	average vertical strain (in./in.)
h	=	thickness of the layer (in.)
$\epsilon_0, \beta_{s1}, p$	=	material properties
ϵ_r	=	resilient strain (in./in.)

Likewise, permanent deformation in the unbound layers is a function of average vertical strain estimated by the multi-layer linear elastic software, and the strain relationships developed under laboratory tests.

Furthermore, it should be noted that the approach utilized by the MEPDG to estimate pavement performance is based upon an incremental damage approach. The design guide breaks up a pavement's life into one-month time intervals, and uses the distress prediction equations to convert the structural responses into incremental distresses. Then the design guide sums up the distresses during each time increment to attain total accumulated damage for the design life.

9.4 Analysis Results

This section presents the results from the impact analysis conducted with the MEPDG. Material characteristics for the *IH-20* and the *FM 1606* pavement structures were input into the design guide along with their respective environmental conditions. Two traffic scenarios, "standard" traffic scenario and "windmill" traffic scenario were applied to each pavement structure for an ***analysis period of 20 years***. An analysis period of 20 years was chosen in order to estimate the impacts of windmill traffic at several stages along a pavement's life. In terms of rutting, the rate of pavement damage progression may be more severe during the initial years of design life as the pavement may not have yet settled under the traffic load. In terms of cracking, the opposite may be truth. These non-constant trends should be accounted for in the analysis.

It should be noted, however, that impacts from windmill traffic *were not* estimated for the entire 20 year analysis period. Windmill traffic comes in cycles and damage only occurs during the construction period of the wind farm. In Texas, an average wind farm is about 200-250 MW in size and requires about 130-160 windmill units to be constructed over a period of 1-2 years (AWEA, ND)³⁸. Often times a developer will construct a section of the wind farm over a course of 8-12 months and then expand it a year or so later. The Horse Hollow Wind Energy Center in Taylor and Nolan County, TX, for example is a 735.5 MW, 421 unit development that was constructed in three main stages over the course of three years (Wikipedia, ND)³⁹.

Since windmill traffic comes and goes, it is important to measure the damage only during the *2-year* construction period, *and not* the entire 20 year analysis period. Therefore, an analysis of 20 years was run in the MEPDG, but pavement performance was evaluated in 2-year segments towards the beginning, the middle, and the end of the pavement's life. The following two sub-sections will present the results from the impact study for the two pavement sections.

9.4.1 IH-20 IMPACT ANALYSIS RESULTS

Figure 46 presents the development of total surface pavement rutting with time for IH-20 under the two traffic scenarios discussed in the previous sections. The standard traffic scenario for IH-20 consisted of 1,209 Class 5 single-unit trucks and 7,817 Class 9 combination-unit trucks. The windmill traffic scenario consisted of standard traffic plus the movement of an additional 5, 10, and 20 windmills (*45, 90, and 180 wind trucks*) per day on that facility. No traffic growth was incorporated in the analysis. Pavement damage was evaluated at three stages of the design life: Initial stage (*1 month-2 years*), Middle-life (*8 years-10 years*), and end-life (*18 years- 20 years*). The three stages at which pavement life was evaluated are highlighted by red squares in Figure 46.

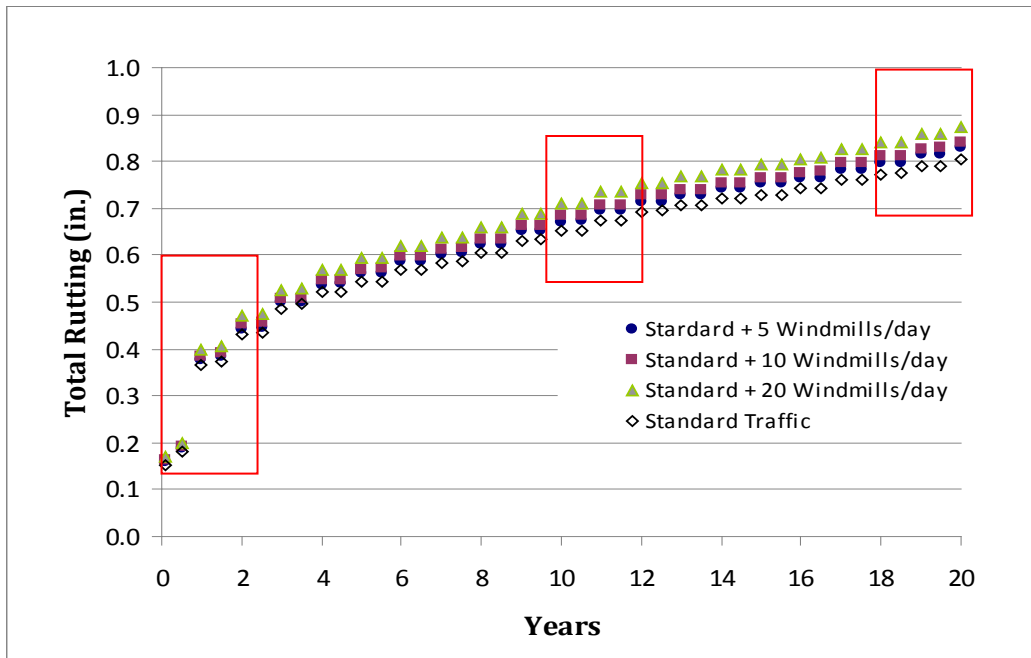


Figure 46: Pavement Performance for IH-20

Performance was first evaluated during the first 2 years of the pavement's design life. Figure 47 illustrates the total rutting accumulated during that period under the two traffic scenarios. In Figure 47, year 0.08 corresponds with the month of October, which is one month after the modeled roadway section was first opened to traffic. The years 0.75 and 1.75 correspond to the months of June, and the years 1.0 and 2.0 correspond to the months of September.

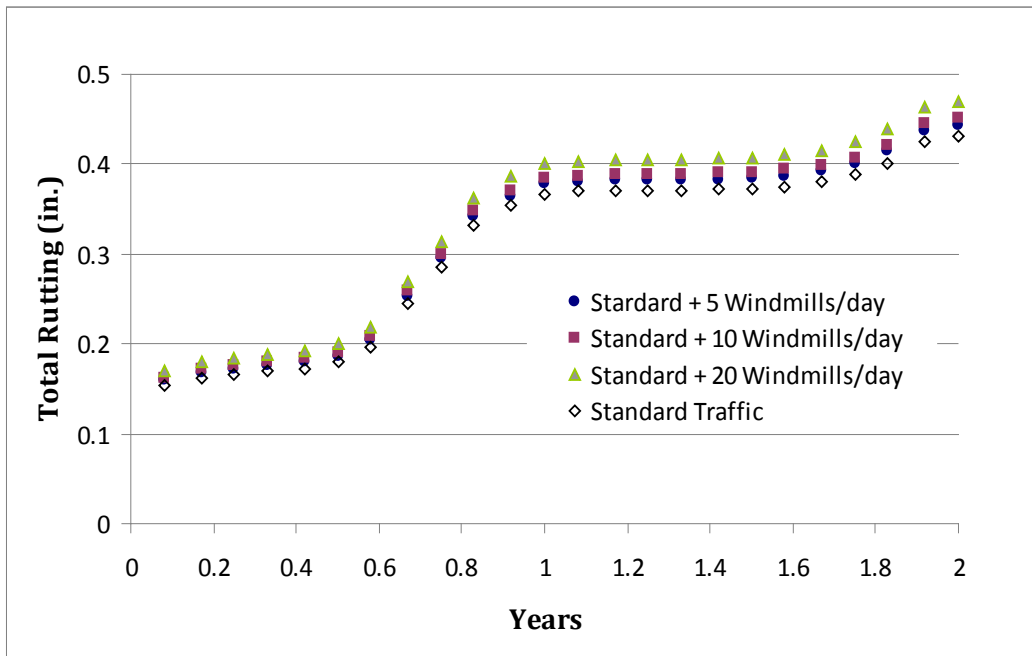


Figure 47: IH-20 Pavement Performance at Initial Stages of Design Life

From the figure, it can be seen that there was a significant amount of rutting experienced by the pavement structure after the first month of traffic and during the first summer season 8 months into the analysis period. This pattern of rutting can be expected from a new pavement structure that has just opened to traffic, as it has not yet had time to settle under the traffic load. The pavement can also be expected to undergo significant rutting during the summer seasons due to extremely hot daytime pavement temperatures. Asphalt is a material that exhibits viscoelastic-plastic properties, and it is therefore highly sensitive to changes in temperature (*NCHRP, 2004*)⁴². In some areas of Texas, during the summer months, pavement surface temperatures can rise as high as 120 °F. Under high temperatures, asphalt binder tends to display plastic behavior, and as a result, asphalt concrete layers undergo significant reductions in the dynamic modulus. “Softer” pavements, or pavements with a lower dynamic modulus, tend to experience more shear deformation under the wheel load. Therefore it was appropriate for the MEPDG to model this behavior. Overall rutting for the first two years is presented in Table 28.

Table 28: Pavement Rutting During First 2 Years

Rutting (in.)	Standard Traffic	+ 5 Windmills	+ 10 Windmills	+ 20 Windmills
Month 1	0.15	0.16	0.16	0.17
Month 24	0.43	0.44	0.45	0.47
Δ	0.28	0.28	0.29	0.30

Performance was next evaluated during the half-way point of the pavement’s design life. Figure 48 illustrates the total rutting accumulated during the period under the two traffic scenarios.

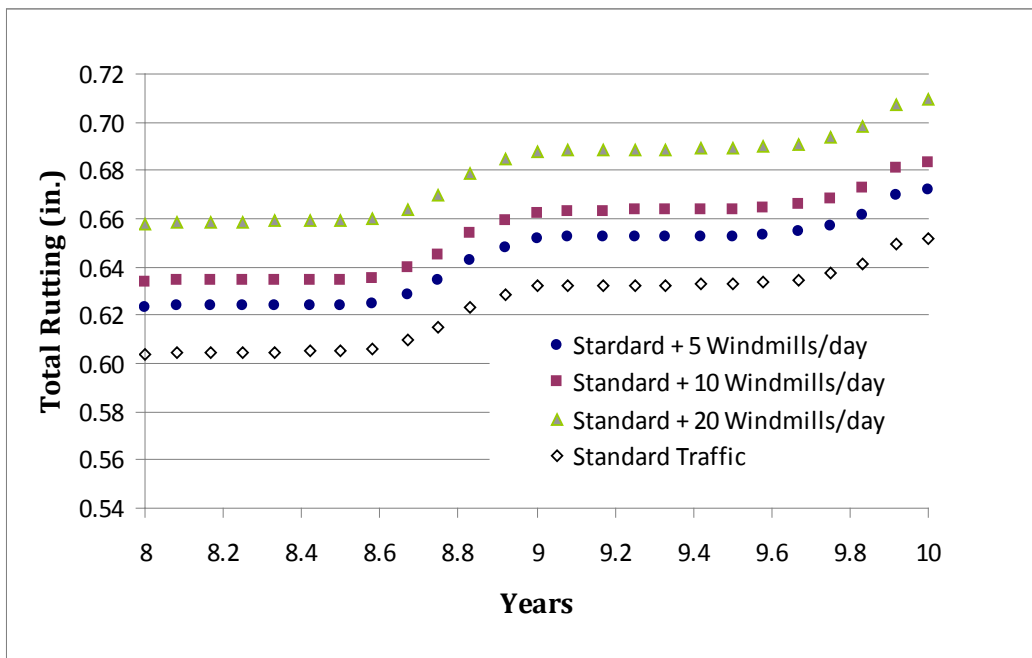


Figure 48: IH-20 Pavement Performance for Years 8-10 of Design Life

From the figure it can be seen that once again, there is a small increase in pavement rutting during the summer periods of year 8 and year 9, however, the rutting is significantly less than what was seen from the initial two years of traffic. Overall rutting for years 8-10 is presented in Table 29.

Table 29: Pavement Rutting During Years 8-10

Rutting (in.)	Standard Traffic	+ 5 Windmills	+ 10 Windmills	+ 20 Windmills
Month 96	0.60	0.62	0.63	0.65
Month 120	0.65	0.67	0.68	0.71
Δ	0.05	0.05	0.05	0.06

Figure 49 illustrates rutting for the last two years of the pavement’s design life. Similarly, overall rutting for years 18-20 is presented in Table 30.

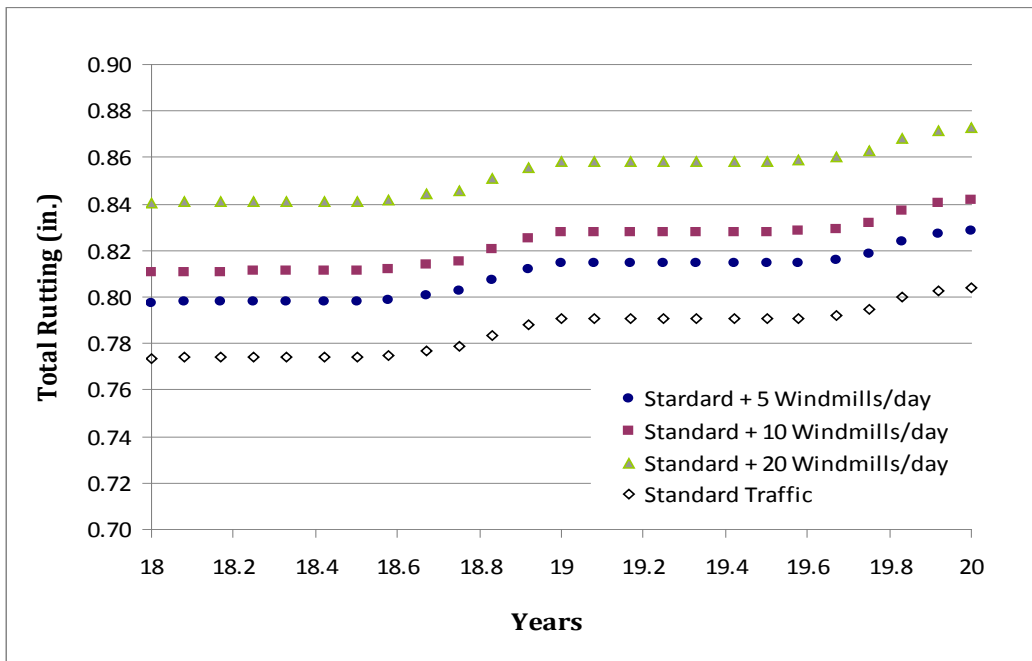


Figure 49: IH-20 Pavement Performance During Years 18-20 of Design Life

Table 30: Pavement Rutting During Years 18-20

Rutting (in.)	Standard Traffic	+ 5 Windmills	+ 10 Windmills	+ 20 Windmills
Month 216	0.77	0.80	0.81	0.84
Month 240	0.80	0.83	0.84	0.87
Δ	0.03	0.03	0.03	0.03

Pavement performance was quantified by comparing the rutting damage accumulated by the pavement due to the windmill traffic scenario against rutting damage accumulated by the pavement due to the standard traffic scenario. This sort of performance measure can be thought of as a damage ratio. Equation 3 illustrates how the damage ratio was calculated.

Equation 3: Damage Ratio for Pavement Rutting

$$DR = \frac{\Delta Rut_{windmill_traffic}}{\Delta Rut_{standard_traffic}} = \frac{\Delta Rut_{standard+windmill_traffic} - \Delta Rut_{standard_traffic}}{\Delta Rut_{standard_traffic}}$$

From the equation it can be seen that rutting damage due to **windmill traffic only**, can be obtained by subtracting the damage due to standard traffic from the damage due to standard traffic plus windmill traffic. The damage ratios for the three windmill traffic scenarios were then calculated and are presented in Table 31.

Table 31: Damage Ratios for Windmill Traffic Compared Against Standard Traffic

Damage Ratio	Standard Traffic	5 Windmills	10 Windmills	20 Windmills
Year 0.08-2	100%	3.0%	4.7%	8.5%
Year 8-10	100%	2.7%	4.2%	7.7%
Year 18-20	100%	2.7%	3.7%	7.3%

From Table 31, it can be seen that the damage ratio changes slightly when performance is monitored at different stages of the pavement’s design life. The damage ratios in Table 31 can be interpreted in the following way:

In this case scenario, the rutting damage caused from moving 5 additional windmills per day for two years on a rural interstate facility, is approximately 3% higher than the rutting damage that would have been caused by normal truck traffic.

9.4.2 FM 1606 IMPACT ANALYSIS RESULTS

A similar impact analysis on *FM 1606* can also be performed. Figure 50 presents total pavement rutting for *FM 1606* under the two traffic scenarios discussed in the previous sections. The standard traffic scenario for *FM 1606* consisted of 182 Class 5 single-unit trucks and 243 Class 9 combination-unit trucks. The windmill traffic scenario consisted of standard traffic plus the movement of an additional 2, 5, and 10 windmills (18, 45, and 90 wind trucks) per day on that facility. As before, no traffic growth was assumed. Pavement damage was once again evaluated at three stages of the design life: initial stage (1 month-2 years), middle-life (8 years-10 years), and end-life (18 years- 20 years). The three stages at which pavement life was evaluated are highlighted by red squares in Figure 50.

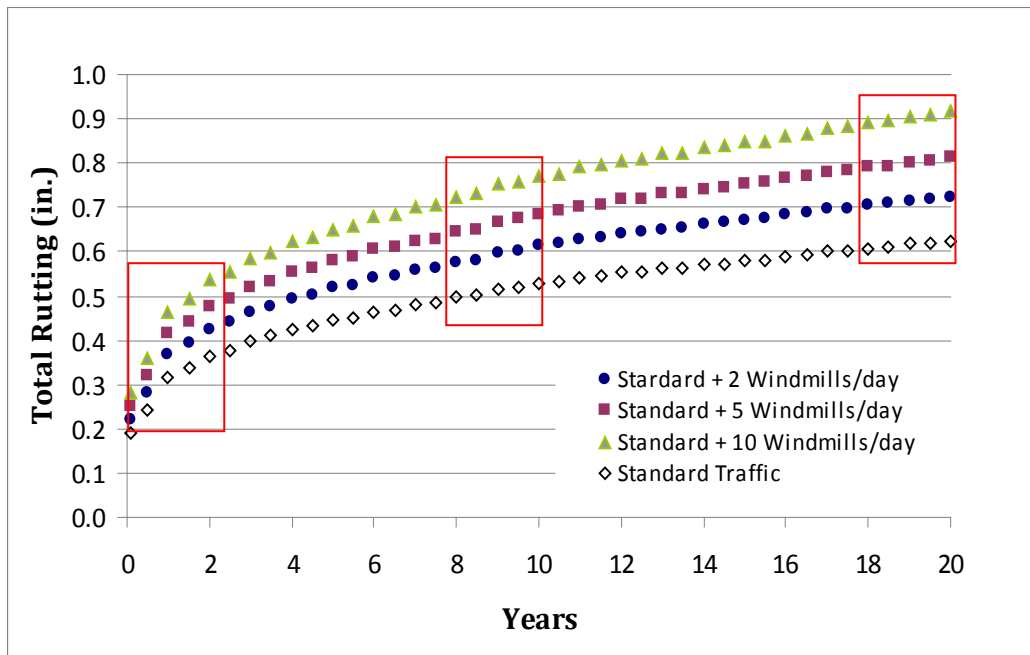


Figure 50: Pavement Performance for FM 1606

Once again, performance was first evaluated during the first 2 years of the pavement’s design life. Figure 51 illustrates the total rutting accumulated during that period under the two traffic scenarios. Overall rutting for the first two years is also presented in Table 32.

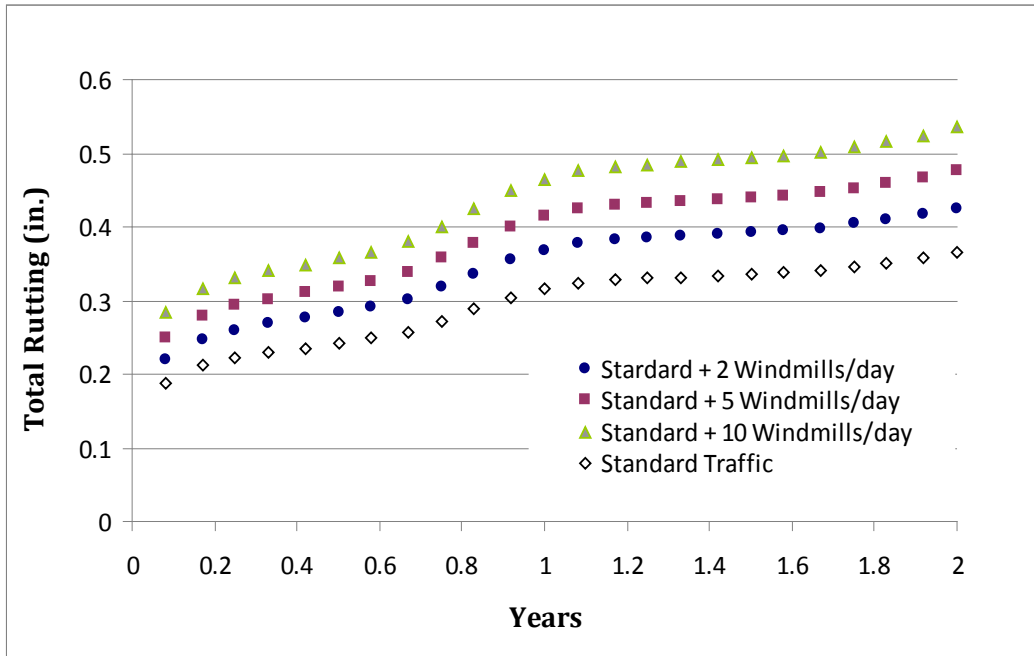


Figure 51: FM 1606 Pavement Performance at Initial Stages of Design Life

Table 32: Pavement Rutting During First 2 Years

Rutting (in.)	Standard Traffic	+ 2 Windmills	+ 5 Windmills	+ 10 Windmills
Month 1	0.19	0.22	0.25	0.28
Month 24	0.36	0.43	0.48	0.54
Δ	0.17	0.21	0.23	0.26

From Figure 51, it can be seen that once again the modeled pavement experienced a significant amount of rutting during the initial months of traffic due to the densification of air voids. Rutting also occurred during the summer seasons, however summer rutting on FM 1606 was not as pronounced as summer rutting on IH-20. This may be attributed

to the structural design of the FM road. FM 1606 was modeled with only one asphalt concrete layer (2.8 inches in thickness) while IH-20 was modeled with three asphalt concrete layers (10.5 inches in thickness). Since temperature has a pronounced effect on the viscoelastic properties of asphalt, in this case it can be reasoned that the FM 1606 section was less affected by summer temperatures than the IH-20 section because it had a thinner asphalt concrete layer.

Performance was next evaluated during the half-way point of the pavement’s design life. Figure 52 illustrates the total rutting accumulated during the period under the two traffic scenarios. Overall rutting for years 8-10 is presented in Table 33.

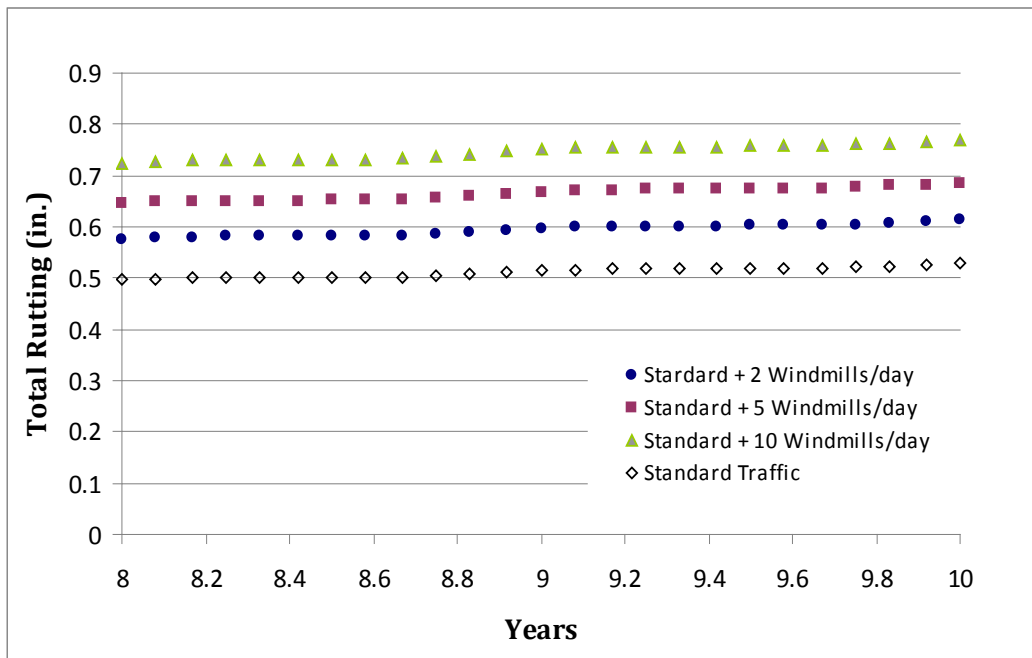


Figure 52: FM 1606 Pavement Performance for Years 8-10 of Design Life

Table 33: Pavement Rutting During Years 8-10

Rutting (in.)	Standard Traffic	+ 2 Windmills	+ 5 Windmills	+ 10 Windmills
Month 96	0.50	0.58	0.65	0.72
Month 120	0.53	0.61	0.69	0.77
Δ	0.03	0.03	0.04	0.05

Lastly, Figure 53 illustrates rutting for the last two years of the pavement’s design life. Similarly, overall rutting for years 18-20 is presented in Table 34.

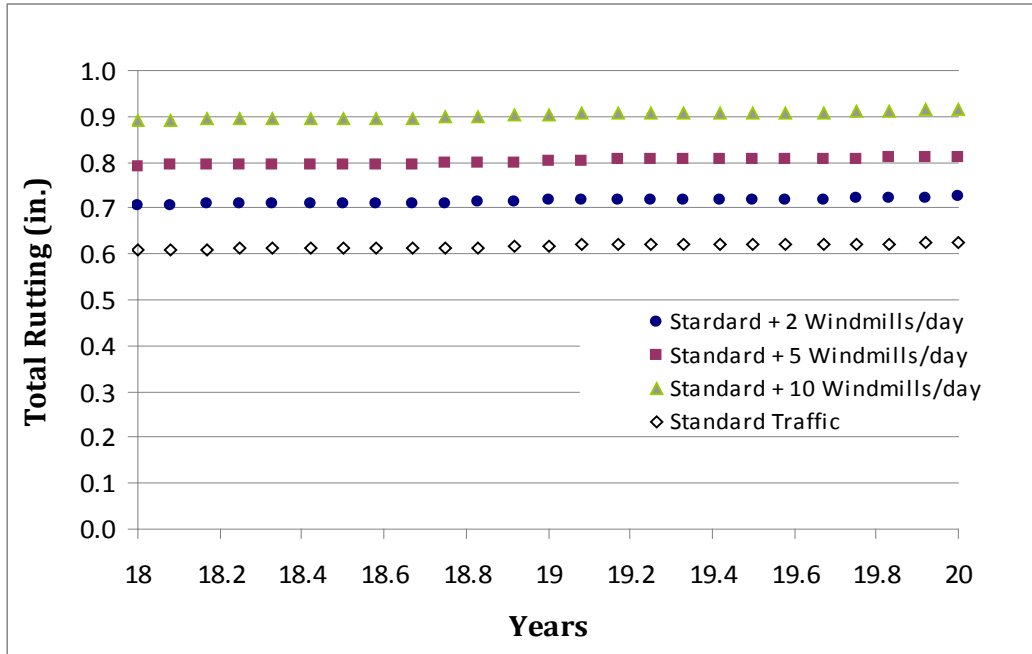


Figure 53: FM 1606 Pavement Performance During Years 18-20 of Design Life

Table 34: Pavement Rutting During Years 18-20

Rutting (in.)	Standard Traffic	+ 2 Windmills	+ 5 Windmills	+ 10 Windmills
Month 216	0.61	0.71	0.79	0.89
Month 240	0.63	0.73	0.81	0.92
Δ	0.02	0.02	0.02	0.03

Once again, pavement performance was quantified by comparing the rutting damage ratios of the two traffic scenarios. The damage ratios for the three windmill traffic scenarios are calculated below in Table 35.

Table 35: Damage Ratios for Windmill Traffic When Compared Against Standard Traffic

Damage Ratio	Standard Traffic	2 Windmills	5 Windmills	10 Windmills
Year 0.8-2	100%	16.5%	29.1%	43.1%
Years 8-10	100%	15.7%	29.8%	48.4%
Year 18-20	100%	15.7%	30.7%	50.6%

From the table, it can be seen that the damage ratio once again changes slightly when performance is monitored at different stages of the pavement's design life. The damage ratios in Table 35 can be interpreted in the following way:

The rutting damage increase caused from moving 2 additional windmills per day for two years on a rural collector facility, is approximately 16% higher than the rutting damage that would have been caused by normal truck traffic.

CHAPTER 10. CONCLUSIONS OF STUDY

This report analyzed the impacts of transporting windmill components on pavement structures. In all, two pavement sections were selected (rural interstate, and rural collector road) and two traffic scenarios were analyzed for the study. To quantify the damage and compare the impacts, a damage ratio was developed. The damage ratio is a unit-less measurement that allows for quick comparison between rutting damage caused from standard traffic and windmill traffic. Rutting damage ratios were developed for each one of the three windmill traffic scenarios for both pavement structures.

In general, it was seen that pavement rutting development for both pavement structures is significantly higher during early life. The damage ratios between the two traffic scenarios, for the most part, remained steady over the pavements' design life. Pavement rutting progression at the end of the design life for both structures was predicted to be in the hundredths of a decimal point of an inch, which can be considered insignificant, and therefore the damage ratios for that time period should not be analyzed with much scrutiny. What is important to take away is that the MEPDG predicted consistent patterns for the damage ratio from the initial stages to the ending stages of the pavements' design lives.

The windmill traffic scenarios revealed that the damage done from moving oversize overweight windmill components had a defining impact on rural collector pavement sections, meanwhile, for rural interstate pavement sections, windmill traffic played a less significant role. For the rural interstate system, the windmill traffic scenario considered the transportation of 5, 10, and 20 windmills on the facility per day. Moving 10-20 windmills per day on any roadway facility for a 2-year period may be excessive. However, during the Route Study conducted for this analysis, some segments of interstate were observed to get a steady flow of windmill traffic throughout the state of Texas. Specifically, these roadways were IH-10 and IH-20 in West Texas, IH-45 from Houston

to San Antonio, and IH-35W north of the Dallas/Ft. Worth metroplex. So, to quantify the impacts of transporting 5 windmills per day on a rural interstate is closer to reality.

For the rural collector facility (FM 1606), the windmill traffic scenario considered the transportation of 2, 5, and 10 windmills on the facility per day. Once again, the 5-10 windmills per day scenario may be a bit far-fetched, and should be taken with practicality only as a sensitivity analysis.

Through the development of the rutting damage ratio it was seen that the transportation of 5 windmills per day (*45 windmill trucks spread over 8 vehicle classes*) on a rural interstate is equivalent to 3% of additional damage to that facility under normal traffic conditions. In terms of number of trucks, this would equal to approximately 268-245 standard traffic trucks per day (*with 13.4% being single unit trucks and 86.6% being combination unit trucks*).

On the rural collector roadway facility, moving 2 windmills per day (*18 windmill trucks spread over 8 vehicle classes*) was equivalent to approximately 16% of additional damage to that facility under normal traffic conditions. On the rural collector road, normal traffic conditions were determined to be 425 trucks per day, therefore moving 2 windmills per day is equivalent to damage caused by 70 to 67 standard trucks (*with 42.9% of trucks being single unit and 57.1% being combination-unit*).

10.1 Further Remarks

It should be mentioned that pavement damage in the development of wind farms is not only caused by the transportation of windmill components. There are other elements of wind farm construction that facilitate a significant amount of truck traffic that may have a more severe impact on the roadway infrastructure. For example, the construction of service roads requires a significant amount of materials and it can generate a substantial volume of traffic. Every windmill is connected to the main collector road by a service road. In Texas, it was seen that most service roads range from 0.25 to 0.5 miles in length, are 20 feet wide and constructed from an 8 inch caliche material base. Typically a

service road requires 4,000 to 4,500 tons of caliche soil per/mile to construct, so a single service road may require anywhere from **67-89 truck trips** to haul the soil to the site.

Thereafter, the concrete foundation which sits underneath the windmill structure needs to be constructed. Figure 54 illustrates the pad-site and the foundation as it is being constructed.



Figure 54: Construction of Pad Site for Windmill Structure

(Stacey Young, TxDOT Pavement Engineer)

The foundation requires approximately 85,000 lbs of rebar, and 600 to 750 tons of concrete. The foundation also requires approximately 5,000 tons of soil material for cover after it has been cast into place. In total, a single windmill may call for an **additional 35 concrete truck hauls** for the pad site and **220 truck hauls** for the cover material.

Windmills are typically developed in segments with the average spacing between windmills being around 2,000 feet. Therefore a single farm-to-market road may facilitate traffic for the construction of 30 to 40 windmills, while an adjoining rural interstate facility may facilitate traffic for the entire wind farm development (Young, 2008)⁴⁰.

It should also be mentioned that in this study, the **reported loads on axles** were used to develop the axle load spectra for the windmill vehicle fleet. These values are provided by the transportation companies to the state DOT during the permitting process.

However, if the actual load spectra for trucks were to be taken from weigh-in-motion (WIM) stations, the results may be far different. Actual data will be more variable. The way the load is spread over the vehicle's axles is heavily dependent on its shape, position, center of mass, and center of symmetry. Based on these parameters, there may be some axles that are heavily overloaded and other axles that are quite under-loaded, and without actual data there is no way to tell.

To conclude, the wind energy industry is a growing sector, and its impacts on the transportation system throughout the United States has not yet been quantified, however, it is affecting the rate of deterioration of our road network. There is much room for research and further analysis in all elements discussed in this report: from the future of the wind industry itself, to the vehicle fleet employed in the transportation of components, and down to the assessment of pavement damage. The transportation system is a vital part of this nation's well being, and it is important to continue to study how various industries use it and impact it in many ways.

Appendix A

The Wilcoxon rank-sum test compares the means of two independent continuous populations. If the difference between the means (u_1 and u_2) of these two populations is insignificant, then it is assumed that both populations belong to the same distribution (Montgomery & Runger, 2007). In this example, the GVW of the tractor vehicle fleet was used as the parameter under study. The tractor vehicle fleet was first sorted in an ascending order by gross vehicle weight, and then split into two category groups:

- Standard tractor vehicles (steering axle and one tandem back axle)
- Non-standard tractor vehicles (steering axle and non-tandem combination back axle)

Standard tractor vehicles were assigned a “+” sign, and non-standard vehicles were assigned a “-” sign. The rank-sum test is typically

By applying the rank-sum test to the problem it can be determined whether the weight of the nacelle has any impact on the type of tractor used to transport it. If the weight of the nacelle *has no* impact on the vehicle fleet, then it can be expected that the mean gross vehicle weights of standard tractors and non-standard will be approximately equal to each other. Applying the procedure of the rank-sum test, the number of standard and non-standard tractors in the vehicle fleet was first determined:

- Standard tractor vehicles (+): 924
- Non-standard tractor vehicles (-): 2,444
- Total number of observations: 3,368

The observations were then arranged in ascending order of magnitude by their reported GVW, and assigned ranks (1-3,368). The sum of the ranks of the smaller sample (standard tractor vehicles) was then determined as W_1 . Since both the samples were

significantly large (>8), the distribution of W_I was approximated to be normal (Montgomery and Runger, 2007), and the mean μ_{w1} and variance σ^2_{w1} were determined using the following equations:

$$\mu_{w1} = \frac{n_1(n_1 + n_2 + 1)}{2} \quad (1)$$

$$\sigma^2_{w1} = \frac{n_1 n_2 (n_1 + n_2 + 1)}{12} \quad (2)$$

Based on the mean and the standard deviation of the entire group of observations, and the W_I statistic, the distribution of the tractor vehicle fleet can be standardized, and the Z_0 statistic obtained using the following equation:

$$Z_0 = \frac{W_1 - \mu_{w1}}{\sigma_{w1}} \quad (3)$$

The resulting statistics of the analysis are presented in Table 1 below.

Table 1: Statistics of Wicoxon Rank-Sum Test

W_1	708290
μ_{w1}	1556478
σ^2_{w1}	6.34E+08
σ_{w1}	25179.46
Z_0	-33.6857

Since Z_0 is significantly low (corresponding to $\alpha \ll 0.05$), it can be concluded that the gross vehicle weight (GVW) and hence the weight of the nacelle unit has a significant impact on the vehicle tractor fleet. The standard and non-standard vehicle fleets are two different populations of fleets that are not used for moving the same types of load.

References

1. AWEA, 2009. *AWEA Annual Wind Industry Report, Year Ending 2008*. American Wind Energy Association, Washington D.C., 2009. available at: www.awea.org/publications
2. TRB, ND. *NCHRP 1-37A: Design Guide*. Transportation Research Board. Available at: <http://onlinepubs.trb.org/onlinepubs/archive/mepdg/home.htm>
3. AASHTO, 2008. *Mechanistic-Empirical Pavement Design Guide, A Manual of Practice*. American Association of State Highway and Transportation Officials, Washington D.C., July 2008.
4. AASHTO, 1993. *AASHTO Guide for Design of Pavement Structures*. American Association of State Highway and Transportation Officials, Washington D.C., 1993.
5. U.S. Department of Energy: Energy Efficiency and Renewable Energy, 2008. *20% Wind Energy by 2030*. Washington, July. available at: <http://www1.eere.energy.gov/windandhydro/>
6. American Wind Energy Association. ND. “*Legislative Affairs*.” Accessed online at: www.awea.org/legislative. June, 2010.
7. AWEA, 2010. *AWEA Wind Power Outlook 2010*. American Wind Energy Association, Washington D.C., 2010. available at: www.awea.org/publications
8. Tombari, C., 2007. “Energy Efficiency and Renewable Energy: Risk Management in the 21st Century.” National Renewable Energy Laboratory. Workshop on Renewable Energy Austin, TX. October, 2007.
9. GE Energy, ND. “Wind Energy at GE.” General Electric Company. Available online at: http://www.gepower.com/businesses/ge_wind_energy/en/index.htm. Accessed on May, 2010
10. U.S. EIA, ND. “Table 5. Average Monthly Bill by Census Division, and State 2008.” Available at: <http://www.eia.doe.gov/cneaf/electricity/esr/table5.html>. U.S. Energy Information Administration Independent Statistics and Analysis. Accessed on May, 2010
11. Wikipedia Online Encyclopedia, ND. “Square-cube law.” Available at: http://en.wikipedia.org/wiki/Square-cube_law. Accessed on May, 2010
12. Model Brochure, 2010. “Siemens SWT-3.0-101.” Available at: www.siemens.com/wind Siemens AG Energy Sector. Erlangen, Germany.

13. Model Brochure, 2010. "Clipper 2.5 MW Liberty." Available at: www.clipperwind.com Clipper Windpower Plc. London, UK.
14. Model Brochure, 2009. "GE Energy 1.5MW Wind Turbine." Available at: www.gepower.com General Electric Company. U.S.A.
15. Model Brochure, 2009. "G90 2.0 MW Wind Turbine." Available at: www.gamesacorp.com Gamesa Corporation. Sarriguren, Spain.
16. Model Brochure, 2010. "AW-3000 3.0 MW Wind Turbine." Available at: www.acciona-energy.com. Acciona Windpower. Navarra, Spain.
17. Model Brochure, 2010. "V80-2.0 MW Wind Turbine." Available at: www.vestas.com
Vestas Americas Inc. Portland, OR.
18. Model Brochure, 2009. "V821-65 1.65 MW Wind Turbine." Available at: www.vestas.com
Vestas Americas Inc. Portland, OR.
19. Model Brochure, 2009. "S82- 1.5 MW Wind Turbine." Available at: www.suzlon.com. Suzlon Energy Limited.
20. American Wind Energy Association. ND. "*Wind Industry Transportation Opportunities and Challenges.*" Accessed online at: www.awea.org. Accessed on June, 2010.
21. BNSF Railway, 2010. "BNSF Case Study: Serving the Transportation Needs of the Wind Energy Market." Burlington Northern Santa-Fe Railway. Available at: <http://www.bnsf.com/customers/wind-energy>. Accessed on June, 2010
22. BNSF Railway, 2010. "Brochure: Wind Power Shipments on the BNSF Railway." Burlington Northern Santa-Fe Railroad. Available at: www.bnsf.com/wind. April.
23. Union Pacific Railway, ND. "Wind Turbines." Union Pacific Railway. Available at: http://www.uprr.com/customers/ind-prod/emerge_mkts/wind.shtml. Accessed on May, 2010
24. Texas Department of Transportation, ND. "Oversize and Overweight Load Permits." Online: http://www.dot.state.tx.us/business/motor_carrier/overweight_permit/default.htm
Accessed on April, 2010.

25. California Department of Transportation, ND. "Truck Size". Available at: <http://www.dot.ca.gov/hq/traffops/trucks/trucksize/width.htm>. Accessed on April 2010.
26. Union Pacific Railway, ND. "Step-by-Step Process for Shipping Dimensional Loads." Available at: <http://www.uprr.com/customers/ind-prod/consumer/stepbystep.shtml>. Accessed on May, 2010
27. CSX Railway, ND. "Customers: Dimensional Shipments." Available at: www.csx.com/?fuseaction=customers.md_shipments. Accessed on May, 2010.
28. BLM Deck Division Incorporated, ND. "Trailer Specifications." Available at: <http://www.apacheinc.com/trailer.html> Accessed on May, 2010.
29. Peerless Limited, ND. "Tandem Blade Trailer." Available at: <http://www.peerless.ca/products/windenergy/tandem30blade.php> Accessed on May, 2010
30. IST Trailers, ND. "Heavy Haul Trailers." Available at: <http://www.isttrailers.com/heavy-haul.cfm> Accessed on May, 2010.
31. Prozzi, J.A., Hong, F., 2004. "Evaluation of Equipment, Methods, and Pavement Design Implications of the AASHTO 2002 Axle Load Spectra Traffic Methodology." FHWA/TX-06/0-4510. Prepared by Center for Transportation Research, Austin, TX.
32. Montgomery, D., Runger, G. 2007. Applied Statistics and Probability for Engineers. John Wiley and Sons, Hoboken, NJ.
33. Huang, Yang H. Pavement Analysis and Design. Pearson Prentice Hall, Upper Saddle River, NJ, 2004.
34. The University of Austin at Texas, ND. *Texas Flexible Pavement Database*. Available at: <http://pavements.ce.utexas.edu>
35. Roberts, F., Kandhal, P., Brown, R., Lee, D., Kennedy, T., 1996. Hot Mix Asphalt Materials, Mixture Design, and Construction. National Asphalt Pavement Association Research and Education Foundation, Lanham, MD.
36. Braja M. Das, 2006. Principles of Geotechnical Engineering, 6th Edition. PWS Publishing Company, Boston, MA.
37. Prozzi, J. (2009). *Review of HERS-ST for Application in Texas*. Center for Transportation Research, University of Texas at Austin.

38. NCHRP, 2004. *Guide for Mechanistic-Empirical Design of New and Rehabilitated Pavement Structures Final Report: Part 3 Flexible Design*. NCHRP 1-37A. National Cooperative Highway Research Program, Washington D.C., March.
39. American Wind Energy Association. ND. “*Wind Power Projects*.” Accessed online at: www.awea.org/projects. June, 2010.
40. Wikipedia Online Encyclopedia, ND. “Horse Hollow Energy Center.” Available at: http://en.wikipedia.org/wiki/Horse_Hollow_Wind_Energy_Center
41. Young, S., Campbell, C. 2008. “Maintenance of FM Roads That Have Been Windmilled.” Presentation. June.
42. NCHRP, 2004. *Guide for Mechanistic-Empirical Design of New and Rehabilitated Pavement Structures Final Report: Part 2 Design Inputs*. NCHRP 1-37A. National Cooperative Highway Research Program, Washington D.C., March.

VITA

Sergey Grebenshikov was raised in Chicago, IL. He received his undergraduate degree in Civil Engineering from Michigan State University. He currently lives in Austin, TX.

Email: grebensc@msu.edu

This thesis was typed by Sergey Grebenshikov.